

PULMONARY DIFFUSION LIMITATION, \dot{V}_A/\dot{Q} MISMATCH AND PULMONARY
TRANSIT TIME IN HIGHLY TRAINED ATHLETES DURING MAXIMAL EXERCISE

by

SUSAN ROBERTA HOPKINS

B. Med. Sci., Memorial University of Newfoundland, 1978
M.D., Memorial University of Newfoundland, 1980
M.P.E., The University of British Columbia, 1988

A THESIS SUBMITTED IN PARTIAL FULFILLMENT OF THE REQUIREMENTS
FOR THE DEGREE OF DOCTOR OF PHILOSOPHY

in

THE FACULTY OF GRADUATE STUDIES
(Interdisciplinary Studies, Medicine/Physical Education/Zoology)

We accept this thesis as conforming to the required standard

THE UNIVERSITY OF BRITISH COLUMBIA

November 1992

© Susan Roberta Hopkins, 1992

In presenting this thesis in partial fulfilment of the requirements for an advanced degree at the University of British Columbia, I agree that the Library shall make it freely available for reference and study. I further agree that permission for extensive copying of this thesis for scholarly purposes may be granted by the head of my department or by his or her representatives. It is understood that copying or publication of this thesis for financial gain shall not be allowed without my written permission.

(Signature)

Department of Interdisciplinary Studies

The University of British Columbia
Vancouver, Canada

Date February 25, 1993

ABSTRACT

To investigate the relationship between pulmonary diffusion limitation, ventilation-perfusion (\dot{V}_A/\dot{Q}) mismatch, pulmonary transit times (PTT) and pulmonary gas exchange during exercise, 10 highly trained male athletes (age=26.4±4.4 years, Height=185.5±5.3 cms, Weight=78.2±8.6 kg, $\dot{V}O_{2\max}=5.15\pm0.52$ l·min⁻¹) underwent exercise testing at rest (R) and 150W, 300W and maximal exercise (372±22W), corresponding to an oxygen consumption ($\dot{V}O_2$) of 0.41±0.09, 2.16±0.17, 4.32±0.35 and 5.13±0.50 l·min⁻¹ respectively, while trace amounts of six inert gases were infused via a peripheral vein. Arterial blood samples, mixed expired gas samples and metabolic data were obtained. Observed alveolar arterial difference ($[A-a]DO_{2(o)}$) was calculated according to the alveolar gas equation. Indices of \dot{V}_A/\dot{Q} mismatch: LogSD \dot{V} and LogSD \dot{Q} and predicted $[A-a]DO_2$ ($[A-a]DO_{2(p)}$) were derived from 50 compartment model analysis of retentions and excretions of the inert gases. Additional indices of \dot{V}_A/\dot{Q} mismatch: DISPR*, DISPE and DISPR*-E and inert gas alveolar difference ($[A-a]D$, R(A-a)D and E(A-a)D) were obtained directly from the inert gas data. One to two weeks later, the subjects underwent first pass radionuclide angiography using a Siemens ZLC wide field of view gamma camera. Following in vitro labeling with ^{99m}Tc, 5-10 ml of the subject's blood, containing 10-20 mCi of activity, were injected at rest. First pass and post-static data were obtained on an ADAC 3003 computer and cardiac output was calculated using the Stewart Hamilton equation. PTT was determined using deconvolution and centroid methods. Gated radionuclide angiography was then performed at rest, 150, and 300W. On a separate occasion, first pass cardiac outputs and pulmonary transit times were obtained at maximal exercise. Mean arterial partial pressure of O₂ (PaO₂) decreased significantly from rest to 150W, and from 150 to 300W to a low value of 86±9 torr, before increasing to near resting values at maximal exercise. $[A-a]DO_{2(o)}$ increased across each exercise level however only the increase from 150 to 300 W was significant. The overall and perfusion-related indices of \dot{V}_A/\dot{Q} mismatch showed a significant increase with exercise, mainly as a

result of increasing perfusion of areas of high \dot{V}_A/\dot{Q} . $[A-a]DO_{2(o)}$ was greater than predicted, becoming significant during heavy exercise, indicating diffusion limitation. Cardiac output increased from $6.9 \pm 0.9 \text{ l}\cdot\text{min}^{-1}$ (R) to $25.2 \pm 2.5 \text{ l}\cdot\text{min}^{-1}$ at 300W and $33.3 \pm 3.7 \text{ l}\cdot\text{min}^{-1}$ at maximal exercise. End diastolic volume increased from R to heavy exercise ($p < 0.001$), accompanied by a decrease in end systolic volume ($p = 0.05$). Stroke volume and ejection fraction also increased significantly from R to 300W ($p < 0.001$). Deconvolution PTT decreased from $9.32 \pm 1.41 \text{ s}$ at rest to $2.91 \pm 0.30 \text{ s}$ during max exercise and was highly correlated with centroid PTT both at rest ($r=0.99$, $p<0.001$) and during maximal exercise ($r=0.96$, $p<0.001$). PTT during maximal exercise was significantly correlated with PaO_2 ($r=0.65$, $p<0.05$) and $[A-a]DO_{2(o)}-[A-a]DO_{2(p)}$ ($r=-0.60$, $p<0.05$). Calculated pulmonary blood volume increased during maximal exercise by 57% over resting values to over 25% of total blood volume and when corrected for body surface area correlated significantly with PaO_2 ($r=0.69$, $p<0.05$). There was a significant correlation between $(A-a)D$, PTT, the ventilatory equivalent for CO_2 and PaO_2 during maximal exercise ($r=0.94$, $p<0.01$) allowing prediction of over 80% of the variance in PaO_2 between subjects. These data indicate that highly trained athletes develop \dot{V}_A/\dot{Q} mismatch accompanied by diffusion limitation during maximal exercise. Observed decrease in PaO_2 during high intensity exercise is the result of a complex interaction between \dot{V}_A/\dot{Q} mismatch, hypoventilation and diffusion limitation secondary to shortened pulmonary transit.

TABLE OF CONTENTS

Abstract	ii
List of Tables	vi
List of Figures	vii
List of abbreviations and symbols	viii
Acknowledgment	x
Introduction	1
Methods	6
Baseline data	6
Subject preparation	7
Test protocol	7
Multiple inert gas analysis	8
Arterial blood gases	9
Cardiac output	10
Pulmonary transit time	12
Data analysis	13
Results	14
General data	14
Ventilation and metabolic data	15
Arterial blood gases and oxygen saturation	16
\dot{V}_A/\dot{Q} inequality	22
Diffusion disequilibrium	25
Cardiac output and cardiac volumes	26
Pulmonary transit time	26
Pulmonary blood volume	32
Discussion	33
Multiple inert gas analysis and exercise	34
MIGET data	35
Indices of dispersion and \dot{V}_A/\dot{Q} mismatch	35
Diffusion limitation	37
Effect of uncertainty in cardiac output on MIGET data	38
Maintenance of steady state conditions	40
Blood and plasma volume	41
Radionuclide cardiography	42
Cardiac function in athletes	43
Comparison with previous investigations	44
Effect of increasing exercise intensity on cardiac volumes	44
Pulmonary transit times	47
Theory	47
Pulmonary transit times and exercise in humans	49
Pulmonary blood volume	49
Relationship of pulmonary transit time and blood volume to pulmonary capillary transit time and blood volume	50
Arterial blood gas and metabolic data	51
Arterial blood measures	51
Mixed venous PO_2	52
Possible mechanisms of exercise induced hypoxemia	52
Summary of findings	56
References	57
Appendix A: Review of literature	70
Introduction	70

Respiration and the respiratory muscles.....	71
Energetics.....	72
Blood flow to the diaphragm and other respiratory muscles.....	72
Oxygen consumption of respiratory muscles.....	74
Lactate Production.....	76
Theoretical calculations of respiratory muscle $\dot{V}O_2$ and \dot{Q} in humans exercising at maximal levels.....	77
Respiratory muscle fatigue.....	79
Histochemical properties of mammalian respiratory muscles.....	79
Evidence for fatigue.....	80
Respiratory drives.....	81
Pulmonary mechanics and expiratory flow limitation.....	83
Pressure-volume relationships.....	83
Characteristics of flow inside tubes.....	83
Flow-volume relationships.....	84
Pulmonary diffusion and gas exchange.....	86
Factors related to diffusion of oxygen.....	86
Factors related to diffusion of carbon dioxide.....	87
Factors affecting pulmonary gas exchange.....	88
Does the pulmonary system constrain exercise?.....	92
Summary.....	96
Appendix B: Methodological background.....	97
Quantitative radiocardiography.....	97
Red blood cell labeling.....	97
First pass determination of cardiac output.....	97
Gated radionuclide angiography.....	99
Measurement of blood volume.....	100
Pulmonary transit time.....	101
Frequency distribution of pulmonary transit times.....	102
Multiple inert gas elimination.....	105
Ventilation and perfusion relationships.....	105
Multiple inert gas elimination theory.....	107
Practical aspects.....	110
Dead space.....	111
Shunt.....	112
V_A/\dot{Q} distributions.....	113
Alveolar arterial difference.....	114
Appendix C: Statistical analyses and raw data.....	116
Anova tables.....	116
Metabolic data.....	116
Blood gas data.....	118
MIGET data for all six gases.....	121
Cardiac data.....	125
Regression.....	127
Appendix D: Individual Subject Data.....	131

LIST OF TABLES

Table 1.	Subject descriptive data.....	14
Table 2.	Plasma volume and calculated whole blood volume - individual subject data.....	15
Table 3.	Arterial blood gases, metabolic data, transit times and MIGET summary data at rest, light, heavy and maximal exercise ($\bar{x} \pm SD$).....	18
Table 4.	Calculated mixed venous and arterio-venous O ₂ difference during rest, light, heavy and maximal exercise.	22
Table 5.	(A-a)D, R(A-a)D and E(A-a)D at rest and during light, heavy and maximal exercise ($\bar{x} \pm SD$).....	24
Table 6.	Cardiac output, volumes and ejection fraction at rest and during, light, heavy and maximal exercise ($\bar{x} \pm SD$).....	26
Table 7.	Pulmonary transit times by the deconvolution and centroid methods.....	28
Table 8.	Pulmonary blood volume at rest and during maximal exercise	32
Table 9.	Comparison of MIGET data from present study with other investigators	38
Table 10.	Effect of varying cardiac output on residual sum of squares and indices of dispersion.....	40
Table 11.	Cardiac output and volume indices comparison with other studies	46
Table 12.	Blood flow of respiratory muscles.....	73
Table 13.	$\dot{V}O_2$ of respiratory muscles.....	75
Table 14.	Oxygen cost of unobstructed hyperventilation.....	76
Table 15.	Alveolar-arterial differences at rest and during exercise	91
Table 16.	Blood gas and cardio-respiratory data obtained at 70-100% of $\dot{V}O_2$ max	95

LIST OF FIGURES

Figure 1.	PaO ₂ , PaCO ₂ and [A-a]DO ₂ (o) for individual subjects during light exercise.....	19
Figure 2.	PaO ₂ , PaCO ₂ and [A-a]DO ₂ (o) for individual subjects during heavy exercise.....	20
Figure 3.	PaO ₂ , PaCO ₂ and [A-a]DO ₂ (o) for individual subjects during maximal exercise.....	21
Figure 4.	Dispersion indices at rest and during light, heavy and maximal exercise.....	24
Figure 5.	Observed and predicted alveolar-arterial O ₂ difference.....	25
Figure 6A.	Raw data and gamma univariate fit for subject one during rest.....	29
Figure 6B.	Frequency distribution of transit times for data in Figure 6A.....	29
Figure 7A.	Raw data and gamma univariate fit for subject one during maximal exercise.....	30
Figure 7A.	Frequency distribution of transit times for data in Figure 7A.....	30
Figure 8.	PaO ₂ and [A-a]DO ₂ (o-p) versus transit time.	31
Figure 9.	Maximal expiratory flow volume loop with exercise and maximum voluntary ventilation manoeuvre	84
Figure 10.	The relationship between end capillary PO ₂ and mixed venous PO ₂ for lung units of differing \dot{V}_A/\dot{Q}	107

LIST OF ABBREVIATIONS AND SYMBOLS

(A-a)D	Inert gas alveolar arterial difference area
[A-a]DO ₂	Alveolar arterial difference for oxygen
(a-v)O ₂ diff	Arterio-venous difference for oxygen
DISP _{R*}	Index of dispersion for retention of MIGET gases
DISP _E	Index of dispersion for excretion of MIGET gases
DISP _{R*-E}	Overall index of dispersion
D _L CO	Diffusing capacity for carbon monoxide
E(A-a)D	Excretion component of inert gas alveolar arterial difference area
EIH	Exercise induced hypoxemia
FVC	Forced vital capacity
FEV ₁	Forced expiratory flow in 1 second
¹³¹ I	Iodine 131 a radioactive isotope of iodine
λ	Lambda – blood gas partition coefficient
Log SD \dot{Q}	Standard deviation of the log normal distribution for blood flow
Log SD \dot{V}	Standard deviation of the log normal distribution for ventilation
MEFV	Maximal expiratory flow volume
MIGET	Multiple inert gas elimination technique
MVV	Maximum voluntary ventilation
pH	Negative logarithm of hydrogen ion concentration
PaO ₂	Arterial partial pressure of oxygen
PAO ₂	Alveolar partial pressure of oxygen
Pa/P \bar{v}	Retention (R) of a MIGET gas defined as the ratio of arterial to mixed venous partial pressure
P _{bar}	barometric pressure
PE	partial pressure in expired gas
PE/P \bar{v}	Excretion (E) of a MIGET gas defined as the ratio of mixed expired to mixed venous partial pressure

P_{IO_2}	Partial pressure of inspired oxygen
$P_{\bar{v}}$	mixed venous partial pressure
$P_{\bar{v}O_2}$	Mixed venous partial pressure of oxygen
\dot{Q}	Cardiac output or blood flow
$R(A-a)D$	Retention component of inert gas alveolar arterial difference area
RER	Respiratory exchange ratio
SaO_2	Arterial oxygen saturation
SF_6	Sulfur hexafluorane
^{99m}Tc	Technetium 99 an meta stable radio-isotope of Technetium
\dot{V}_A/\dot{Q}	Ventilation-perfusion ratio
V_c	Pulmonary capillary blood volume
$\dot{V}CO_2$	Minute production of carbon dioxide
V_D	Dead space
$\dot{V}E$	Minute ventilation
$\dot{V}E/\dot{V}CO_2$	Ventilatory equivalent for carbon dioxide
$\dot{V}E/\dot{V}O_2$	Ventilatory equivalent for oxygen
$\dot{V}O_2$	Minute consumption of oxygen
V_T	Tidal volume

ACKNOWLEDGMENT

I would like to take this opportunity to thank everyone who helped in the preparation of this thesis:

Dr. Don McKenzie, my supervisor for his helpful advice, sense of humor, support and endless proof reading,

Dr. Tom Robertson, Dave Frazer, and Thien Tran, their help and patience in analyzing, programming, printing and interpreting mountains of MIGET data,

Dr. Brownie Schoene for his help in providing technical support, creative financing, accommodation and beer; Dr. Rob Glenny and Ron Saxon for their enthusiastic help in data collection,

Dr. Al Belzberg, and the technical staff at St. Paul's Hospital Nuclear Medicine for the excellent help with the nuclear medicine data,

Barry Wiggs, for his help with deconvolution,

My subjects who endured $\dot{V}O_2$ max tests, big needles, radiation and blizzards in the name of Science,

My committee members Peter Hochachka, Bob Schutz and Jeremy Road for their advice,

My parents, Bob and Barbara Hopkins for supporting me in the decision to return to school,

and Trevor Cooper, for providing a shoulder to cry on.

The financial assistance of the Medical Research Council of Canada, and the British Columbia Lung Association is also gratefully acknowledged.

INTRODUCTION

Dissecting the factors that limit maximal exercise performance has been a fundamental area of investigation in exercise physiology in both human and animals. Factors such as oxygen (O_2) transport and the circulatory system, peripheral blood flow, and O_2 diffusion and mitochondrial O_2 utilization have been discussed (39). The effects of endurance type physical training on the cardiovascular and musculoskeletal system are well known and include increases in cardiac output (\dot{Q}), stroke volume, arterio-venous [(a-v) O_2] difference, plasma volume and peripheral muscle blood flow (20) all of which contribute to the increase in maximal oxygen consumption ($\dot{V}O_{2max}$). Similarly, effects of training on the respiratory system have been documented and include: increased respiratory muscle enzyme activities (82, 113), and increased maximal voluntary ventilation (MVV) (150) maximal ventilation (51) maximal sustainable ventilation (47, 91) and flow velocities (16). In the gas exchanging portions of the lung however, development is complete in childhood (113) and a training effect (aside from blood volume or hemoglobin alterations) on gas exchanging areas is unlikely (10, 135). As a result, the lung has attracted attention as a potential constraint to maximal performance particularly at altitude (55, 74, 161, 177, 178) and in highly trained athletes (4, 34, 35, 72, 105, 127) where a supra-normal cardiovascular system may unmask the respiratory system's limited capacity to adapt.

Exercise induced hypoxemia (EIH) was first reported by Harrop (65) who made arterial blood gas measurements on patients with a variety of clinical problems as well as healthy normal subjects. Included in these measures were samples taken from a healthy Caucasian male who performed "fifteen minutes of brisk exercise consisting of arm and trunk movements and vigorous hopping about the room until quite dyspneic." He documented a decline in % saturation of arterial blood (SaO_2) from 95.6% at rest to 85.5% following exercise. Sporadic reports of impaired gas exchange during exercise followed (146, 159, 185) however the lung was not widely recognized as a potential limiting factor to exercise performance as the preponderance of evidence indicated that arterial oxygenation

was maintained during exercise (9, 17, 156). More recently, a number of authors (35, 72, 126, 127) have confirmed the findings of Harrop (65), Rowell (146), Thompson (159) and others, stimulating interest in this avenue of exploration.

Two causes of the decline in PaO_2 with exercise can be outlined, based on alveolar partial pressure of oxygen (PAO_2) and arterial partial pressure of oxygen (PaO_2). If PaO_2 is low and PAO_2 is also low (< 105 torr) this suggests inadequacy of ventilation either as a result of mechanical limitation of flow or as a result of blunted respiratory drives. If PaO_2 is low and PAO_2 is high (>110) resulting in very wide alveolar-arterial difference ($[\text{A-a}]\text{DO}_2$) this suggests an inadequacy of gas exchange either as a result of ventilation-perfusion (\dot{V}_A/\dot{Q}) mismatch or diffusion limitation. In fact, both of these situations have been described in the literature. Dempsey et al., (35) exercised sixteen subjects at 60-90% of $\dot{V}\text{O}_2\text{max}$ and reported PaO_2 of less than 60 torr associated with little or no alveolar hyperventilation. Administration of normoxic helium-oxygen mixtures improved PaO_2 only to the extent that PAO_2 was increased and it was concluded that the magnitude of the hyperventilatory response to exercise was a major determining factor of the hypoxemia observed. In contrast to this, Hopkins and McKenzie (72) found that alveolar PO_2 was high in their subjects who developed hypoxemia, with no evidence of inadequate ventilation. Both groups raised the possibility of impaired gas exchange as a possible explanation for some of the hypoxemia seen in their subjects.

As exercise intensity increases, cardiac output to the working muscles also increases, in some highly trained individuals to over $40 \text{ l}\cdot\text{min}^{-1}$ (43). The time that the red blood cell spends in the pulmonary vascular bed is directly related to flow and pulmonary capillary blood volume; as flow increases, expansion of the pulmonary vascular bed by dilation and recruitment (59) becomes of paramount importance in ensuring adequate time for equilibration of gas exchange. The average resting pulmonary capillary transit time has been estimated to be $\sim 0.75 \text{ s}$ (80, 144) falling to about 0.3 s during exercise. These represent mean capillary transit times as a whole, and it is possible that, given regional

differences in pulmonary transit (70), some red cells may travel too rapidly through the pulmonary vasculature resulting in arterial hypoxemia.

Transfer of a gas across the pulmonary blood gas barrier can be described by the equation (166) :

$$P_{\chi}(t) = P_{A\chi} + (P_{\bar{v}\chi} - P_{A\chi}) \cdot e^{-\left[\frac{100}{60} \cdot \frac{kA}{dV_c} \cdot \frac{\alpha_{\chi}}{\beta_{\chi} \sqrt{MW_{\chi}}} \right] t}$$

where P_{χ} is the partial pressure of gas χ , t is time, P_A and $P_{\bar{v}}$ are alveolar and mixed venous partial pressures of gas χ , k is the diffusion coefficient of gas χ , A is the cross-sectional area of diffusion, d is the thickness of the blood gas barrier, α_{χ} is the solubility of the gas χ in the blood gas barrier, β_{χ} is the solubility of gas χ in the blood and MW is the molecular weight of the gas χ . The effect of decreasing transit time can be seen by inspection of the above equation. All other factors being equal, as transit time decreases P_{χ} will fall as a function of e^{-t} , such that when $t=0$ the partial pressure is equal to the mixed venous partial pressure. In the exercising athlete, the time for equilibration of oxygen is further lengthened by low mixed venous PO_2 (34) and a right-ward shifted oxygen-hemoglobin equilibrium curve secondary to temperature increase, high mixed venous PCO_2 , and low pH, which in addition to possible rapid pulmonary transit may compromise gas exchange.

Two recent technological advances have made possible further detailed investigations into diffusion limitation and gas exchange in exercising athletes. The multiple inert gas elimination technique (MIGET) as it is currently in use, was developed by Wagner and co-workers (45, 167, 168) and is discussed in detail in Appendix B. It utilizes a multi-compartment model of pulmonary gas exchange calculated from data obtained from elimination of infused inert gases (usually six) based on the relationship:

$$\frac{P_{A\chi}}{P\bar{V}_\chi} = \frac{P_{c'\chi}}{P\bar{V}_\chi} = \frac{\lambda_\chi}{\lambda_\chi + \dot{V}_A/\dot{Q}}$$

where $P_{A\chi}$ is the alveolar partial pressure, $P\bar{V}_\chi$ is the mixed venous partial pressure, $P_{c'\chi}$ is the end capillary partial pressure and λ_χ is the blood gas partition coefficient of gas χ . Inert gases will approach equilibrium across the alveolus faster than oxygen, therefore if diffusion dis-equilibrium occurs, the observed [A-a]DO₂ will exceed that predicted from inert gas exchange and will be improved by administration of 100% oxygen. Post pulmonary shunt via the bronchial and thesbian veins will not affect inert gases as they are not metabolized, however administration of 100% O₂ will disproportionately increase the [A-a]DO₂ because it will increase alveolar PO₂ with less effect on arterial PO₂ as shunted blood bypasses the gas exchanging areas. These techniques thus allow the contributing factors to [A-a]DO₂ to be dissected.

Inert gas studies in normal subjects exercising at a $\dot{V}O_2$ of about 3.0 l·min⁻¹ (161) and in moderately trained individuals exercising at a $\dot{V}O_2$ of 4.0 l·min⁻¹ (63) have suggested diffusion limitation, secondary to rapid pulmonary transit, as a cause of impaired gas exchange. Right heart to left heart whole lung transit time can be measured using radioisotopically labeled RBC and a frequency distribution of pulmonary transit times can be calculated (70, 71, 96). The time required for an indicator to flow past an observation point down stream from an entry point is related not only to the time it take the bolus to flow past the point but also how quickly it arrived there. In this case the gamma camera provides the observational point to observe the bolus curve derived from labeled RBC traversing the right ventricle and the output curve derived from the left ventricle. Transit time is determined by subtracting the first moment of the right ventricular curve from the first moment of the left ventricular curve. Deconvolution is a mathematical process by which a frequency

distribution of transit times (a transfer function, $h(t)$) can be derived from the input (right ventricular) and output (left ventricular) time activity curves.

It was the purpose of this study to investigate pulmonary gas exchange and transit times during exercise in a population of highly trained male athletes exercising near $\dot{V}O_2$ max who on the basis of high pulmonary blood flow may develop shortened pulmonary transit and diffusion limitation.

METHODS

Baseline data

Sixteen non-smoking healthy male athletes with no prior history of respiratory or cardiac disease underwent preliminary studies. After giving informed consent, a history was obtained and a physical examination was performed, seeking evidence of cardio-pulmonary abnormality. All subjects were screened for pulmonary disease with pulmonary function tests consisting of forced expiratory volume in 1 second (FEV_1), forced vital capacity (FVC), peak flow rates, and 12 second maximum voluntary ventilation (MMV) using a Medical Graphic CAD/Net 2001 metabolic cart equipped with Medical Graphics 1070 pulmonary function testing software.

Maximal oxygen uptake was determined on an electronically braked cycle ergometer (Minjardt KEM-3) equipped with a racing saddle and pedals. After a 10 minute warm-up (75-100 watts), the subjects rode a progressive exercise test with the work intensity ramped at $30 \text{ watt}\cdot\text{min}^{-1}$ until they were unable to continue. Minute ventilation (\dot{V}_E), oxygen consumption ($\dot{V}O_2$) and carbon dioxide production ($\dot{V}CO_2$) were measured on a breath-by-breath basis and tabulated every 15 seconds with a Medical Graphics CAD/Net 2001 Metabolic Cart equipped with Medical Graphics 2001 software. Heart rate was monitored and recorded by cardiac monitor (Lifepak 6) interfaced with the metabolic cart. $\dot{V}O_2$ max was considered to be the average of the four highest consecutive 15 second measures of oxygen uptake. These results were used to calculate a work-load which represented greater than 90% of $\dot{V}O_2$ max. Subjects were excluded from further testing unless their $\dot{V}O_2$ max was greater than $5.0 \text{ l}\cdot\text{min}^{-1}$ or $60 \text{ ml}\cdot\text{kg}^{-1}\cdot\text{min}^{-1}$. On a separate occasion single breath carbon monoxide diffusing capacity (D_LCO) was obtained at the UBC Hospital Pulmonary Laboratory (7).

Ten subjects fulfilling the entry criteria were transported the following week to the Cardio-Pulmonary Laboratory at the Harborview Medical Center (Seattle Wa.).

Subject Preparation

Prior to the exercise test, an indwelling arterial cannula (Arrow # 20 gauge) was inserted in the right radial artery. Cannula patency was maintained by frequent flushing with normal saline to which heparin sodium ($2000 \text{ u}\cdot\text{l}^{-1}$) had been added. Under sterile technique, and cardiac monitoring, a number 7.5F triple lumen Swan-Ganz catheter (for temperature monitoring) was introduced into the venous circulation via the left antecubital vein and positioned in the region of the superior vena cava. Cannula patency was maintained as described for the arterial cannula. A second venous line (#18 gauge) was inserted via the right antecubital vein into the peripheral venous circulation for infusion of the inert gases. The subjects were instructed to discontinue if any unusual symptoms developed. At least three physicians were present at all times during the exercise testing one of whom had primary responsibility for the subject. EKG tracing (lead II) was monitored continuously.

Test protocol

Subjects were seated on the bicycle ergometer previously described and connected to a respiratory circuit. This consisted of a Rudolph (2700) valve connected by large diameter heated tubing to a heated 13 l Plexiglas mixing chamber which in turn was connected to a pneumotach. Breath by breath analysis of $\dot{V}O_2$ and $\dot{V}CO_2$ was obtained by a Medical Graphics 2000 system equipped with 2001 software similar to the system previously described for $\dot{V}O_2$ max testing. After a ten minute rest period to allow stabilization of ventilatory data the testing protocol was started. Arterial blood gases, $\dot{V}E$, $\dot{V}O_2$, $\dot{V}CO_2$, heart rate were obtained at rest and every minute at each of the exercise levels. The exercise levels consisted of five minutes each of light (150w, mean $\dot{V}O_2 = 42\%$ of $\dot{V}O_2$ max), heavy (300w, mean $\dot{V}O_2 = 86\%$ of $\dot{V}O_2$ max) and near maximal exercise ($>90\%$ $\dot{V}O_2$ max, mean power output = 371 ± 30 watts). Mixed expired gases and arterial blood samples

for inert gas analysis were collected at rest and during the last minute at each exercise level. The subjects rested approximately 5 minutes between each exercise level to allow recalibration of the instruments.

Multiple inert gas analysis

Six inert gases (SF₆, ethane, cyclopropane, halothane, ether and acetone) dissolved in 5% dextrose (55, 63, 167, 168, 180) were infused starting 20 min before the start of the experiment, at a rate in ml·min⁻¹ corresponding to one quarter of the expected \dot{V}_E in l·min⁻¹ (range 5 - 50 ml·min⁻¹). Duplicate arterial (8 ml) and expired gas (30 ml) samples were collected in pre-heparinized glass syringes during the last minute at each exercise level and analyzed by gas chromatography. The time delay between arterial and expired samples due to the hoses and mixing chamber was calculated by dividing the mixing chamber volume by the \dot{V}_E and the time of collection of the expired gas sample was adjusted accordingly. Mixed venous inert gas concentrations were calculated from the Fick equation. Retention ($P_a/P_{\bar{v}}$) and excretion ($P_E/P_{\bar{v}}$) values were used to estimate \dot{V}_A/\dot{Q} and standard deviation of the log normal distribution of perfusion (LogSD \dot{Q}) and ventilation (LogSD \dot{V}) distribution were used as an index of \dot{V}_A/\dot{Q} inequality (168). Retention (R(A-a)D) and excretion (E(A-a)D) components of the inert gas alveolar-arterial difference area ([A-a]D) were also derived directly from the inert gas data (42, 69). Three additional indices were derived directly from the data as described by Gale et al., (53). $DISP_{R^*}$ analogous to log SD \dot{Q} and R(A-a)D, $DISP_E$ analogous to log SD \dot{V} and E(A-a)D, and $DISP_{R^*-E}$ analogous to (A-a)D were calculated as follows:

$$DISP_{R^*-E} = 100 \times \sqrt{\frac{\sum_{i=1}^n (R_i - E_i^*)^2}{n}}$$

$$\text{DISP}_{R^*} = 100 \times \sqrt{\frac{\sum_{i=1}^n (\text{R}_i - \text{R}_{\text{homoi}}^*)^2}{n}}$$

$$\text{DISP}_E = 100 \times \sqrt{\frac{\sum_{i=1}^n (\text{E}_{\text{homoi}}^* - \text{E}_i^*)^2}{n}}$$

where

$$\text{E}_{\text{homoi}} = \text{R}_{\text{homoi}} = \frac{\lambda_i}{\lambda_i + \frac{\dot{V}_A}{\dot{Q}_T}}$$

n is the number of gases, E_i and R_i represent excretions and retentions of the gas of interest and E_i^* is excretion corrected for dead space:

$$E_i^* = \frac{E_i}{1 - \frac{V_D}{V_T}}$$

Predicted values for PaO_2 , PaCO_2 and $[\text{A-a}]\text{DO}_2$, ($[\text{A-a}]\text{DO}_2(\text{p})$) based on the derived \dot{V}_A/\dot{Q} distribution were then calculated (174, 180). These values, calculated from inert gas data, reflect only that predicted by intra-pulmonary shunt and ventilation perfusion inequality, therefore an indirect estimate of diffusion impairment $[\text{A-a}]\text{DO}_2(\text{o-p})$, is possible. It should be noted that the inert gas analysis assumes steady state and the absence of post-pulmonary shunt.

Arterial blood gases

The arterial samples were anaerobically collected in pre-heparinized glass syringes and were maintained in ice until the test session was complete. Each 2 ml sample was analyzed for pH, PaO_2 and PaCO_2 using a Corning Blood Gas/ pH Analyzer, which is calibrated daily and after each exercise test against a known standard. Resting samples and the last sample drawn had hemoglobin and hematocrit determined. Using Kelman's routines

(85-87) SaO_2 , PaO_2 and PaCO_2 were also corrected for arterial blood temperature measured at the superior vena cava via the Swan-Ganz catheter.

Cardiac output

One to two weeks later in the Department of Nuclear Medicine at St. Paul's Hospital cardiac output was measured at each exercise intensity using a combination of first pass and gated radiocardiography. Right ventricle to left ventricle first pass transit time was also measured during rest and near maximal exercise. Plasma volume was measured using ^{131}I labeled albumin (RISA) (76).

Ten ml of whole blood was withdrawn from the subject into a pre-heparinized syringe via an antecubital vein. The blood was labeled with $^{99\text{-m}}\text{Tc}$ ($^{99\text{-m}}\text{Tc}$) using a standard commercial red blood cell (RBC) labeling kit (152) (Brookhaven National Laboratories, Upton, N.Y.). A 5-10ml aliquot of RBC injectate containing 10-20 mCi of activity was obtained. A 20 gauge plastic cannula was inserted in the right median basilic vein and maintained patent with normal saline. The subjects were seated on the bicycle ergometer previously described in front of a Siemens ZLC 3700 gamma camera with a wide field of view, medium energy columnator. The subjects were studied in the left anterior oblique position by placing the ergometer at angle to the camera and having the subject lean forward placing his chest directly in contact with the camera and grasping the camera with the left hand. In all cases, except for one at near maximal exercise, the images obtained were of excellent technical quality and allowed good separation of the right and left ventricle. Heart rate was recorded using a Lifepak 6 monitor/defibrillator.

After stabilization of heart rate to the level observed during resting level of the inert gas experiments, one half the labeled RBC were injected into the dead space of the plastic cannula and flushed into the venous circulation with a rapid bolus of 15 ml of normal saline. Data were acquired and processed on an ADAC 3003 computer (ADAC Laboratories, Sunnyvale, Ca) at $0.5 \text{ frames}\cdot\text{second}^{-1}$ during the first pass through the

central circulation. Without changing the position of the camera a 2 minute static image was obtained after the bolus injection. In the static projection, a large region of interest was drawn over the left ventricle using the light-pen and applied to the dynamic view. A first pass time activity curve and static or equilibrium counts were obtained. Cardiac output (\dot{Q}) was calculated from the Stewart Hamilton equation:

$$\dot{Q} = C_{eq} \cdot \frac{TBV}{\int C(t) dt}$$

where C_{eq} represents the static counts from the left ventricle region of interest, TBV is blood volume (from measured plasma volume and hematocrit) and $\int C(t) dt$ is the area under the left ventricle first pass curve. The upstroke and down stroke of this curve are extrapolated to zero to exclude counts from the right ventricle and recirculation of blood.

The remainder of RBC were then administered and the gated studies were conducted. Using the same experimental setup as described above, count data was obtained at a framing rate of 16 frames per R-R interval of the EKG and stored on the hard disk in a 64x64 pixel matrix. Data were acquired for two minutes, after the third minute of each exercise level. Gated ventricular imaging was conducted at rest, 150 watts and 300 watts. Each of the 16 images acquired was then displayed and the left ventricular region of interest was manually drawn using a light-pen. A background region of interest was drawn laterally and inferiorly to the left ventricle. Left ventricular ejection fraction was then calculated from the difference between background subtracted end-diastolic and end-systolic counts and expressed as a percentage of end-diastolic counts.

Two, 5 ml samples of blood were drawn at the end of each exercise period and imaged in petri dishes for five minutes. The average background subtracted count rate for 5 ml of blood was thus obtained. The left ventricular count rate at each exercise level was corrected for loss by decay of ^{99m}Tc using standard tables and the left ventricular end-diastolic volume was obtained by dividing the left ventricular count rate by the 5 ml count rate; cardiac output was then obtained by multiplying by the ejection fraction and the

average heart rate during data acquisition. Correction for attenuation of counts by the chest wall for the gated studies was made by comparing the first pass cardiac output at rest with the result obtained from the resting gated study, and the results obtained during the gated studies at 150 and 300w were adjusted accordingly. Of the 40 gated determinations of cardiac output and cardiac volumes, 7 were lost for technical reasons. For the purpose of MIGET calculations, \dot{Q} was calculated from a linear regression of \dot{Q} vs $\dot{V}O_2$ for the remaining subjects. On a separate occasion, at least a week apart to minimize the effect of residual radioactivity, the first pass study was repeated at the near maximal exercise level.

Pulmonary transit time

Right ventricle to left ventricle RBC pulmonary transit times were calculated from the first pass time-activity curves (70, 96). In the static image, large regions of interest were drawn with the light pen outlining the right and left ventricle. These regions of interest were then applied to the dynamic images and time activity curves were obtained. In a similar fashion, the quality of the bolus injection was checked by drawing a region of interest in the superior vena cava. The numerical data thus obtained was then down loaded directly into a Zenith 386 PC for further processing. Each time-activity curve was fitted using linear least squares to a gamma (γ) function using the method of Starmer and Clark (153) programmed into a Lotus 123 spread sheet. The transit time across the lungs was then obtained by subtracting the first moment of the right ventricular time-activity curve from that of the left ventricle (96). To confirm these results and obtain a frequency distribution of transit times (also known as a transfer function) deconvolution analysis was applied to the gamma fitted curves. This was done using Gauss 386 statistical software. The area underneath both the input (right ventricular) curve and the output (left ventricular) curve was set equal to 1. A series of fifty transfer functions was then generated with a mean transit time equal to that obtained by the subtraction of first moments, and a variance ranging from that of the input curve to that of the output curve. The transfer functions were then convoluted with the input

curve and ridge regression was applied to determine contribution of each output curve derived by this process to the final output curve. This process was repeated with slight alterations in the variance and mean transit times of the transfer functions until a satisfactory visual fit was obtained. Pulmonary blood volume was calculated by dividing the cardiac output in $\text{ml}\cdot\text{second}^{-1}$ by the transit time.

Data analysis

Data were analyzed using analysis of variance for repeated measures to determine differences in blood gas, cardiac output, stroke volume, indices of dispersion and metabolic data between the rest, 150w, 300w, and near maximal exercise conditions. A similar analysis was used to determine differences in end systolic volume, end diastolic volume and ejection fraction between rest, 150w and 300w. Where overall significance was obtained, Scheffe's testing was applied post-hoc to determine where these differences occurred. Student's t test was used to evaluate changes in pulmonary transit time and pulmonary blood volume between rest and maximal exercise. Linear regression was used to determine the relationship between $[A-a]DO_2(o-p)$ during maximal exercise and pulmonary transit time, and between blood volumes and PaO_2 and $[A-a]DO_2(o)$. Multiple linear regression was used to examine the relationships between $\dot{V}E/\dot{V}CO_2$, PTT, $(A-a)D$, and PaO_2 .

RESULTS

General data

Subject descriptive information is given in Table 1. The high levels attained for $\dot{V}O_2$ max indicate that the subjects were highly trained males. Blood volume indices from measured plasma volume and hematocrit are given in Table 2. The subjects exhibited above normal values for plasma volume and red cell mass. Plasma volume was as high as 159% of predicted based on norms calculated from the subjects height, weight and age. Mean hematocrit was at the low end of the normal range however calculated red cell mass was also more than 130% of predicted. In all cases plasma and red cell volumes were outside the upper limit of the normal range. Mean hematocrit for the subjects was 42.6% pre-exercise and increased to 44.2% post exercise. This change was statistically significant ($t=1.98$, $p<0.05$)

Table 1. Subject descriptive data

	Age (years)	Height (cm)	Weight (kg)	$\dot{V}O_2$ max (l·min ⁻¹)	FVC (l)	FEV ₁ (l)	$\dot{V}E$ max (l·min ⁻¹)	MVV (l·min ⁻¹)	D _L CO (ml·min ⁻¹ ·mm Hg ⁻¹)
1	31	188.5	89.7	6.31	7.02	6.73	218.5	230	44.70
2	28	180.7	67.5	4.37	5.52	4.62	186.1	198	41.99
3	23	193.5	79.5	5.07	6.73	6.37	240.2	257	44.98
4	30	181.5	81.0	5.17	5.34	4.68	201.0	223	42.94
5	20	188.4	82.3	5.12	6.47	5.26	211.5	219	49.74
6	25	185.2	76.5	5.36	7.07	6.10	199.4	241	49.90
7	19	183.5	68.5	4.91	6.05	5.16	209.2	204	43.47
8	28	185.1	77.2	4.81	5.94	5.17	212.1	178	*
9	29	176.5	68.2	4.84	5.49	4.84	186.2	194	34.19
10	31	192.5	92.0	5.57	6.02	4.91	201.6	208	43.04
Mean	26.4	185.5	78.2	5.15	6.17	5.38	206.6	215.2	43.88
± SD	4.4	5.3	8.6	0.52	0.63	0.75	16.3	23.6	4.63

*Subject failed to complete this portion of the testing

Table 2. Plasma volume and calculated whole blood volume - individual subject data.

	Whole Blood Vol.(ml)	ml·kg ⁻¹	% Predicted	Plasma Vol.(ml)	ml·kg ⁻¹	% Predicted	RBC Vol. (ml)	% Predicted
1	8075	90.0	152	5140	57.3	161	2934	137
2	5720	84.7	130	3621	53.6	136	2100	121
3	6959	87.5	134	4231	53.2	134	2727	133
4	6142	75.8	127	3859	47.6	133	2283	117
5	7467	90.7	145	4912	59.7	159	2556	125
6	6802	88.9	140	4249	55.5	145	2553	133
7	6759	98.7	145	4359	63.6	157	2400	135
8	6757	87.5	139	3848	49.8	131	2906	151
9	5643	82.7	130	3499	51.3	133	2144	125
10	8126	88.3	144	5143	55.9	153	2983	131
Mean	6845	87.5	139	4286	54.8	144	2559	131
±SD	868	5.9	8	606	4.7	12	325	10

Ventilation and metabolic data

Respiratory and metabolic data are given in Table 3. Statistical information in brackets refers to Scheffe's F test unless otherwise stated. Mean blood temperature measured at the superior vena cava was 36.8 ± 0.5 °C at rest and rose significantly at each exercise level to 38.0 ± 0.7 °C at the end of the heaviest exercise task (omnibus $F_{(3,27)}=24.3$ $P < 0.001$). $\dot{V}E$ increased from 13.4 ± 2.6 l·min⁻¹ at rest to 178.1 ± 16.3 l·min⁻¹ at the end of maximal exercise, and was significantly less than peak values (mean= 206.6 l·min⁻¹) reached during the initial $\dot{V}O_2$ max test ($t=5.76$, $p<0.001$). $\dot{V}O_2$ increased from 0.41 ± 0.09 l·min⁻¹ at rest to 2.16 ± 0.17 l·min⁻¹, 4.32 ± 0.35 l·min⁻¹, and 5.13 ± 0.50 l·min⁻¹ at light (150 watts), heavy (300 watts) and maximal exercise respectively. $\dot{V}CO_2$ at the corresponding exercise levels was 0.36 ± 0.10 l·min⁻¹, 1.85 ± 0.11 l·min⁻¹, 4.39 ± 0.35 l·min⁻¹ and 5.97 ± 0.68 l·min⁻¹. The respiratory exchange ratio (RER) was not significantly different between rest and light exercise (0.88 ± 0.11 rest vs 0.86 ± 0.05 light exercise $F=0.06$, $p=NS$); however it increased significantly from light to heavy exercise ($F=7.74$, $p<0.05$) to 1.02 ± 0.11 during heavy exercise indicating that the subjects were close to their

anaerobic threshold during this workload. During maximal exercise RER increased significantly from heavy exercise ($F=6.50$, $p<0.05$) to 1.17 ± 0.08 . The ventilatory equivalent for carbon dioxide ($\dot{V}E/\dot{V}CO_2$) decreased significantly from rest to light exercise ($F=20.5$, $p<0.05$), then increased slightly from light to heavy exercise and from heavy to maximal exercise, although $\dot{V}E/\dot{V}CO_2$ at max was significantly less than resting values ($F=7.6$, $p<0.05$). The ventilatory equivalent for oxygen ($\dot{V}E/\dot{V}O_2$) also decreased significantly from rest to light exercise ($F=18.2$, $p<0.05$) and increased from light to heavy exercise ($F=5.08$, $p<0.05$) and from heavy to maximal exercise ($F=6.26$, $p<0.05$). $\dot{V}E/\dot{V}O_2$ at rest was not significantly different from maximal exercise ($F=0.25$, $p=NS$). There were modest correlations between $\dot{V}E/\dot{V}CO_2$ and PaO_2 during heavy and maximal exercise ($r=0.43$ and $r=0.53$ respectively) for these 10 subjects but they were not statistically significant. There was a similar correlation between $\dot{V}E/\dot{V}O_2$ and PaO_2 during heavy exercise ($r=0.40$), again not statistically significant.

Arterial blood gases and oxygen saturation

Group mean blood gas values are given in Table 3 and individual subject data for PaO_2 , $PaCO_2$ and $[A-a]DO_2(o)$ during light, heavy and maximal exercise are given in Figures 1, 2 and 3. Mean PaO_2 was 98 ± 6 torr at rest and decreased significantly ($F=36.3$, $p<0.05$) to 91 ± 8 torr during light exercise. PaO_2 declined further to 86 ± 9 torr during heavy exercise ($F=12.8$ compared to rest, $p<0.05$) and increased to near resting levels (94 ± 8 torr) at the end of maximal exercise. Alveolar arterial difference did not increase significantly from rest to light exercise ($F=0.29$, $p=NS$); however the increase in $[A-a]DO_2(o)$ from light to heavy exercise was significant ($F=27.5$, $P<0.05$). There was no further increase in $[A-a]DO_2(o)$ between heavy and maximal exercise ($F=0.14$, $p=NS$); therefore any improvement in PaO_2 was due to improved alveolar PO_2 . There was little evidence of hypoventilation at the end of maximal exercise as mean PAO_2 calculated by the alveolar gas equation was 121 ± 3 torr. $PaCO_2$ was slightly depressed during the rest measurements

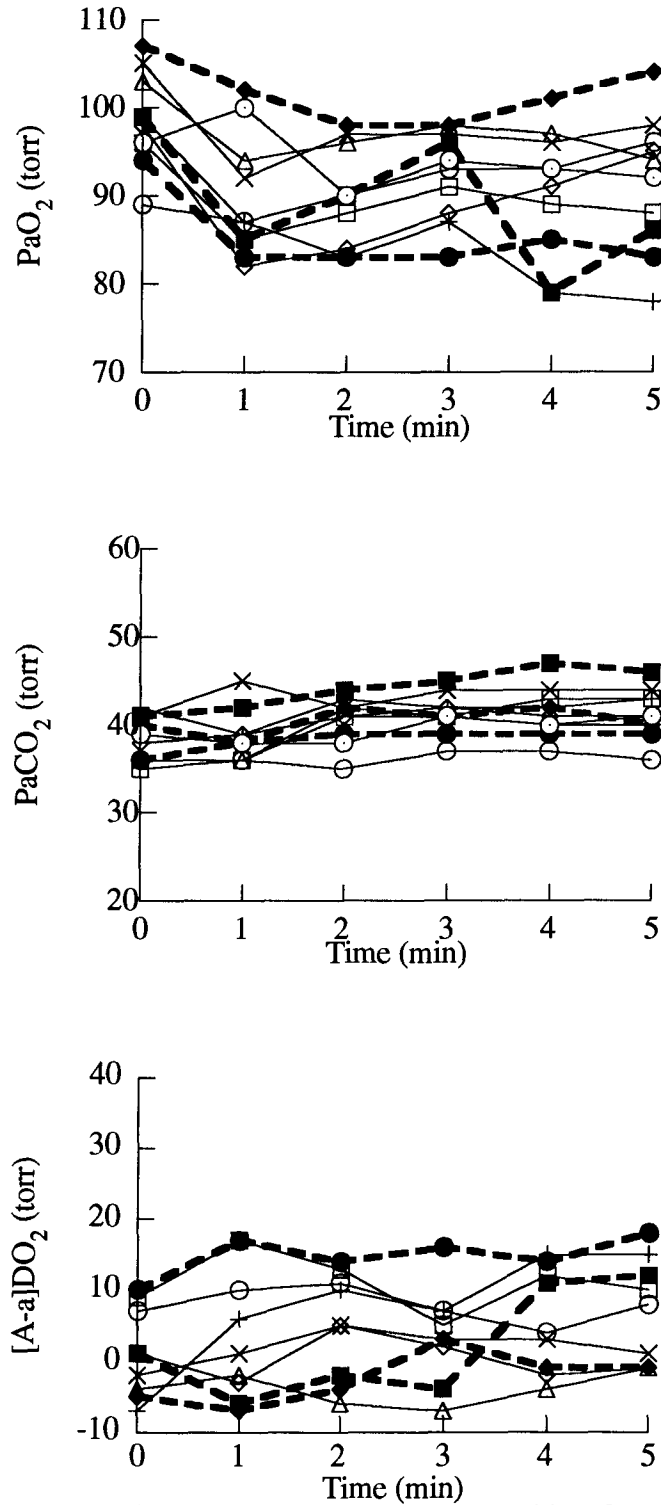
(38 ± 3 torr), likely indicating some anxiety on the part of our subjects; it then rose to more normal levels during light exercise, before decreasing significantly during heavy and maximal exercise ($F=8.4, p<0.05$ and $F=6.5, p<0.05$ for heavy and maximal exercise vs rest). Blood pH did not change significantly from rest to light exercise, but decreased significantly from light to heavy exercise ($F=7.94, p<0.05$) and from heavy to maximal exercise ($F=15.0, p<0.05$). SaO_2 decreased significantly over the exercise levels (omnibus $F_{(3,27)}= 18.5, p<0.0001$) to a mean of $94.2 \pm 2.3\%$.

There was considerable inter-subject variability in the blood gas response over the five minute exercise period at each exercise intensity (see Figures 1, 2 and 3). For example, subject six maintained PaO_2 above 98 torr during heavy exercise and above 105 torr during maximal exercise. Corresponding $[A-a]DO_2(o)$ was less than 11 torr throughout testing and PAO_2 was above 110 torr at the end of heavy exercise and 115 torr at the end of maximal exercise, confirming adequate ventilation and gas exchange. In contrast to this, subject 4 developed hypoxemia ($PaO_2 = 74$ torr) during heavy exercise associated with an $[A-a]DO_2(o)$ of 38 torr. At maximal exercise the PaO_2 increased to 81 torr as a result of increasing PAO_2 (123 torr) and $[A-a]DO_2(o)$ widened further to 42 torr. Subject 5, also demonstrated hypoxemia during heavy exercise with PaO_2 at the end of exercise of 74 torr, however there is also evidence of hypoventilation, as $PaCO_2$ was elevated above resting levels and PAO_2 was 102 torr.

Table 3. Arterial blood gases, metabolic data, transit times and MIGET summary data at rest, light, heavy and maximal exercise ($\bar{x}\pm SD$)

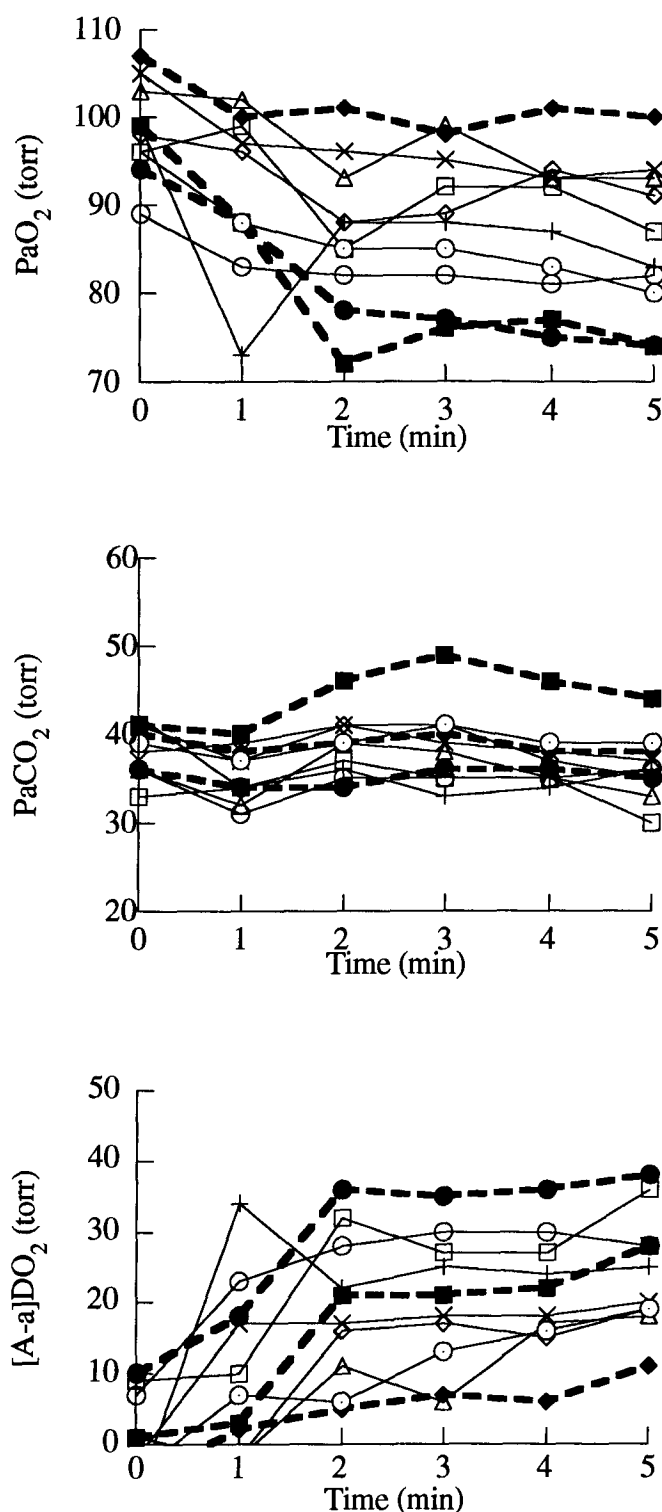
	Rest	Light Exercise (150 watts)	Heavy Exercise (300 watts)	Maximal Exercise (371±30 watts)
Heart Rate	70±10	116±9	156±8	166±8
\dot{Q} (l·min ⁻¹)	6.9±0.9	16.1±1.5	25.3±2.5	33.3±3.7
$\dot{V}E$ (l·min ⁻¹)	13.4±2.6	45.5±3.5	119.3±27.3	178.1±16.3
$\dot{V}E/\dot{V}O_2$	33.5±6.2	21.2±1.5	27.6±6.5	34.9±3.8
$\dot{V}E/\dot{V}CO_2$	38.5±6.8	24.6±1.6	27.1±5.3	30.0±2.8
$\dot{V}O_2$ (l·min ⁻¹)	0.41±0.09	2.16±0.17	4.32±0.35	5.13±0.50
$\dot{V}CO_2$ (l·min ⁻¹)	0.36±0.1	1.85±0.11	4.39±0.35	5.97±0.68
RER	0.88±0.11	0.86±0.05	1.02±0.11	1.17±0.08
PAO ₂ (torr)	102±8	98±5	111±6	121±3
PaO ₂ (torr)	98±6	91±8	86±9	94±8
SaO ₂ (%)	97.6±0.4	96.7±0.9	95.3±1.8	94.2±2.3
[A-a]DO ₂ (o) (torr)	4±16	6±8	26±9	27±9
[A-a]DO ₂ (p) (torr)	7±8	10±4	17±7	17±3
[A-a]DO ₂ (o-p) (torr)	-3±15	-4±9	9±13	10±12
PaCO ₂ (torr)	38±3	41±3	36±4	32±3
pH	7.44±0.03	7.41±0.03	7.34±0.05	7.24±0.06
Log SD \dot{V}	1.09±0.55	0.90±0.47	1.09±0.29	1.18±0.14
Log SD \dot{Q}	0.38±0.20	0.44±0.12	0.64±0.17	0.78±0.11
DISP _{R*}	2.527±2.129	2.827±2.092	4.631±2.291	5.733±1.332
DISP _E	3.881±3.070	3.918±3.015	5.549±2.712	5.459±1.034
DISP _{R*-E}	5.408±4.466	6.090±4.653	9.343±4.509	10.385±2.124
Transit time (sec)	9.32±1.41			2.91±0.30
Pulmonary blood volume (l)	1.08±0.17			1.61±0.27

Figure 1. PaO₂, PaCO₂ and [A-a]DO₂(o) for individual subjects during light exercise.



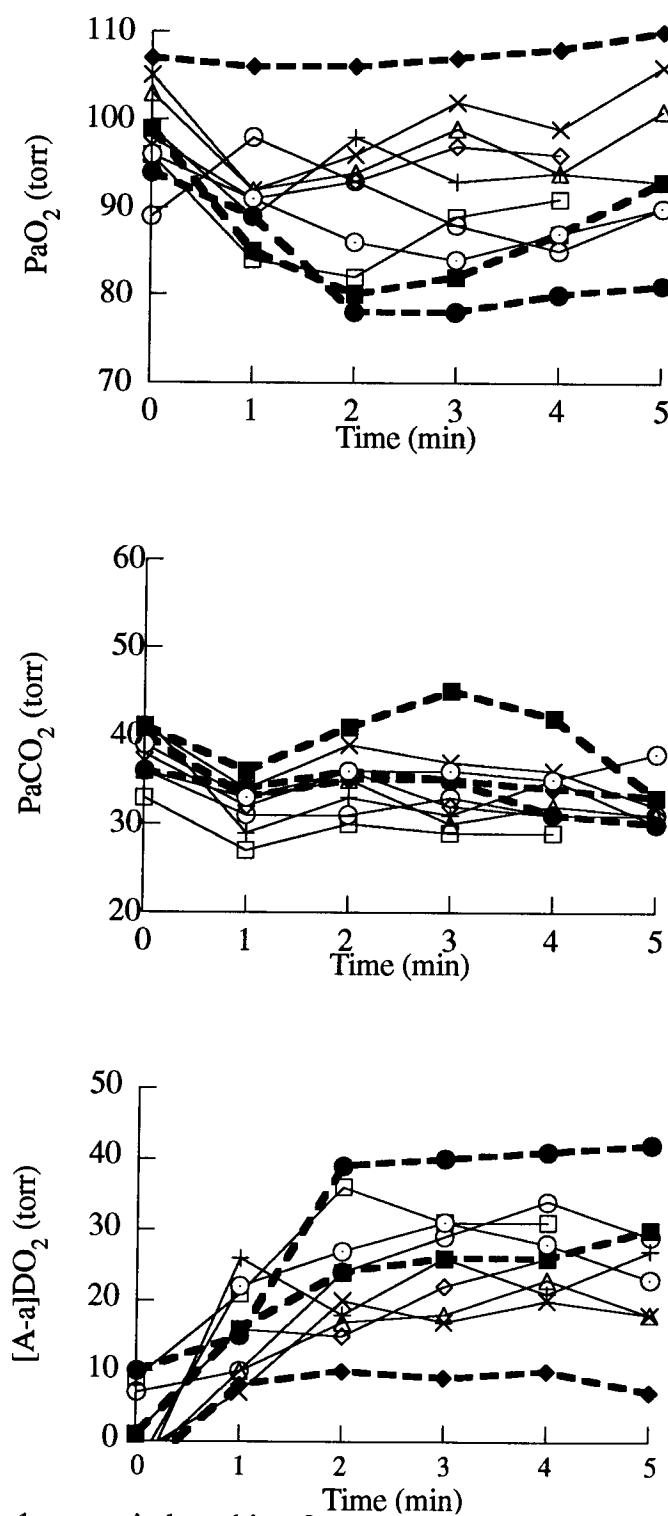
Legend: subject 1=open circle, subject 2=open square, subject 3=open diamond, subject 4=closed circle, subject 5=closed square, subject 6=closed diamond, subject 7=diagonal cross, subject 8=horizontal cross, subject 9=open triangle, subject 10=open circle with dot.

Figure 2. PaO₂, PaCO₂ and [A-a]DO₂(o) for individual subjects during heavy exercise.



Legend: subject 1=open circle, subject 2=open square, subject 3=open diamond, subject 4=closed circle, subject 5=closed square, subject 6=closed diamond, subject 7=diagonal cross, subject 8=horizontal cross, subject 9=open triangle, subject 10=open circle with dot.

Figure 3. PaO₂, PaCO₂ and [A-a]DO₂(o) during maximal exercise.



Legend: subject 1=open circle, subject 2=open square, subject 3=open diamond, subject 4=closed circle, subject 5=closed square, subject 6=closed diamond, subject 7=diagonal cross, subject 8=horizontal cross, subject 9=open triangle, subject 10=open circle with dot.

Mixed venous PO_2 ($P\bar{v}O_2$) and arterio-venous difference ($a-\bar{v}O_2$ diff) were calculated from the Fick equation and are given in Table 4. Mean $P\bar{v}O_2$ was 36 ± 4 torr at rest and decreased significantly ($F=17.9$, $P<0.05$) during light exercise. A further decrease between light and heavy exercise was not statistically significant ($F=2.49$, $p>0.05$), nor was the slight increase from heavy to maximal exercise (\bar{x} $P\bar{v}O_2 = 15\pm 6$ torr heavy exercise vs 17 ± 7 torr maximal exercise). The $a-\bar{v}O_2$ diff increased between rest and light exercise ($F=3.98$, $p<0.05$), was the same for light and heavy exercise (71 ± 7 and 71 ± 9 torr respectively) and increased further ($F=1.69$, $p>0.05$) during heavy exercise to a maximum value of 77 ± 11 torr.

Table 4. Calculated mixed venous and arterio-venous O_2 difference during rest, light, heavy and maximal exercise.

Subject	Rest		150 watts		300 watts		Maximal	
	$P\bar{v}O_2$ (torr)	(a-v) O_2 (torr)						
1	30	59	19	77	14	68	11	77
2	40	48	21	67	24	63	19	72
3	31	67	17	78	20	71	29	68
4	36	58	19	64	13	61	19	62
5	34	65	24	62	13	61	25	65
6	43	64	24	80	18	82	12	97
7	32	73	22	76	17	77	19	83
8	40	59	18	60	14	69	15	78
9	35	68	22	72	5	88	11	86
10	35	61	17	75	8	72	7	82
$\bar{x}\pm$ SD.	36 ± 4	62 ± 7	20 ± 3	71 ± 7	15 ± 6	71 ± 9	17 ± 7	77 ± 11

$P\bar{v}O_2$ = mixed venous partial pressure of oxygen, [(a-v) O_2] = arterio-venous difference for oxygen.

\dot{V}_A/\dot{Q} inequality

Considerable difficulty was experienced in fitting the data from the present study to the MIGET model of Wagner et al., (168) as evidenced by high residual sum of squares at

rest. There was a significant improvement in the residual sum of squares during heavy and maximal exercise when compared to rest ($F=3.3$, and $F=3.5$, $p<0.05$) and an acceptable fit was achieved in the maximal exercise data. The mean of the log normal perfusion (mean of \dot{Q}) distribution increased significantly over the exercise levels (omnibus $F_{(3,27)}=45.6$, $p<0.001$) as did the mean of the log normal ventilation distribution (mean of \dot{V}) (omnibus $F_{(3,27)}=61.2$, $p<0.0001$). There was a non significant increase in the \dot{V}_A/\dot{Q} heterogeneity, as measured by log $SD\dot{Q}$ from rest to light exercise; however the increase from light to heavy exercise and from heavy to maximal exercise was significant ($F=6.6$, $p<0.05$ and $F=3.14$, $p<0.05$). There was no significant change in the log $SD\dot{V}$ over the exercise levels (omnibus $F_{(3,27)}=1.35$, $P>0.05$).

Elimination of SF_6 data from the analysis resulted in low residual sums of squares (4.27 ± 2.7 at rest, which increased to a maximum value of 12.2 ± 11.1 at max exercise) indicating adequate model fit. The results of the statistical analyses for the mean \dot{Q} , mean \dot{V} and log $SD\dot{V}$ were unchanged when the SF_6 data were eliminated, however no statistically significant change in log $SD\dot{Q}$ was found with exercise (omnibus $F_{(3,27)}=1.12$).

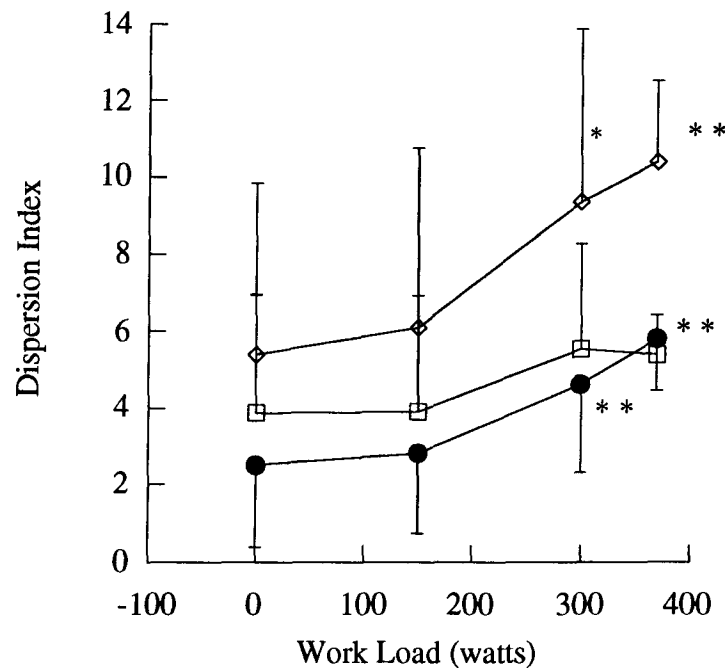
The independent indices of \dot{V}_A/\dot{Q} mismatch $DISP_{R^*}$, $DISP_E$ and $DISP_{R^*-E}$ are presented in Figure 4. There was a significant increase in dispersion as measured by two of the three indices. There was a highly significant increase in $DISP_{R^*}$ across exercise levels (omnibus $F_{(3,27)}=25.8$, $p<0.0001$), as was the increase in $DISP_{R^*-E}$ ($F_{(3,27)}=8.45$, $p<0.001$). The increase in $DISP_E$ was not significant ($F_{(3,27)}=2.45$, $p=0.09$). The area under the curve described by the plot of alveolar arterial difference for the six inert gases as a function of λ , $(A-a)D$ and the retention and excretion components of the area $R(A-a)D$ and $E(A-a)D$ are given in Table 5. $DISP_{R^*}$, $R(A-a)D$ and log $SD\dot{Q}$ are all measures of the perfusion distribution and therefore should be comparable. Similarly $DISP_E$, $E[A-a]$ and log $SD\dot{V}$, are comparable measures of the ventilation distribution and $DISP_{R^*-E}$ and $(A-a)D$ are comparable overall indices of dispersion.

Table 5. (A-a)D, R(A-a)D and E(A-a)D at rest and during light, heavy and maximal exercise ($\bar{x} \pm SD$).

	Rest	150 Watts	300 Watts	Maximal Exercise
(A-a)D	0.211±0.171	0.233±0.185	0.360±0.178	0.411±0.098
R(A-a)D	0.066±0.060	0.088±0.066	0.146±0.073	0.181±0.043
E(A-a)D	0.259±0.341	0.161±0.139	0.201±0.088	0.231±0.047

There was a significant increase in (A-a)D and R(A-a)D over the exercise levels (omnibus $F_{(3,27)}=9.1, p<0.001$ and omnibus $F_{(3,27)}=21.0, p<0.0001$) paralleling the increases in the corresponding parameters of the other methods of analysis. There was no significant change in E(A-a)D over the exercise levels (omnibus $F_{(3,27)}=1.7, p=0.64$).

Figure 4. Dispersion indices at rest and during light, heavy and maximal exercise.

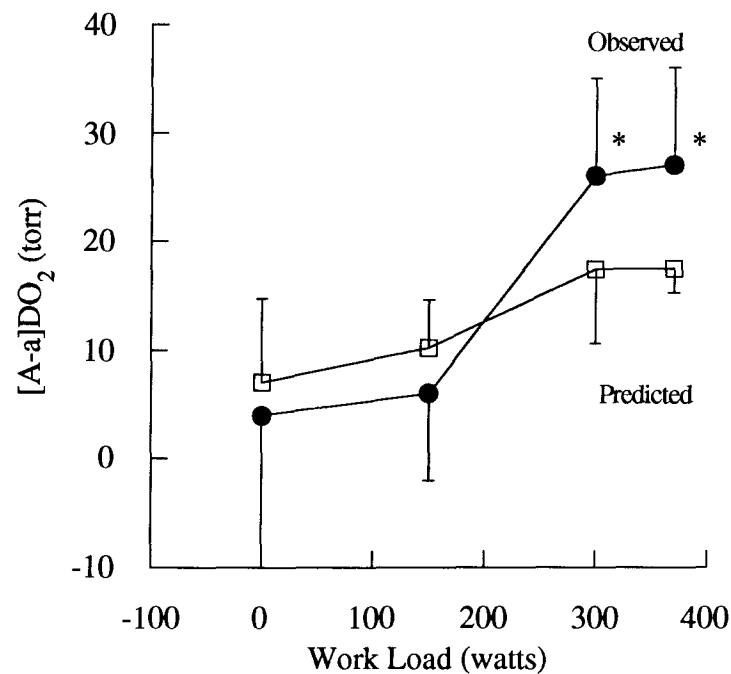


Legend: Closed circles = $DISP_{R^*} (\bar{x} \pm SD)$, open squares = $DISP_E (\bar{x} \pm SD)$, open diamonds = $DISP_{R^*-E} (\bar{x} \pm SD)$, * = significantly different from rest ($p<0.05$), ** = significantly different from light exercise and rest ($p<0.05$).

Diffusion disequilibrium

[A-a]DO₂ predicted on the basis of the model of Wagner et al.(164), [A-a]DO₂(p), and that not accounted for by the inert gas analysis [A-a]DO₂(o-p) is given in Table 3. [A-a]DO₂(p) is compared to observed [A-a]DO₂ in Figure 5. [A-a]DO₂(p) increased significantly over the exercise levels (omnibus F= 12.2, p<0.0001), paralleling the dispersion indices. There were a non-significant increases in [A-a]DO₂(p) between rest and light exercise. The increase between light and heavy exercise was significant (F=3.7, p<0.05) and there was no further increase from heavy to maximal exercise. During heavy and maximal exercise [A-a]DO₂(o) was 9-10 torr greater than that predicted by the inert gas exchange (F=5.3, and F=11.4, p<0.05) suggesting diffusion limitation.

Figure 5. Observed and predicted alveolar-arterial O₂ difference



Legend: Open squares=predicted [A-a]DO₂ (mean±SD), closed squares=observed [A-a]DO₂ (mean±SD) * = significantly different than predicted (p<0.05)

Cardiac output and cardiac volumes

The results of the first pass and gated cardiac studies are given in Table 6. Data were processed by three independent observers and the results were averaged. The correlation was 0.90 between observers and the mean difference in cardiac output between observers was approximately 3% at each exercise level. Cardiac output rose from 7.0 ± 0.9 $l \cdot \text{min}^{-1}$ at rest to 33.3 ± 3.7 $l \cdot \text{min}^{-1}$ at maximal exercise, accompanied by a significant increase in ejection fraction from 0.63 ± 0.05 % at rest to 0.76 ± 0.05 % during light exercise ($F=35.8$ $p < 0.05$). A further increase in ejection fraction to 0.80 ± 0.04 % at 300 watts approached but did not reach statistical significance ($F=3.2$, $p > 0.05$ compared to 150 watts). End diastolic volume increased significantly (omnibus $F_{(2,12)}=20.1$, $p < 0.05$) from rest to heavy exercise as did stroke volume ($F=22.5$, $p < 0.05$). There was also a decrease in end systolic volume between rest and heavy exercise (omnibus $F_{(2,12)}=4.4$, $p < 0.05$).

Table 6. Cardiac output, volumes and ejection fraction at rest and during, light, heavy and maximal exercise. ($\bar{x} \pm \text{SD}$).

	Rest	150 watts	300 watts	Maximal
\dot{Q}	7.0 ± 0.9	16.2 ± 1.5	25.3 ± 2.6	33.3 ± 3.6
Heart Rate	70 ± 10	116 ± 9	156 ± 8	166 ± 8
Stroke Volume	102 ± 21	140 ± 17	163 ± 22	201 ± 23
End Diastolic Volume	149 ± 16	184 ± 25	198 ± 22	*
End Systolic Volume	55 ± 10	44 ± 12	41 ± 10	*
Ejection Fraction	0.63 ± 0.04	0.76 ± 0.05	0.80 ± 0.04	*

* = cardiac volumes obtained during gated study only which was not conducted during maximal exercise.

Pulmonary transit time

Figures 6A and 7A contain representative raw data and gamma univariate fits for regions of interest drawn over the right and left ventricles. Figure 6B and 7B show the frequency distribution of transit times (transfer function) obtained by the deconvolution

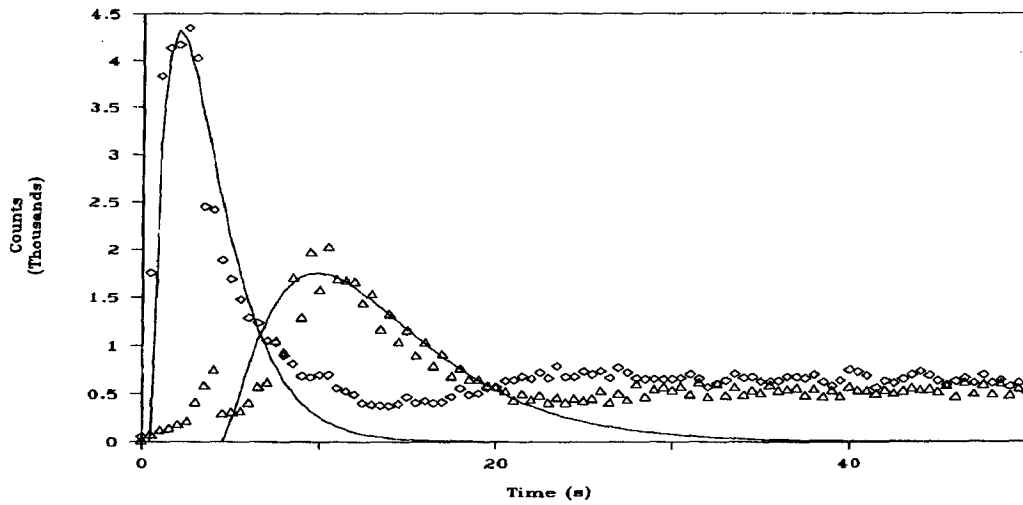
method for the same subject and the output curve obtained when the transfer function is convoluted with the input curve from the right ventricle. Mean transit times at rest and maximal exercise obtained by both deconvolution and centroid techniques are presented in Table 7. In one subject, (subject 10) a satisfactory fit was not obtained by deconvolution analysis and results are reported for the centroid method only in this individual. Mean transit time at rest was 9.31 ± 1.45 seconds by the centroid method and 9.32 ± 1.41 by deconvolution. These were highly correlated ($r = 0.99$, $p < 0.0001$). During exercise mean transit times decreased significantly to less than 3 seconds (2.90 ± 0.35 centroid, 2.91 ± 0.30 deconvolution; $t_{\text{deconvolution}} = 12.3$, $p < 0.001$) and these were also highly correlated ($r = 0.96$, $p < 0.001$). The mean duration of the right ventricular curve did not change significantly from rest to exercise (4.96 ± 1.37 vs 4.19 ± 0.80 seconds, $t = 1.54$, $p = 0.1$) however there was a significant decrease in the mean duration of the left ventricular curve from 14.29 ± 1.52 to 7.09 ± 1.06 seconds ($t = 11.2$, $p < 0.001$). Pulmonary transit time was significantly correlated with PaO_2 (Figure 8) ($r = 0.65$, $p < 0.05$) during maximal exercise and $[\text{A-a}]\text{DO}_2(\text{o})$ ($r = -0.59$, $p < 0.05$). There was also a significant relationship (Figure 8) between $[\text{A-a}]\text{DO}_2(\text{o-p})$ and transit time ($r = -0.60$, $p < 0.05$). When multiple linear regression was used to determine the relationship between transit time, $\dot{V}_E/\dot{V}_{\text{CO}_2}$, $[\text{A-a}]\text{D}$ and PaO_2 there was a highly significant relationship ($R = 0.94$, $R^2 = 0.88$, adjusted $R^2 = 0.83$, $p < 0.01$). Thus at maximal exercise, over 80% of the variance between subjects in PaO_2 can be explained on the basis of transit time, \dot{V}_A/\dot{Q} mismatch and the ventilatory equivalent for CO_2 .

Table 7. Pulmonary transit times by the deconvolution and centroid methods ($\bar{x} \pm S.D.$)

	Rest (s)		Exercise (s)	
	Centroid	Deconvolution	Centroid	Deconvolution
1	10.09	10.19	2.99	2.92
2	7.24	7.37	2.77	2.78
3	8.60	8.75	3.18	3.16
4	7.72	7.45	2.68	2.67
5	9.12	9.23	2.74	2.99
6	8.96	8.85	3.76	3.56
7	8.63	8.73	2.95	2.91
8	9.80	9.82	2.60	2.58
9	11.36	11.35	2.68	2.69
10	11.75	11.43	2.71	*
Mean \pm SD	9.33 \pm 1.45	9.32 \pm 1.41	2.90 \pm 0.35	2.91 \pm 0.30

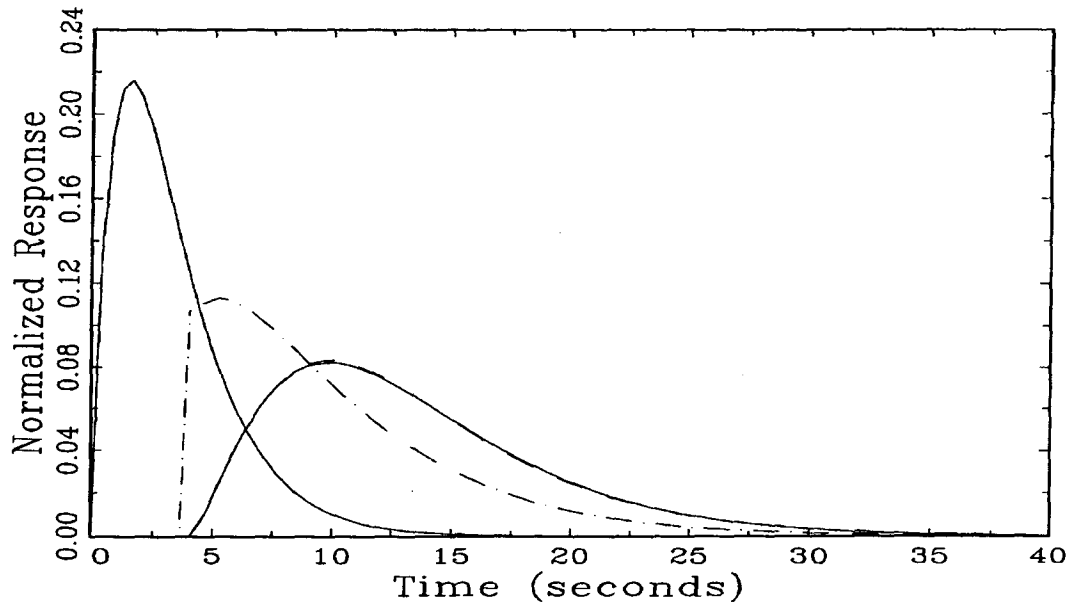
* = unable to fit satisfactory deconvolution analysis

Figure 6A. Raw data and gamma univariate fit for subject one during rest



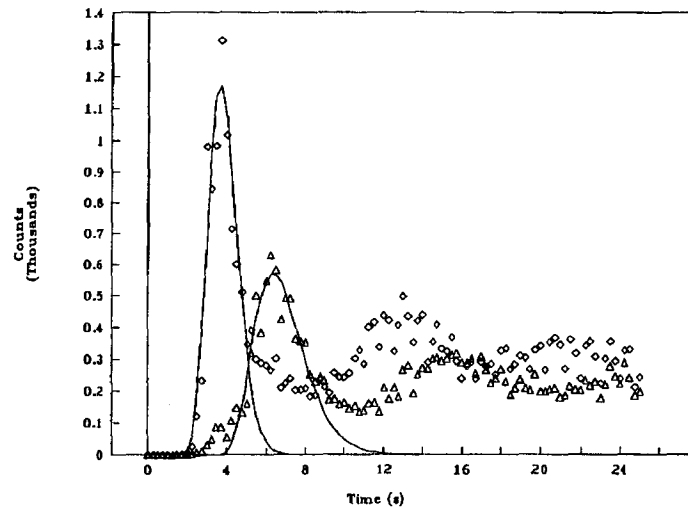
Legend: Open triangles = left ventricular counts, open diamonds = right ventricular counts. Solid lines = gamma univariate fit for the right and left ventricular curves.

Figure 6B. Frequency distribution of transit times for data in Figure 6A.



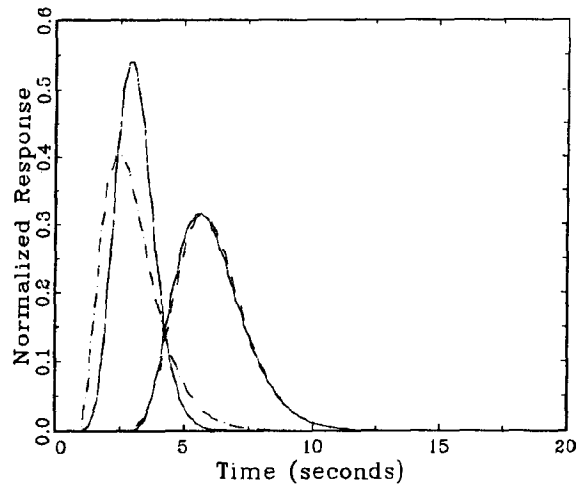
Legend: Solid lines = gamma univariate fit for the right ventricle and left ventricle, dashed and dotted line = frequency distribution of transit times (transfer function), dashed line = resulting output curve when the right ventricular curve is convoluted with the transfer function.

Figure 7A. Raw data and gamma univariate fit for subject one during maximal exercise.



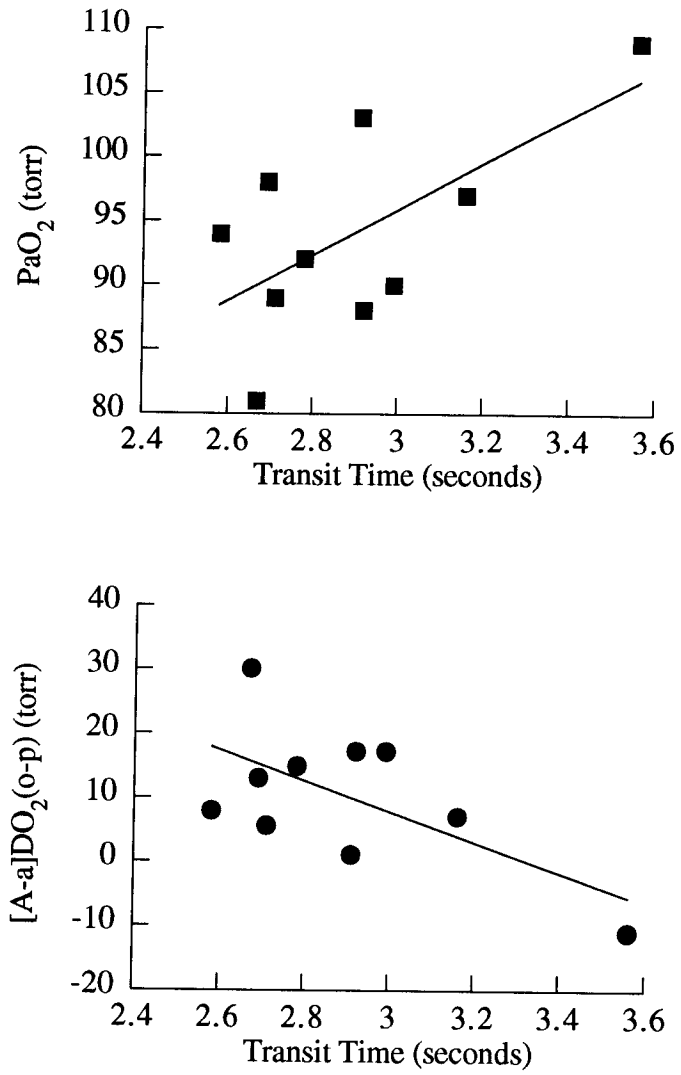
Legend: Open triangles = left ventricular counts, open diamonds = right ventricular counts.
Solid lines = gamma univariate fit for the right and left ventricular curves.

Figure 7B. Frequency distribution of transit times for data in Figure 7A.



Legend: Solid lines = gamma univariate fit for the right ventricle and left ventricle, dashed and dotted line = frequency distribution of transit times (transfer function), dashed line = resulting output curve when the right ventricular curve is convoluted with the transfer function.

Figure 8. PaO₂ and [A-a]DO₂ (o-p) versus transit time.



Pulmonary blood volume

Pulmonary blood volume and pulmonary blood volume index obtained at rest and during maximal exercise are presented in Table 8. Pulmonary blood volume increased significantly during exercise ($t=6.1$, $p<0.001$) by over 50%. Pulmonary blood volume was significantly correlated with whole blood volume at rest ($r=0.67$, $p<0.05$) and there was a similar trend during exercise although the relationship did not attain statistical significance ($r=0.52$, $p=0.06$). Resting pulmonary blood volume index (pulmonary blood volume/BSA) correlated significantly with resting $[A-a]DO_2$ ($r=-0.65$, $p<0.05$). Exercising pulmonary blood volume index correlated significantly with PaO_2 ($r=0.69$, $p<0.01$) and $[A-a]DO_2(o)$ ($r=-0.57$, $p<0.05$). Pulmonary blood volume index correlated significantly with $[A-a]DO_2(o-p)$ during exercise ($r=-0.68$, $p<0.05$), as did whole blood volume (in $ml \cdot kg^{-1}$) ($r=-0.61$, $p<0.05$).

Table 8. Pulmonary blood volume at rest and during maximal exercise

	Rest			Maximal exercise			
	Pulmonary Blood Volume (l)	Pulmonary Blood Volume Index	% of Total Blood Volume	Pulmonary Blood Volume (l)	Pulmonary Blood Volume Index	% of Total Blood Volume	% increase in pulmonary blood volume
1	1.24	0.58	15	1.67	0.78	21	40
2	0.74	0.40	13	1.28	0.69	22	73
3	0.95	0.45	13	1.82	0.87	26	97
4	1.06	0.52	18	1.42	0.70	23	30
5	1.17	0.56	15	1.79	0.86	22	42
6	1.21	0.61	18	2.05	1.03	32	77
7	0.90	0.48	13	1.82	0.96	27	107
8	1.08	0.54	16	1.54	0.76	23	44
9	1.11	0.60	20	1.18	0.64	21	6
10	1.33	0.61	17	1.53	0.69	19	11
MEAN	1.08	0.53	16	1.65	0.82	24	57
±SD	0.18	0.07	2	0.30	0.15	4	34

DISCUSSION

Several authors have reported hypoxemia and arterial desaturation during short term heavy or maximal exercise which increases with physical conditioning (146) and is more common in highly trained athletes (184). In this population the reported incidence of hypoxemia during exercise may be as high as 52% (126).

The etiology of the hypoxemia continues to attract considerable debate. Dempsey and co-workers (35) exercised sixteen highly trained athletes at 70-90% of $\dot{V}O_2$ max breathing different gas mixtures. At this exercise intensity, several subjects exhibited little alveolar hyperventilation and the authors concluded that "the magnitude of the hyperventilatory response was a major determinant of the hypoxemia seen in our athletes". The effect of hypoventilation is to reduce alveolar PO_2 and thus the arterial PO_2 without an effect on $[A-a]DO_2$. Additional evidence in support of inadequacy of ventilation as a causative factor include the observations that during MVV testing and exercise, peak expiratory flows may approach or exceed those defined by the maximal expiratory flow-volume curve (67, 78, 118) and the observation that administration of He: O_2 mixtures increases ventilation, decreases $PaCO_2$, and improves arterial oxygenation, without altering $[A-a]DO_2$ (35, 36, 170). Humans also exhibit entrainment to a variable extent with running, walking, rowing and cycling (13, 158) and this has been implicated as a cause of hypoxemia in galloping horses (34). Aside from the mechanical factors described above, hypoventilation could also be caused by blunted respiratory drives (26, 106, 148).

Pulmonary diffusion limitation secondary to shortened pulmonary transit represents an attractive alternate hypothesis to hypoventilation as a cause of exercise induced hypoxemia. Multiple inert gas studies have shown evidence of diffusion limitation in men capable of sustaining $\dot{V}O_2 \sim 4 \text{ l}\cdot\text{min}^{-1}$, however since MIGET studies have not been made in very highly trained athletes who exhibit exercise induced hypoxemia, the arguments are largely theoretical. The consistent observation that $[A-a]DO_2$ widens with increasing exercise intensity, (35, 63, 72, 161, 182) offers indirect support to this idea.

Multiple inert gas analysis and exercise

The multiple inert gas analysis technique is based on the observation that the retention of a gas in the blood is related to the solubility of the gas (λ) and the \dot{V}_A/\dot{Q} distribution. By using gases that bracket the solubility of O_2 and CO_2 and measuring arterial and mixed expired concentrations, it is possible to estimate shunt, dead space and the shape of the \dot{V}_A/\dot{Q} distribution. It is also possible using the derived \dot{V}_A/\dot{Q} distribution to predict the behavior of O_2 and CO_2 . Assumptions that are made in the multiple inert gas analysis are: 1. there is steady state gas exchange, 2. the lung units are arranged in parallel and behave as independent compartments 3. ventilation and perfusion is non-pulsatile, 4. diffusion dis-equilibrium and extra-pulmonary shunt are absent. It is the exploitation of this last point that has formed the basis of detection of diffusion dis-equilibrium, as any observed $[A-a]DO_2$ that exceeds that predicted from the MIGET \dot{V}_A/\dot{Q} distribution is likely due to diffusion limitation or extra-pulmonary shunt. The advantages of the MIGET technique are that a change in PiO_2 which may alter the \dot{V}_A/\dot{Q} distribution is not required, and that the trace amounts of gases infused are not sufficient to alter concentrations of the physiologic gases.

Despite more than ten years experience with this method, studies involving humans are few, and are mostly confined to normals rather than highly trained athletes. Gledhill et al., (60) studied five male subjects at rest and during light exercise ($\dot{V}O_2$ $1.8 \text{ l}\cdot\text{min}^{-1}$) and found an increase in \dot{V}_A/\dot{Q} as measured by $\log SD\dot{V}$ and $\log SD\dot{Q}$, associated with a widening of $[A-a]DO_2$ which was improved by the breathing of a high density gas. In contrast, Derks (37) found no changes in dispersion in his subjects, again at levels of exercise less than $2.0 \text{ l}\cdot\text{min}^{-1}$. The next studies, published in 1985 as companion papers by Torre-Bueno et al.(161), and Gale et al. (55), contributed substantially to knowledge of the effects of exercise and altitude on ventilation and perfusion mismatch and diffusion limitation. Nine subjects were studied at various exercise levels up to a $\dot{V}O_2$ of almost $3 \text{ l}\cdot\text{min}^{-1}$, at sea-level and simulated altitude corresponding to 5,000, 10,000 and 15,000 feet.

At sea-level there was a trend towards worsening of \dot{V}_A/\dot{Q} relationships with exercise although the results did not reach statistical significance. Resting \dot{V}_A/\dot{Q} did not increase with altitude, although the combination of exercise and altitude did produced significant deterioration in the \dot{V}_A/\dot{Q} relationships (55). There was no evidence of diffusion disequilibrium at rest for any altitude although there was evidence for diffusion limitation during exercise at altitudes above 10,000 ft. There was a suggestion that, in subjects capable of higher levels of exercise, diffusion limitation might be present although small "n" hampered definitive conclusions (161).

This last observation was addressed further in a paper by Hammond et al., (63) who was able to exercise moderately trained athletes to a $\dot{V}O_2$ of almost $4.0 \text{ l}\cdot\text{min}^{-1}$. Evidence of diffusion disequilibrium was found at the highest exercise intensity (300 watts), as the average measured $[A-a]DO_2$ exceeded that predicted from the derived \dot{V}_A/\dot{Q} distribution by more than 12 torr. These results were confirmed by Bebout et al., (12) who found evidence of diffusion limitation during exercise that was worsened by altitude and improved by two weeks of acclimatization. The authors concluded that the effect of acclimatization was to lower cardiac output at any given exercise level and improve diffusion limitation through an effect on pulmonary transit time.

MIGET data

Indices of dispersion and \dot{V}_A/\dot{Q} mismatch

Significant increases in overall indices of dispersion and in the indices of dispersion related to the blood flow distribution were observed with exercise regardless of the index used. There was little change between rest and light exercise, marked increases between light and heavy exercise and little further change between heavy and maximal exercise. No significant change was apparent in any of the indices of dispersion related to ventilation. These data indicate increasing \dot{V}_A/\dot{Q} mismatch predominantly related to heterogeneity of blood flow. When blood flow was examined with respect to areas of low ($\dot{V}_A/\dot{Q} < 0.1$),

normal ($0.1 < \dot{V}_A/\dot{Q} < 10$) and high ($\dot{V}_A/\dot{Q} > 10$) \dot{V}_A/\dot{Q} (40) it was evident that the heterogeneity in flow resulted from significantly increasing flow to areas of high \dot{V}_A/\dot{Q} rather than areas of shunt or low \dot{V}_A/\dot{Q} . Perfusion of areas of high \dot{V}_A/\dot{Q} accounted for over 10% of blood flow during maximal exercise compared with less than 2% at rest. At maximal exercise perfusion of areas of low \dot{V}_A/\dot{Q} accounted for less than 1% of blood flow and intrapulmonary shunt was not found. Similar patterns of dispersion of the perfusion indices have been reported resulting from hypoxic pulmonary vasoconstriction in lobar preparations in the dog (41) which is exacerbated in oleic acid induced pulmonary edema (40). Difficulty in interpreting these data stems from an overall right shift of the compartmental ventilation versus $\log \dot{V}_A/\dot{Q}$ curves as a result of an approximately twenty-fold increase in \dot{V}_E compared to a six-fold increase in \dot{Q} . During exercise, therefore, perfusion to areas of low \dot{V}_A/\dot{Q} may be obscured by this shift and will be manifest by an increase in $\log SD\dot{Q}$ and other perfusion related indices.

At rest and during exercise to a $\dot{V}O_2$ of $4.0 \text{ l}\cdot\text{min}^{-1}$ the mean of the \dot{Q} and distribution and $\log SD\dot{Q}$ compare favorably with those at comparable exercise levels obtained during similar studies (12, 63, 147) (Table 9). The mean of the \dot{V} distribution and $\log SD\dot{Q}$ are higher at all exercise levels and are due to the recovery of areas with apparently very high \dot{V}_A/\dot{Q} distributions. In some cases the excretion of acetone (the gas of highest solubility) exceeded the retention, violating laws of mass balance. This apparent paradox can likely be explained on the basis of a complex interaction between airways heating and cooling, as it was much more pronounced at maximal exercise. Areas of very high \dot{V}_A/\dot{Q} have been reported in many experimental situations including high frequency ventilation (68, 108, 138), and have been considered to be artifactual. No alveolar zones with such a high \dot{V}_A/\dot{Q} seem anatomically likely, but gas exchange of soluble gases by the airways is possible (162). Gas solubility and transport is related to airways temperature, mucous temperature, water content and thickness. During high intensity exercise there will be both heating of the airways secondary to increased bronchial blood flow and increases in core

temperature, as well a cooling secondary to hyperventilation. It is possible that excretion of the soluble gases deposited in the airway mucosa and mucous earlier during the experiment may be enhanced by the increase in body temperature. The indices of ventilation heterogeneity $E(A-a)D$, $DISP_E$ and $\log SD\dot{V}$ would be most likely to be affected and do not explain the significant increases in the perfusion related indices.

The increase in \dot{V}_A/\dot{Q} heterogeneity with exercise, manifest by increasing $[A-a]DO_2(p)$ is greater than reported in other studies (12, 63) and is not an effect of the higher exercise intensity achieved since $[A-a]DO_2(p)$ was higher even at the submaximal workloads. The reasons for this are not apparent but may reflect an unique characteristic of this highly trained subject population.

Diffusion limitation

The MIGET analysis of pulmonary gas exchange accounts for \dot{V}_A/\dot{Q} mismatch and intra-pulmonary shunt. $[A-a]DO_2(o-p)$ therefore represents that portion of the $[A-a]DO_2$ which is not accounted for by those factors and represents diffusion limitation or extrapulmonary shunt. A 1% extra-pulmonary shunt would result in a fall in SaO_2 of about 0.7% and a decrease in PaO_2 of about 7 torr accounting for most of the difference between observed and predicted values of $[A-a]DO_2$. The issue of extrapulmonary shunt therefore becomes crucial in the detection of diffusion limitation. Since extrapulmonary shunt was not measured in this study this possibility cannot be dismissed. Previous work (161) during exercise at sea level and altitude has shown minimal (< 0.18 %) shunt, although these measurements are extremely difficult to make. If it is assumed that the subjects in the present study are similar with respect to extrapulmonary shunt then a 0.18% shunt in the present study would account for approximately 1 torr of the $[A-a]DO_2(o-p)$.

Although the $[A-a]DO_2(o-p)$ demonstrated a correlation of 0.60 with pulmonary transit time over 60% of variance between subjects is not accounted for by PTT. There are many possible explanations and making a direct comparison is fraught with difficulties. The

comparison is only as good as the measures used to make it. Pulmonary transit time is only an indirect indicator of pulmonary capillary transit time and therefore the relationship described above reflects uncertainty in this measure as well as uncertainty related to the detection of diffusion limitation by MIGET.

Table 9. Comparison of MIGET data from present study with other investigators

$\dot{V}O_2$ l·min ⁻¹	Mean \dot{Q}	Mean \dot{V}	Log SD \dot{Q}	Log SD \dot{V}	DISP _{R*}	DISP _E	DISP _{R*-E}	Study
	1.00 ±0.23	1.91 ±0.99	0.38 ±0.20	1.09 ±0.55	2.53 ±2.13	3.88 ±3.07	5.41 ±4.47	p
Rest	1.11 ±0.17	1.28 ±0.20	0.35 ±0.05	0.42 ±0.10	1.08 ±0.29	1.07 ±0.29	1.99 ±0.51	1
	0.63 ±0.09	0.68 ±0.23	0.28 ±0.13	0.26 ±0.04	0.68 ±0.43	0.59 ±0.27	1.16 ±0.61	2
	2.46 ±0.62	4.21 ±1.50	0.44 ±0.12	0.90 ±0.47	2.83 ±2.09	3.92 ±3.01	6.09 ±4.65	p
2-3	3.16 ±0.66	3.91 ±0.83	0.44 ±0.05	0.46 ±0.05	1.64 ±0.25	1.38 ±0.17	2.72 ±0.32	1
	2.79 ±0.69	2.98 ±0.77	0.34 ±0.07	0.31 ±0.03	0.93 ±0.28	0.82 ±0.28	1.48 ±0.54	2
	2.94 ±0.62	7.27 ±3.67	0.64 ±0.17	1.09 ±0.29	4.63± 2.29	5.55 ±2.71	9.34 ±4.51	p
>3-4.5	*	*	0.55 ±0.17	0.49 ±0.20	*	*	*	3
	3.33 ±0.50	3.96 ±0.61	0.58 ±0.30	0.36 ±0.09	1.44 ±0.81	0.96 ±0.47	2.14 ±1.10	2
>5.0	4.44 ±0.53	11.82 ±2.90	0.78 ±0.11	1.18 ±0.14	5.73 ±1.33	5.45 ±1.03	10.39 ±2.12	p

* = not reported. P= present study, 1= study of Schaffartzik et al., group 1 subjects (147), 2= Hammond et al., (63), 3= Bebout et al., (12)

Effect of uncertainty in cardiac output on MIGET data

Small non significant differences were noted in heart rate between measures made during the cardiac output determinations and the inert gas measures, at rest and submaximal

exercise. During maximal exercise, the two measures were nearly identical. On average, heart rate was 6-7 beats per minute higher during the nuclear medicine studies, resulting in an error of 12% at rest, 5.7% during light exercise and 4.4% during heavy exercise. The likely explanation, relates to small differences in posture during the two studies; during the inert gas studies the subjects were free to assume the posture that they were the most comfortable with, usually in a relaxed position holding on to the bars of the ergometer. In contrast, during the cardiac output determinations the subjects were required to hold on to the gamma camera, an awkward position at best, which likely changed their pedaling efficiency slightly.

Although cardiac output was not measured simultaneously with the MIGET determinations, uncertainty of the cardiac output measurements is unlikely to affect the inert gas calculations with respect to the recovered \dot{V}_A/\dot{Q} distributions or the predicted [A-a]DO₂. In theory, uncertainty in measurement of cardiac output, would be most apparent in the insoluble gases (small λ) as the mixed venous levels ($P\bar{v}$) of the inert gases are calculated from arterial and mixed expired ($P\bar{E}$) levels:

$$P\bar{v} = P_a + \frac{P\bar{E}\dot{V}_E}{\lambda\dot{Q}_T}$$

For highly soluble gases, λ is large and P_a dominates the right hand side of the equation. For insoluble gases such as SF₆, the term $(P\bar{E}\dot{V}_E)/(\lambda\dot{Q}_T)$ dominates the equation and uncertainty in \dot{Q}_T will be transmitted directly to calculations of retention and excretion data and from there into the calculation of the \dot{V}_A/\dot{Q} distribution.

This issue has been addressed by Wagner et al., (169) who compared recovered \dot{V}_A/\dot{Q} distributions, residual sum of squares (model fit), [A-a]DO₂ (p), and PaO₂ for detection of diffusion limitation in ten patients at rest using measured cardiac output and a sensitivity analysis over assumed cardiac outputs of 2 to 12 l·min⁻¹. Little effect of assumed cardiac output was observed on most of the variables of interest. Log SD \dot{Q} was insensitive

to large changes in cardiac output, although slightly more effect was observed on $\log SD\dot{V}$. The predicted values of PaO_2 , $PaCO_2$ and $[A-a]DO_2$ were also insensitive to assumed cardiac output and residual sum of squares was unaltered. These findings were also confirmed in the present study. Table 10 gives the residual sum of squares (RSS) and mean \dot{Q} , mean \dot{V} , $\log SD\dot{Q}$ and $\log SD\dot{V}$ for a poorly fitting data set varying cardiac outputs from 15 to 40 $l \cdot \text{min}^{-1}$.

Table 10. Effect of varying cardiac output on residual sum of squares and indices of dispersion

\dot{Q} $l \cdot \text{min}^{-1}$	RSS	mean of \dot{Q} distribution	mean of \dot{V} distribution	Log $SD\dot{Q}$	Log $SD\dot{V}$
15	114	6.52	12.35	0.558	1.025
20	113	4.83	9.92	0.535	1.153
25	112	3.84	8.40	0.515	1.253
30	111	3.17	7.35	0.496	1.134
35	110	2.71	6.52	0.486	1.398
40	109	2.37	5.90	0.473	1.457

The mean of the ventilation and perfusion distributions are sensitive to alterations in cardiac output but are not of great importance since it is dispersion that determines \dot{V}_A/\dot{Q} mismatch. The indices of dispersion $\log SD\dot{Q}$ and $\log SD\dot{V}$ as described by Wagner et al., (169) are relatively insensitive to changes in cardiac output; for an increase in cardiac output of over 150%, $\log SD\dot{Q}$ decreased by 15% while $\log SD\dot{V}$ increased by 14%. It can be concluded that the pattern of the \dot{V}_A/\dot{Q} relationship recovered from inert gas data is not affected by uncertainties in cardiac output, and cannot explain the difficulties in fitting the SF_6 data.

Maintenance of steady state conditions

Steady state conditions in the strictest sense cannot be attained at exercise levels above the anaerobic threshold and mean ventilation changed from 164.2 to 178.1 $l \cdot \text{min}^{-1}$ over the data collection during maximal exercise. This was an increase of 7.8%, which is

relatively small and unlikely to affect the results as the very high levels of blood flow and ventilation ensure rapid equilibration rates.

Blood and plasma volume

Methods for determination of blood and plasma volume are based on measurement of dilution of a known amount of a tracer material. The use of radiolabelled human serum albumin (RISA) is currently the accepted method for routine measurement of plasma volume in human subjects (76), although the use of albumin as an intravascular marker likely overestimates the volume of distribution by a factor of over 5% when compared to larger macromolecules such as fibrinogen (15). The RISA method for measurement of plasma volume compares favorably to measurements made with Evans blue dye, carbon monoxide gas, and ^{99m}Tc labeled erythrocytes (160), although, as would be expected from the preceding statement, RISA measurements agree closest with Evan blue dye measures which also uses albumin as the carrier molecule for the tracer. When red cell mass is not measured independently, but estimated from venous hematocrit, the accuracy of the determination is dependent on correction of venous hematocrit to whole body hematocrit (76).

The subjects were both plasma volume expanded and had increased red blood cell mass. These findings have been documented in the past by a number of authors. Cross-sectional studies indicate that highly trained men and women have blood volumes that are approximately 25% larger than sedentary subjects (38, 88) with the proportionate increase in plasma volume being greater than the proportionate increase in red cell mass (21). The subjects had plasma volumes 44% greater than predicted for normal subjects although the mean value of $87.5 \text{ ml}\cdot\text{kg}^{-1}$ whole blood volume for this study compares favorably with values reported by Kjellberg et al., (88) and others (21, 38). Little is known about the mechanisms of the changes in hematological parameters, however it is postulated that increases in circulating plasma proteins are an important factor in chronic hypervolemia, as

are renal mechanisms involving renin-angiotensin-aldosterone, and vasopressin (31). This hypervolemia may offer advantages with respect to thermoregulation and hemodynamics and has shown a strong correlation with $\dot{V}O_2$ (31). Changes in blood volume associated with chronic endurance exercise may account for up to one half of the difference in stroke volume between trained and untrained men (73) and a decrease in plasma and blood volume with detraining has been shown to decrease both $\dot{V}O_2$ max and stroke volume in endurance athletes (32).

Radionuclide cardiography

First pass and gated radionuclide cardiography offer many advantages over other methods for determination of cardiac output and cardiac volumes. The method is relatively non-invasive requiring only an intravenous line and serial measurements can be made making these techniques suitable for exercise studies, particularly those involving more than one exercise level. A combination of first pass and gated determination of cardiac output was chosen for the following reasons: First pass techniques also allowed simultaneous determination of right-heart to left heart pulmonary transit times, and measurement of cardiac output at rest by both methods enabled the subsequent gated determinations to be corrected for attenuation of counts by the chest wall without on relying assumptions about ventricular geometry or depth. We used the gated technique during light and heavy exercise to minimize radiation exposure to the subjects, and first pass was only done during maximal exercise because of concern regarding motion artifact and data acquisition time.

First pass radionuclide cardiography has been compared with more traditional methods of cardiac output determination both at rest and exercise and shows good agreement with values obtained by thermodilution (83), contrast ventriculography and gated equilibrium radionuclide angiography (122). Gated equilibrium radionuclide angiography, similarly has shown excellent agreement with contrast ventriculography (122, 151), direct

Fick method (111) and thermodilution (33). Thus both radionuclide methods can be used with confidence that they are valid means of determining cardiac output.

Cardiac function in athletes

The term "athletes heart" has been used to describe the alteration in cardiac structure and function which accompany regular physical conditioning. In recent years, M-Mode echocardiography and gated and first pass radionuclide angiography have allowed a more accurate picture of the effects of exercise on the heart. Maron (103) extensively reviewed 28 echocardiographic studies in athletes from a variety of athletic backgrounds. Regular athletic training produces an increase in left ventricular mass, even when corrected for body size and increases in left ventricular cavity dimension especially in endurance athletes. Left ventricular end-systolic dimension is usually increased, and many studies report increases in posterior left ventricular wall as well as ventricular septal thickness (103). Enlargement of the left atrium is also commonly reported, as is an increase in right ventricular mass. The effects of training on the heart has been examined longitudinally (94, 95, 115, 134) and the available data indicate that the nature of alterations in cardiac structure are somewhat dependent on the type of training stimulus, with strength athletes exposed to predominantly a pressure load tending to show an increase in left ventricular thickness while those exposed to endurance training, and hence a volume load, showed an increase in ventricular volume.

In a longitudinal study, Rerych et al., (134) studied collegiate level swimmers with first pass radionuclide angiography and found an increase in resting stroke volume, end diastolic volume, end systolic volume and a decrease in ejection fraction after six months of swim training. During exercise, maximal cardiac output was increased predominantly as a result of increases in end diastolic volume, while ejection fraction was unchanged from pre-training levels. Fagard et al., (46) studied highly trained amateur and professional cyclists with echocardiography in both the competitive and rest seasons and compared them to recreationally active controls. During the resting season the athletes had smaller heart size

and significant decreases in total left ventricle end systolic diameter, due to reductions in wall thickness than in the competitive season. When compared to controls the cyclists had much higher ratios of wall thickness to internal dimensions in both the competitive season and the resting season suggesting that both volume and pressure (presumably due to isometric upper body exercise during cycling) were responsible for the increase in cardiac dimensions.

Comparison with previous investigations

The data from the present study are similar to those obtained by direct Fick technique, radioangiography and echocardiography (Table 11). At rest, the cardiac output was slightly higher in both the present study and the other radioangiographic study (134), but resting heart rate and cardiac output would be expected to be the most influenced by extraneous variables such as subject arousal etc. The resting stroke volume index from the present study is comparable to the mean value for the other studies cited. During exercise at a $\dot{V}O_2$ of 1.5-2 l·min⁻¹ and $\dot{V}O_2$ of 3-4 l·min⁻¹ the present data again are very similar to those previously reported. During maximal exercise, although cardiac output is very similar to that obtained in the other studies, stroke volume index is higher. This may possibly be explained by the study design. Collecting clean first pass data was of paramount importance for measurement of pulmonary transit times and motion artifact was of great concern. It was elected to inject the labeled red blood cells at the end of 3 minutes of exercise and data were acquired for 150 seconds after injection. At this work intensity heart rate clearly had not fully stabilized and it may be possible that stroke volume may have fallen and heart rate risen, with redistribution of blood flow as the exercise continued, which would not be evident during the data collection.

Effect of increasing exercise intensity on cardiac volumes

Exercise physiology text books (20) report that stroke volume levels off with increasing exercise intensity, possibly as a result of decreased diastolic filling time and

reduced end diastolic volume. Indeed, some authors have reported a decrease in end diastolic volume with increasing exercise (57) while others have reported a decrease, no change or an increase in end diastolic volume (49, 124). A decrease in stroke volume with increasing exercise intensity was not found in any of the subjects, and only one subject (#9) showed a plateau in stroke volume between heavy and maximal exercise. These data would tend to support the recent observations by Gledhill et al., (61) who found increasing stroke volume with increasing exercise in endurance trained athletes without a shortening of left ventricular ejection time compared to sedentary controls, leading the authors to conclude that enhanced preload and Frank-Starling mechanism were important factors for maintenance of stroke volume in athletic subjects.

Table 11. Cardiac output and volume indices comparison with other studies

Exercise intensity	Cardiac Index ml·m ⁻²	End Diastolic Volume index ml·m ⁻²	End Systolic Volume Index ml·m ⁻²	Stroke Volume Index ml·m ⁻²	Study
Rest	3.4±0.4	73±8	27±5	51±10	present R-G
	3.4±0.5	85±20	22±6	64±15	Rerych R-FP, (134)
	3.0±0.9	85±14	37±11	48±15	Ginzton E (57)
	2.4±0.03			38±6	Hermannsen D (66)
$\dot{V}O_2$ 1.5-2.0 l·min ⁻¹	8.0±0.7	91±13	22±7	69±8	present R-G
	8.8±1.7	90±17	24±7	66±13	Ginzton E (57)
	8.2±1.3			67±9	Ekblom F (43)
$\dot{V}O_2$ 3-4 l·min ⁻¹	12.5±1.2	98±11	21±5	81±11	present study R-G
	13.8±1.3			90±7	Ekblom F (43)
	11.1±1.5			66±9	Hermannsen D (66)
$\dot{V}O_2$ 4+ l·min ⁻¹	16.5±1.8			100±12	present study R-FP
	16.3±4.4	104±19	14±7	90±20	Rerych R-FP (134)
	18±0.6			95±4	Ekblom F (43)

R-FP = Radioangiography first pass method, R-G = radioangiography gated method, E= echocardiography, F = Fick method, D= Dye dilution technique.

Pulmonary transit times

Theory

The mean transit time for a well mixed indicator to flow through a specific volume at a given flow rate is described by the relationship: $\text{transit time} = \text{volume}/\text{flow}$. The time required for an indicator to flow past an observation point down stream from an entry point is related not only to the time it takes the bolus to flow past the point but also how quickly it arrived there. Transit time is the time that a bolus remains in a compartment if it is injected directly and instantaneously into the compartment. The first moment describes not only the time that the indicator is in the compartment but also how quickly or slowly it arrived there. The first moment therefore represents the summation of all transit times up to that point. If it were possible to deliver indicator material instantaneously into the compartment of interest the first moment would be the same as the transit time. Transit time of a compartment can be determined by subtracting the first moment of the bolus from that of the output curve derived from the compartment.

In the case of pulmonary transit times, the bolus or input curve is derived from a time activity curve of the right ventricle and the output curve is derived from the left ventricle; transit time is determined by subtracting the first moment of the right ventricular curve from the first moment of the left ventricular curve. This method is referred to as the centroid method. Deconvolution is a mathematical process by which a frequency distribution of transit times (a transfer function, $h(t)$) can be derived from the input (right ventricular) and output (left ventricular) time activity curves. The assumption is made that since both the input curve and output curve can be described by a gamma function (153) that $h(t)$ is also a gamma function. A series of 20 to 50 curves is then generated with mean transit times similar to that obtained by the centroid method and convoluted with the input curve producing a series of unique output curves. Ridge regression is then applied to determine the contribution of the curves obtained to the actual output curve and the final transfer function is obtained. These data when convoluted with the input curve produces a derived

output curve. The process is repeated until a satisfactory result is obtained. It is important to note that the transit time obtained from either method represents the delay of the bolus through pulmonary arteries, arterioles, capillaries, venules, veins, left atrium and left ventricle and does not just represent pulmonary capillary transit time. Incomplete mixing of the bolus can lead to either over or underestimation of times, therefore it is preferable to measure transit time downstream from the site of injection. Other sources of error include poor bolus technique and cross contamination of time activity curves from overlying structures in the chest.

Pulmonary transit times have been measured in humans and animals in a variety of experimental conditions. There is a clear gravitational difference in regional transit times with the shortest transit times at the base and longest times at the apex of the lung (70, 96). As pulmonary blood flow increases, recruitment of blood volume prevents a drastic decrease in transit time (70). In animals, very close agreement has been obtained between radioisotopic methods and dye techniques (44). Similar support for the validity of this technique has been established in humans: MacNee et al.,(96) compared pulmonary regional transit times obtained by centroid and deconvolution methods pre-operatively with those obtained intra-operatively in five patients undergoing lung resection for carcinoma. Excellent agreement between in vivo and in vitro techniques was found with the mean difference between methods less than 0.5 seconds. There were no significant differences between those results obtained by deconvolution (mean over all regions = 4.83 sec) and centroid (mean = 4.53 sec) methods.

Pulmonary transit times and exercise in humans

Exercise results in a decrease in transit time from resting values of about 5 seconds to less than 2.5 seconds in normal subjects (77). The effect of exercise training on pulmonary transit time have also been demonstrated. Rerych et al., (134) reported an increase in pulmonary transit times in collegiate swimmers after six months of intensive exercise training, likely reflecting increases in both total blood volume and pulmonary blood volume. Resting values in that study and the present one were greater by more than a factor of two, compared to sedentary subjects. Mean pulmonary transit time during exercise was 2.8 ± 0.3 seconds, a result very similar to that of the present study.

Pulmonary blood volume

Pulmonary blood volume has also been measured during a variety of clinical situations and during maximal exercise. Radionuclide methods for determination of pulmonary blood volume have correlated closely with dye dilution techniques (44), but it is important to recognize that both techniques measure the volume of blood between the point of input of the marker and the downstream measurement. Guintini et al., (58) reported pulmonary blood volumes in patients with a variety of cardiopulmonary conditions and in 5 normal men. Pulmonary blood volume at rest was $293 \pm 50 \text{ ml} \cdot \text{m}^{-2}$ comprising approximately 10% of total blood volume and increased with mild exercise. Slightly higher resting values were obtained by Iskandrian et al., (77), with a non significant increase during exercise. Exercise training has been shown to produce an increase in pulmonary blood volume of approximately 10% at rest and 50% during maximal exercise (134) compared to pre-training values. Maximal exercise in trained individuals led to an 80% increase in pulmonary blood volume index from $465 \text{ ml} \cdot \text{m}^{-2}$ at rest to $772 \text{ ml} \cdot \text{m}^{-2}$ during maximal exercise, similar to values of $530 \text{ ml} \cdot \text{m}^{-2}$ at rest and $820 \text{ ml} \cdot \text{m}^{-2}$ obtained during the present study.

Relationship of pulmonary transit time and blood volume to pulmonary capillary transit time and blood volume

A central issue with respect to the interpretation of the present data concerns the relationship between whole lung transit time and blood volume and pulmonary capillary transit time and blood volume, since it is the latter two factors which affect pulmonary gas exchange. Unfortunately data addressing this question are sparse and can only give an estimate of these relationships. Backmann and Hartung(8) measured whole lung blood volume in cadavers and then estimated the arterial and venous contributions by the injection of a very viscous fluid that did not enter the capillaries. They estimated that 53% of the whole lung blood volume or 270 ± 50 ml was in the pulmonary capillaries and suggested that this was an upper limit of the measure, as small arterioles and venules would be included using this technique. In contrast to this, studies that calculate capillary blood volume from diffusing capacity (64, 171) estimate values of less than one half of that value (about 100 ml) and may underestimate the true value, as it is a functional rather than an anatomical measure. If these values for blood volume are applied to the resting data from the present study, calculated pulmonary capillary transit time would be between 1.15 and 2.34 seconds and whole lung transit times would be between 4 and 8 times greater than capillary transit times. During exercise, there are even less data on which to base calculations. Warren et al., (171) measured pulmonary capillary blood volume at 215 ml using diffusing capacity during exercise at a $\dot{V}O_2$ of greater than $4.0 \text{ l} \cdot \text{min}^{-1}$. Using this information and again accepting a value of 270 ml as the upper anatomical limit of pulmonary capillary blood volume, these values would give an estimated pulmonary capillary transit time for the present study of 0.39-0.49 seconds and whole lung transit time would be some 6 to 7.5 time greater than the capillary transit time. It is important to recognize that these represent average values for transit time and because of the skewed nature of both the pulmonary and pulmonary capillary transit curves a significant portion of the cells may have very short transit times.

Arterial blood gas and metabolic data

Arterial blood measures

Our subjects exhibited PaO_2 s ranging from 74 to 100 torr (mean SaO_2 of 95.3%) during heavy exercise and from 81 to 109 torr (mean SaO_2 of 94.2%) during maximal exercise. These values are higher than the previous values reported by this laboratory (72) and that of Dempsey et al.,(35) however it is likely that this is as a result of the different means of exercising the subjects; running in the previous studies versus cycling in the present one. Cycling was chosen as the method of exercising subjects in the present study because it facilitated the MIGET data collection, and because measurement of pulmonary transit times, cardiac output and cardiac volumes is not currently possible using other exercise forms due to motion artifact. The relatively high values for pH in the present study of 7.24 ± 0.06 , compared with the previous study value of 7.21 ± 0.06 in a very similar group of subjects exercising at the same relative intensity, likely are as result of the smaller muscle mass involved in cycling. This factor may also contribute to the higher values for PaO_2 . Three subjects from the 1989 study participated in the current one: all had higher values for SaO_2 , PaO_2 and lower values for pH than in the study involving running. No correction was made for temperature in the previous study, and it is likely that the degree of hypoxemia in those subjects was overestimated. A temperature increase of about 1°C was seen after 5 minutes of exercise at $\dot{\text{V}}\text{O}_2$ max in the current study, which may underestimate the increase in temperature seen with running.

The subjects were screened for EIH during the initial $\dot{\text{V}}\text{O}_2$ max testing with a pulse oximeter and recorded a mean saturation of $92.2 \pm 2.18\%$. This suggest that either the exercise tests were not of sufficient duration to elicit maximal hypoxemia or that the readings of the pulse oximeter were unreliable during maximal exercise.

Mixed venous PO₂

Mixed venous blood gas data is calculated from the Fick equation and small errors in measurement of cardiac output and $\dot{V}O_2$ will be transmitted directly to the $P\bar{v}O_2$ calculation. This may be more of a problem with the current study as cardiac output and $\dot{V}O_2$ were not measured simultaneously, as they were in other studies using similar methodology (63, 161). This is not likely to affect $[A-a]DO_2(p)$ (63) or indicators of diffusion limitation, $[A-a]DO_2(o-p)$. Bearing this in mind, the $P\bar{v}O_2$ data from the present study should be interpreted with some caution. At rest, the calculated mean $P\bar{v}O_2$ is similar to values reported by several other studies employing both direct measurement and calculation from the Fick equation (28, 89, 139, 161). During light exercise, the values are similar to those reported by Cerretelli et al., (28) although they are approximately 6 torr lower than values reported by Torre-Bueno et al., (161). During heavy and maximal exercise, calculated $P\bar{v}O_2$ was substantially lower than reported for normal subjects exercising at sea level, although values lower than 17 torr have been reported for subjects exercising at simulated altitude (161) and breathing hypoxic gas mixtures (139).

Possible mechanisms of exercise induced hypoxemia

Although marked hypoxemia was not seen in the majority of the subjects in this study the individual variation makes it possible to speculate as to causes of exercise induced hypoxemia in highly trained subjects. The data presented in this paper is consistent with hypoventilation, $\dot{V}A/\dot{Q}$ mismatch and diffusion limitation as viable mechanisms in the genesis of EIH, both in groups of subjects and in individuals, although clearly one mechanism may predominate over the other depending on exercise intensity and individual variability. This is perhaps best illustrated by comparing subject 4 to subject 5. Subject 5, who hypoventilated to the point of CO₂ retention at 300 watts, despite a PaO₂ of 74 torr, also had evidence for diffusion limitation both at 300 watts and at maximal exercise, with $[A-a]DO_2(o-p)$ of 6 and 17 torr respectively. It is not likely that the source of this subject's

hypoventilation was purely mechanical in nature as PaCO_2 decreased to 31 torr and PAO_2 rose to 123 torr at the end of maximal exercise, indicating increased effective alveolar ventilation, when given the appropriate stimulation. Subject 4 had little evidence of hypoventilation as PaCO_2 was 35 torr or less during heavy and maximal exercise, however the inert gas data suggests marked diffusion limitation with $[\text{A-a}]\text{DO}_2(\text{o-p})$ greater than 30 torr at both exercise levels.

From the data in the present study, it is now possible to present an explanation of the conflicting findings of the previous study (72) and that of Dempsey et al., (35). Dempsey exercised very highly trained individuals at 70-90% of $\dot{V}\text{O}_2$ max whereas the subjects in the previous study were exercised at 100% of $\dot{V}\text{O}_2$ max. This is evidenced by similar oxygen consumption between the two groups but higher $\dot{V}\text{CO}_2$ and lower pH for the subjects in the study of Hopkins and McKenzie. It is proposed that three main mechanisms contribute to exercise induced hypoxemia. During heavy exercise, hypoxemia results from relative hypoventilation, \dot{V}_A/\dot{Q} mismatch and diffusion limitation. During maximal exercise, diffusion limitation and \dot{V}_A/\dot{Q} mismatch continues and may in some individuals worsen, but arterial oxygenation may improve, as ventilation increases in response to stimuli such as marked acidosis. In this study, as in the previous work, there is little evidence for hypoventilation at maximal exercise in young, highly trained subjects. All of the subjects had significantly lower values for PaO_2 and higher values for PaCO_2 at the heavy exercise level when compared to maximal exercise. In addition, maximal ventilation during the exercise test was significantly less than during the $\dot{V}\text{O}_2$ max determination, indicating that at least under some circumstances, our subjects were capable of higher levels of ventilation. It seems unlikely that mechanical restriction of ventilation is an important factor in these subjects and suggests that the relative hypoventilation and lower levels of arterial oxygen observed during heavy exercise may have been related to complex interactions between the work of breathing and drives to breathe.

The relationships between whole blood volume, pulmonary blood volume index and $[A-a]DO_2(o-p)$ suggest that in some endurance athletes with EIH that this problem could be compounded by dehydration and or cardiovascular drift which would lower blood volume and possibly affect pulmonary blood volume and pulmonary transit. These results must be interpreted with caution, recognizing that due to the small sample size these subjects may not be representative of the population at large. There is no direct evidence in the present study to support this hypothesis, and there are no published papers that directly examine the effect of volume contraction on exercising pulmonary blood volume and EIH. However, a recent study in this laboratory examined the effect of administration of a single dose of furosemide on EIH using ear oximetry (163). Plasma volume was not measured directly but changes in plasma volume were estimated from changes in hematocrit. Although there was considerable intersubject variability, there was a strong correlation between the difference in the change in plasma volume between placebo and furosemide administration and the change in saturation between the two conditions ($r=0.75$, $p<0.01$). That is, the subjects who had the greatest decrease in plasma volume with furosemide and exercise also had the greatest decrease in SaO_2 when compared to the placebo condition. Furosemide has many systemic effects aside from that of diuresis, and it is difficult to make firm conclusions however this would suggest that the role of plasma volume and pulmonary blood volume in the genesis of EIH is worthy of further investigation.

Several authors have described alterations in a number of indirect indicators of barrier function post-exercise including increases in residual volume, decrease in diffusing capacity for carbon monoxide (D_LCO), and decreases in transthoracic electrical impedance that are consistent with pulmonary edema (22, 23, 104, 129, 130). Additionally Hammond et al., (63) described widened $[A-a]DO_2$ and \dot{V}_A/\dot{Q} inequality following heavy exercise and suggested that a structural change in the lung could account for their findings. Despite this, little further investigative work has been done in this area, particularly in athletic populations. Vaughan et al., (164) failed to find an increase in lung water (measured by the

indicator dilution method) with sustained exercise, although an initial increase in lung water was attributed to a redistribution of blood flow, however, their subjects were exercising at a work load of less than 150 watts and a cardiac output of less than $20 \text{ l}\cdot\text{min}^{-1}$. An interesting study by Gallagher et al., (56) examined chest radiographs in five males following a $\dot{V}O_2$ max test. No evidence of pulmonary edema was found, however this study suffered from the same problem as the one of Vaughn et al., the subjects studied were normal non-athletic males who have not been shown to have evidence for inadequate gas exchange during exercise. Pulmonary capillary failure has been demonstrated in the rabbit lung at 40 mmHg of transmural pressure and it has been estimated in human lungs, during exercise of less than $4.0 \text{ l}\cdot\text{min}^{-1}$, that transcapillary pressures of 36 mmHg would be likely, leaving little safety margin (179). The consequences of such capillary failure in humans would be increased capillary permeability at the lower end of the spectrum and frank pulmonary hemorrhage with higher pressures.

Recently Schaffartzik et al., (147) have argued that sustained increases in $\log SD\dot{Q}$ persisting during recovery from exercise, during exercise and normobaric hypoxia is indicative of pulmonary edema. This subgroup of subjects had significant impairment of pulmonary function after exercise compared to controls and also had lower arterial saturation and pH associated with exercise. In the present study, it was possible to define two subgroups with respect to $\log SD\dot{Q}$ however, there were no significant differences between groups with respect to pH, SaO_2 , PaO_2 or other measured parameters. It is not possible to comment on the possibility of pulmonary edema in the present study as no inert gas samples were taken during recovery and the overall shift in the \dot{V}_A/\dot{Q} distribution may obscure alterations in blood flow distribution towards zones of low \dot{V}_A/\dot{Q} . Also the screening process used in selecting subjects excluded any who had post-exercise cough, hemoptysis or decrease in pulmonary flows which could be indicative of pulmonary edema.

Summary of findings

This paper describes \dot{V}_A/\dot{Q} mismatch, diffusion limitation and a variable decrease in PaO_2 in highly trained athletes during exercise. The decrease in PaO_2 is less than previously described for similar athletic populations and may reflect the small muscle mass used in cycling exercise. The increase in \dot{V}_A/\dot{Q} mismatch was largely due to increases in the perfusion related indices of dispersion and does not rule out pulmonary edema as a plausible explanation for these findings. The $[\text{A-a}]\text{DO}_2(\text{o-p})$ was significantly correlated with pulmonary transit time and PaO_2 during maximal exercise could be predicted on the basis of pulmonary transit time, $\dot{V}_E/\dot{V}\text{CO}_2$ and \dot{V}_A/\dot{Q} as indicated by (A-a)D. $[\text{A-a}]\text{DO}_2(\text{o-p})$ was correlated with both pulmonary blood volume index and whole blood volume suggesting that blood volume expansion seen in highly trained athletes and the ability to expand pulmonary blood volume may provide important defenses against pulmonary diffusion limitation.

REFERENCES

1. Akabas, S.R., A.R. Bazy, H. Reichman, G.G. Haddad. Training with inspiratory flow resistive (IFR) loads increases the oxidative capacity of the sheep diaphragm. *Am. Rev. Respir. Dis.* 1985;131:A307.
2. Andersen, P., B. Saltin. Maximal perfusion of skeletal muscle in man. *J. Physiol. (Lond.)* 1985;366:233-249.
3. Anholm, J.D., R.L. Johnson, M. Ramanathan. Changes in cardiac output during sustained maximal ventilation in man. *J. Appl. Physiol.* 1987;63(1):181-187.
4. Anholm, J.D., J. Stray-Gundersen, M. Ramanathan, R.L. Johnson. Sustained maximal ventilation after endurance exercise in athletes. *J. Appl. Physiol.* 1989;67(5):1759-1763.
5. Åstrand, P.-O., T.E. Cuddy, B. Saltin, J. Stenberg. Cardiac output during submaximal and maximal work. *J. Appl. Physiol.* 1964;19(2):268-274.
6. Aubier, M., N. Viires, G. Syllie, R. Mozes, C. Roussos. Respiratory muscle contribution to lactic acidosis in low cardiac output. *Am. Rev. Respir. Dis.* 1982;126:684-652.
7. Ayres, L.N. Carbon monoxide diffusing capacity. In: Wilson AF, ed. Pulmonary function testing: indications and interpretation. New York: Grune and Stratton, 1985:
8. Backmann, R., W. Hartung. Differentiating measurements of blood volumes in isolated human lungs. International Symposium on Pulmonary Circulation. Prague: Karger, 1969: 327-337.
9. Barr, P.O.-2., M. Beckman, H. Bjurstedt, J. Brismar, C.M. Hesser, G. Matel. Time course of blood gas changes provoked by light and moderate exercise in man. *Acta Physiol. Scand.* 1964;60:1-17.
10. Bartlett, D. Post-natal growth of the mamalian lung : influence of exercise and thyroid activity. *Resp. Physiol.* 1970;9:50-57.
11. Bartlett, R.G., H.F. Brubach, H. Specht. Oxygen cost of Breathing. *J. Appl. Physiol.* 1958;12(3):413-424.
12. Bebout, D.E., D. Storey, J. Roca, et al. Effects of altitude acclimatization on pulmonary gas exchange during exercise. *J. Appl. Physiol.* 1989;67(6):2286-2295.
13. Bechbache, R.R., J. Duffin. The entrainment of breathing frequency by exercise rhythm. *J. Physiol.* 1977;271:553-561.
14. Bender, P.R., B.J. Martin. Maximal ventilation after exhausting exercise. *Med. Sci. Sports Exercise* 1985;17(1):164-167.
15. Bent-Hansen, L. Initial plasma disappearance and distribution volume of [¹³¹I]albumin and [¹²⁵I]fibrinogen in man. *Acta Physiol Scand.* 1989;136:455-461.

16. Bertolin, J.F., J. Carles, A. Tellac. Assessment of the ventilatory performance of athletes using the maximal expiratory flow-volume curve. *Int. J. Sports Med.* 1986;7:80-85.
17. Bjurstedt, H., O. Wigertz. Dynamics of arterial oxygen tension in response to sinusoidal work load in man. *Acta Physiol. Scand.* 1971;82:236-249.
18. Bradley, M.E., D.E. Leith. Ventilatory muscle training and the oxygen cost of sustained hyperpnea. *J. Appl. Physiol.* 1978;45(6):885-892.
19. Brancatisano, A., T.C. Amis, A. Tully, L.A. Engel. Blood flow distribution within rib cage muscles. *J. Appl. Physiol.* 1991;70(6):2559-2565.
20. Brooks, G.A., T.D. Fahey. *Exercise Physiology: Human Bioenergetics and its Applications.* Toronto: John Wiley & Sons, 1984:726.
21. Brotherhood, J., B. Borzovic, L.G.C.E. Pugh. Hematological status of middle- and long-distance runners. *Clin. Sci. Mol. Med.* 1975;48:139-145.
22. Buono, M.J., S.H. Constable, A.R. Morton, T.C. Rotkis, P.R. Stanford, J.H. Wilmore. The effects of an acute bout of exercise on selected pulmonary function measurements. *Med. Sci. Sports Exerc.* 1981;13:290-293.
23. Buono, M.J., J.H. Wilmore, F.B. Roby. Indirect assessment of thoracic fluid balance following maximal exercise in man. *J. Sports Sci.* 1983;1:217-226.
24. Bye, P.T., S.A. Esau, K.R. Walley, P.T. Macklem, R.L. Pardy. Ventilatory muscles during exercise in air and O₂ in normal men. *J. Appl. Physiol.* 1984;56:464-471.
25. Bye, P.T.B., G.A. Farkas, C. Roussos. Respiratory factors limiting exercise. *Ann. Rev. Physiol.* 1983;45:439-451.
26. Byrne-Quinn, E., J.V. Weil, I.E. Sodal, G.F. Filley, R.F. Grover. Ventilatory control and the athlete. *J. Appl. Physiol.* 1971;30(1):91-98.
27. Casaburi, R., J. Daly, J.E. Hansen, R.M. Effros. Abrupt changes in mixed venous blood gas composition after the onset of exercise. *J. Appl. Physiol.* 1989;67(3):1106-1112.
28. Cerretelli, P., R. Sikand, L.E. Farhi. Readjustments in cardiac output and gas exchange during onset of exercise and recovery. *J. Appl. Physiol.* 1966;21(4):1345-1350.
29. Coast, J.R., R.A. Jensen, S.S. Cassidy, M. Ramanathan, J. R. L. Johnson. Cardiac output and O₂ consumption during inspiratory threshold breathing. *J. Appl. Physiol.* 1988;64(4):1624-1628.
30. Coates, J., G. Johnson, A. MacDonald. Breathing frequency and tidal volume: relationship to breathlessness. In: Porter R, ed. *Breathing: Herring-Breuer Centenary Symposium.* London: Churchill, 1970: 297-314.

31. Covertino, V.A. Blood volume: Its adaptation to endurance training. *Med. Sci Sports Exerc* 1991;23(12):1338-1348.
32. Coyle, E.F., M.K. Hemmert, A.R. Coggan. Effects of detraining on cardiovascular responses to exercise: role of blood volume. *J. Appl. Physiol.* 1986;60(1):95-99.
33. Dehmer, G.J., B.G. Firth, L.D. Hillis, P. Nicod, J.T. Willerton, S.E. Lewis. Nongeometric determinations of right ventricular volumes from equilibrium blood pool scans. *Am. J. Cardiol.*, 1982;49:79-84.
34. Dempsey, J.A. Is the lung built for exercise? *Med. Sci. Sports Exerc.* 1986;18(2):143-155.
35. Dempsey, J.A., P.G. Hanson, K.S. Henderson. Exercised-induced arterial hypoxaemia in healthy human subjects at sea level. *J. Physiol. (Lond)* 1984;355:161-175.
36. Dempsey, J.A., D. Pegelow, R. Fregosi. Mechanical vs chemical determinants of hyperventilation in heavy exercise (Abs.). *Med. Sci. Sports Exerc.* 1982;14 (suppl.):131.
37. Derks, C.M. Ventilation-perfusion distribution in young and old volunteers during mild exercise. *Bull. Eur. Pathophysiol. Respir.* 1980;16:145-154.
38. Dill, D.B., K. Braithwaite, W.C. Adams, E.M. Bernauer. Blood volume of middle distance runners: effects of 2300 m altitude and comparison with non-athletes. *Med. Sci. Sports Exerc.* 1974;6:1-7.
39. DiPrampo, P.E. Metabolic and circulatory limitations to $\dot{V}O_2$ max at the whole animal level. *J. Exp. Biol.* 1985;115:319-331.
40. Domino, K.B., F.W. Cheney, B.L. Eisenstein, M.P. Hlastala. Effect of regional alveolar hypoxia on gas exchange in pulmonary edema. *J. Appl. Physiol.* 1992;145:340-347.
41. Domino, K.B., B.L. Eisenstein, F.W. Cheney, M.P. Hlastala. Pulmonary blood flow and ventilation-perfusion heterogeneity. *J. Appl. Physiol.* 1991;71(1):252-258.
42. Domino, K.B., M.P. Hlastala, B.L. Einstein, F.W. Cheney. Effect of regional alveolar hypoxia on gas exchange in dogs. *J. Appl. Physiol.* 1989;67(2):730-735.
43. Ekblom, J., L. Hermansen. Cardiac output in athletes. *J. Appl. Physiol.* 1968;25:619-625.
44. Ellis, J.H., P.P. Steele. Comparison of pulmonary blood volume in dogs by radiocardiography and dye dilution. *J. Appl. Physiol.* 1974;37(4):570-574.
45. Evans, J.W., P.D. Wagner. Limits on $\dot{V}A/\dot{Q}$ distributions from analysis of experimental inert gas elimination. *J. Appl. Physiol.* 1977;42:889-898.

46. Fagard, R.J., A. Aubert, R. Lysens, J. Staessen, L. Vanees, A. Amery. Noninvasive assessment of seasonal variations in cardiac structure and function in cyclists. *Circulation* 1982;67(4):896-901.
47. Fairbarn, M.S., K.C. Coutts, R.L. Pardy, D.C. McKenzie. Improved respiratory muscle endurance of highly trained cyclists and the effects on maximal exercise performance. *Int J Sports Med* 1991;12(1):66-70.
48. Farkas, G.A., C. Roussos. Histochemical and biochemical correlates of ventilatory muscle fatigue in emphysematous hamsters. *J. Clin. Invest.* 1984;74:1214-1220.
49. Fisman, E.Z., G. Frank, E. Ben-Ari, et al. Altered left ventricular volume and ejection fraction responses to supine dynamic exercise. *J. Am Coll Cardiol* 1990;15(3):582-588.
50. Fixler, D.E., J.M. Atkins, J.H. Mitchell, L.D. Horowitz. Blood flow to respiratory, cardiac, and limb muscles during graded exercise. *Am. J. Physiol.* 1976;231(5):1515-1519.
51. Folinsbee, L.J., E.S. Wallace, J.F. Bedi, S.M. Horvath. Exercise respiratory pattern in elite cyclists and sedentary subjects. *Med. Sci. Sports Exerc.* 1983;15(6):503-509.
52. Freedman, S., N. Cooke, J. Moxham. Production of lactic acid by respiratory muscles. *Thorax* 1983;38:50-54.
53. Fregosi, R.F., M. Sanjak, D.J. Paulson. Endurance training does not affect diaphragm mitochondrial respiration. *Resp. Physiol.* 1987;67(2):225-237.
54. Fritts, H.W., J. Filler, A.P. Fishman, A. Courand. The efficiency of ventilation during voluntary hyperpnea. *J. Clin. Invest.* 1959;38:1339-1348.
55. Gale, G.E., J. R. Torre-Bueno, R. E. Moon, H. A. Saltzman and P. D. Wagner. Ventilation-perfusion inequality in normal humans during exercise at sea level and simulated altitude. *J. Appl Physiol.* 1985;58(3):978-988.
56. Gallagher, C.G., W. Huda, M. Rigby, D. Greenberg, M. Younes. Lack of radiographic evidence of interstitial pulmonary edema after maximal exercise in normal subjects. *Am. Rev. Respir. Dis.* 1988;137:474-476.
57. Ginzton, L.E., R. Conant, M. Brizendine, M.K. Laks. Effect of long-term high intensity aerobic training on left ventricular volume during maximal upright exercise. *J Am Coll Cardiol* 1986;14(2):364-371.
58. Giuntini, C., M.L. Lewis, A.S. Luis, R.M. Harvey. A study of the pulmonary blood volume in man by quantitative radiocardiography. *J. Clin. Invest.* 1963;42(10):1963.
59. Glazier, J.B., J.M.B. Hughes, J.E. Maloney, J. West. Measurements of capillary dimensions and blood volume in rapidly frozen lungs. *J. Appl. Physiol.* 1969;26:65-76.

60. Gledhill, N., A.B. Froese, F. J. Buick and A. C. Bryan. Va/Q inhomogeneity and AaDO₂ in man during exercise: Effect of SF₆ breathing. *J. Appl Physiology* 1978;45(4):512-515.
61. Gledhill, N.L., D. Cox, V. Jamnik. Stroke volume of endurance athletes does not plateau and the related cardiac time intervals are paradoxical. *Med. Sci. Sports Exerc.* 1992;24(5(Suppl.)):S29.
62. Górski, J., Z. Naimiot, J. Giedrojc. Effect of exercise on metabolism of glycogen and triglycerides in the respiratory muscles. *Pflügers Archiv.* 1978;377:251-254.
63. Hammond, M.D., G.E. Gale, S. Kapitan, A. Ries, P.D. Wagner. Pulmonary gas exchange in humans during exercise at sea level. *J. Appl. Physiol.* 1985;60(5):1590-1598.
64. Harris, P., D. Heath. The measurement of blood volume in the lungs. In: Human pulmonary circulation its form in health and disease. Edinburg, London and New York: Churchill Livingstone, 1977: 105-117.
65. Harrop, G.A. The oxygen and carbon dioxide content of arterial blood in normal individuals and in patients with anemia and heart disease. *J. Exp. Med.* 1919;30:241-257.
66. Hermansen, L., B. Ekblom and B. Saltin. Cardiac output during submaximal and maximal treadmill and cycle exercise. *J. Appl. Physiol.* 1970;29(1):82-86.
67. Hesser, C.M., D. Linnarsson, L. Fagraeus. Pulmonary mechanics and work of breathing at maximal ventilation and raised air pressure. *J. Appl. Physiol.* 1981;50(4):747-753.
68. Hlastala, M.P., D.D. Ralph, A.L. Babb. Influence of gas physical properties on pulmonary gas exchange. *Adv. Exp. Med. Biol.* 1988;227:33-38.
69. Hlastala, M.P., H.T. Robertson. Inert gas elimination characteristics of the normal and abnormal lung. *J. Appl. Physiol.* 1978;44(2):258-266.
70. Hogg, J.C., B.A. Martin, S. Lee, T. McLean. Regional differences in erythrocyte transit in normal lungs. *J. Appl. Physiol* 1985;62:1236-1243.
71. Hogg, J.C., T. McLean, B.A. Martin, B. Wiggs. Erythrocyte transit and neutrophil concentration in the dog lung. *J. Appl. Physiol.* 1988;65(3):1217-1225.
72. Hopkins, S.R., D.C. McKenzie. Hypoxic ventilatory response and arterial desaturation during heavy work. *J. Appl. Physiol.* 1989;67(3):1119-1124.
73. Hopper, M.K., A.R. Coggan, E.F. Coyle. Exercise stroke volume relative to plasma-volume expansion. *J. Appl. Physiol.* 1988;64(1):404-408.
74. Houston, C.S., J.R. Sutton, A. Cymerman, J.T. Reeves. Operation Everest II: man at extreme altitude. *J. Appl. Physiol.* 1987;63(2):887-882.
75. Ianuzzo, C.D., M.J. Spaulding, H. Williams. Exercise-induced glycogen utilization by the respiratory muscles. *J. Appl. Physiol.* 1987;62(4):1405-1409.

76. International Committee for Standardization in Hematology. Recommended methods for measurement of red-cell and plasma volume. *J. Nucl. Med.* 1980;21:793-800.
77. Iskandrian, A.S., A.-H. Hakki, S.A. Kane, B.L. Segal. Changes in pulmonary blood volume during upright exercise. *Chest* 1982;82(1):54-58.
78. Jensen, J.I., S. Lyager, O.F. Pedersen. The relationship between maximal ventilation, breathing pattern and mechanical limitation of ventilation. *J. Physiology* 1980;309:521-532.
79. Johnson, R.L., M. Reid. Limits of oxygen transport to the diaphragm. *Am. Rev. Respir. Dis.* 1979;119:113-114.
80. Johnson, R.L.J., W.S. Spicer, J.M. Bishop, R.E. Forster. Pulmonary capillary blood volume, flow and diffusing capacity during exercise. *J. Appl. Physiol.* 1960;15:893-902.
81. Jones, N.L., K.J. Killian, D. Stubbing. The thorax in exercise. In: Roussos C, ed. *Thorax*. New York: Marcel Dekker, 1985:
82. Keens, T.G., V. Chen, P. Patel, P. O'Brien, H. Levison, C.D. Ianuzzo. Cellular adaptations of the ventilatory muscles to a chronic increased respiratory load. *J. Appl. Physiol.* 1978;44(6):905-908.
83. Kelbæk, H., L. Heslet, K. Skagen, O. Munck, J. Godtfredsen. First pass radionuclide cardiography for determination of cardiac output: evaluation of an improved method. *Int. J. Cardiol.* 1989;23:79-85.
84. Kelbæk, H., H. Jensen, P.V. Madsen, O. Munck, J. Godtfredsen. Determination of cardiac output by first passage radiocardiography. *Scand J. Clin Lab Invest* 1987;47:469-474.
85. Kelman, G.R. Digital computer procedure for the conversion of oxygen tension into saturation. *J. Appl. Physiol.* 1966;21:1375-1376.
86. Kelman, G.R. Digital subroutines for the conversion of PCO₂ into blood CO₂ content. *Resp. Physiol.* 1967;3:111-116.
87. Kelman, G.R. Computer programs for the production of O₂-CO₂ diagrams. *Resp. Physiol.* 1968;4:260-269.
88. Kjellberg, S.R., U. Rudhe, T. Sjostrand. Increase of the amount of hemoglobin and plasma volume in connection with endurance training. *Acta Physiol. Scand.* 1949;19:146-151.
89. Lang, F., S. Daum. Mixed venous PO₂ during exercise in patients with different cardiopulmonary function. *Respiration* 1983;44(3):161-170.
90. Leiberman, D.A., J.A. Faulkner, A.B. Craig, L.C. Maxwell. Performance and histochemical composition of guinea pig and human diaphragm. *J. Appl. Physiol.* 1973;34(2):233-237.

91. Leith, D.E., M. Bradley. Ventilatory muscle strength and endurance training. *J. Appl. Physiol.* 1976;41(4):508-516.
92. Levinsky, N.G. Acidois and Alkalosis. In: Thorn GW, Adams RD, Braunwald E, Isselbacher KJ, Petersdorf RG, ed. *Harrison's Principals of Internal Medicine.* Eighth ed. New York: McGraw-Hill, 1977: 377.
93. Loke, J., D.A. Mahler, J.A. Virgulto. Respiratory muscle fatigue after marathon running. *J. Appl. Physiol.* 1982;52:821-824.
94. Longhurst, J.C., A.R. Kelly, W.J. Gonyea, J.H. Mitchell. Echocardiographic left ventricular masses in distance runners and weight lifters. *J. Appl. Physiol.* 1980;48:154-162.
95. Longhurst, J.C., A.R. Kelly, W.J. Gonyea, J.H. Mitchell. Chronic training with static and dynamic exercise: cardiovascular adaptation and response to exercise. *Circ Res* 1981;48(suppl 1)(I):171-8.
96. MacNee, W., M. B. A, B. Wiggs, A.S. Belzberg, J.C. Hogg. Regional pulmonary transit times in humans. *J. Appl. Physiol.* 1989;66:844-50.
97. Mador, M.J., F.A. Acevedo. Effect of respiratory muscle fatigue on subsequent exercise performance. *J. Appl. Physiol.* 1991;70(5):2059-2065.
98. Manohar, M. Blood flow to the respiratory and limb muscles and to abdominal organs during maximal exertion in ponies. *J. Physiol. (Lond)* 1986;377:25-35.
99. Manohar, M. Costal vs. crural diaphragmatic blood flow during submaximal and near-maximal exercise in ponies. *J. Appl. Physiol.* 1988;65(4):1514-1519.
100. Manohar, M. Inspiratory and expiratory muscle perfusion in maximally exercised ponies. *J. Appl. Physiol.* 1990;68(2):544-548.
101. Manohar, M., T.E. Goetz, L.C. Holste, D. Nganwa. Diaphragmatic O₂ and lactate extraction during submaximal and maximal exertion in ponies. *J. Appl. Physiol.* 1988;64(3):1203-1209.
102. Manohar, M., T.E. Goetz, D. Nganwa. Costal diaphragmatic O₂ and lactate extraction in laryngeal hemiplegic ponies during exercise. *J. Appl. Physiol.* 1988;65(4):1723-1728.
103. Maron, B.J. Structural features of the athlete heart as defined by echocardiography. *J Am Coll Cardiol* 1986;7(1):190-203.
104. Maron, M.B., L.H. Hamilton, M.G. Maksud. Alterations in pulmonary function consequent to competitive marathon running. *Med. Sci. Sports Exerc.* 1979;11(3):244-249.
105. Martin, B., M. Heintzelman, H.I. Chen. Exercise performance after ventilatory work. *J. Appl. Physiol.* 1982;52(6):1581-1585.

106. Martin, B., J.V. Wiel, K.E. Sparks, R.E. McCullough, R.F. Grover. Exercise ventilation correlates positively with ventilatory chemoresponsiveness. *J. Appl. Physiol.* 1978;45(4):557-564.
107. Martin, B.A., J.M. Stager. Ventilatory endurance in athletes and non athletes. *Med. Sci. Sports Exercise* 1981;13(1):21-26.
108. McEvoy, R.D., N.J.H. Davies, F.L. Manino, et al. Pulmonary gas exchange during high frequency ventilation. *J. Appl. Physiol.* 1982;52(5):1278-1287.
109. McKerrow, C.B., A.B. Otis. Oxygen cost of hyperventilation. *J. Appl. Physiol.* 1956;9:375-379.
110. Mead, J. Control of respiratory frequency. *J. Appl. Physiol.* 1960;15:325-336.
111. Melin, J.A., W. Wijns, A. Robert, M. Nannan, P. De Coster, C. Beckers and J. M. Detry. Validation of radionuclide cardiac output measurements during exercise. *J. Nucl. Med* 1985;26(12):1386-1393.
112. Milic-Emili, J., J.M. Petit, R. Deroanne. Mechanical work of breathing during exercise in trained and untrained subjects. *J. Appl. Physiol.* 1962;17:43-46.
113. Moore, K.L. *The Developing Human*. Philadelphia: W. B. Saunders Company, 1974
114. Moore, R.L., P.D. Gollnick. Response of ventilatory muscles of the rat to endurance training. *Pflügers Arch.* 1982;392:268-271.
115. Morganroth, J., B.J. Maron, W.L. Henry, S.E. Epstein. Comparative left ventricular dimensions in trained athletes. *Ann. Int. Med.* 1975;82:521-524.
116. Muche, T.I. Skeletal muscle blood flow in exercising dogs. *Med. Sci. Sports Exerc.* 1988;20(5(suppl.)):s104-s108.
117. NHLBI, w. summary. Respiratory muscle fatigue: report of the respiratory muscle fatigue workshop group. *Am. Rev. Respir. Dis.* 1990;142:474-480.
118. Olafsson, S., R.E. Hyatt. Ventilatory mechanics and expiratory flow limitation during exercise in normal subjects. *J. Clin. Invest.* 1969;45:564-573.
119. Otis, A.B. The work of breathing. *Physiol. Rev.* 1954;34:449-458.
120. Otis, A.B., W.O. Fenn, H. Rahn. Mechanics of breathing in man. *J. Appl. Physiol.* 1950;2:592-603.
121. Pan, L.G., H.V. Forster, G.E. Bisgard, S.M. Dorsey, M.A. Busch. Cardiodynamic variables and ventilation during treadmill exercise in ponies. *J. Appl. Physiol.* 1984;57:753-759.
122. Pfisterer, M.E., D. R. Ricci, G. Schuler, S. S. Swanson, D. G. Gordon, K. E. Peterson and W. L. Ashburn. Validity of left ventricular ejection fractions measured at rest and peak exercise by equilibrium radionuclide angiography using short acquisition times. *J. Nuc. Med.* 1979;20:484-490.

123. Pfisterer, M.E., B. A, S.M. Swanson, R. Slutsky, V. Froelicher, W.L. Ashburn. Reproducibility of ejection-fraction determinations by equilibrium radionuclide angiography in response to supine bicycle exercise: concise communication. *J. Nucl Med.* 1979;20:491-495.
124. Pouliner, L.R., G.J. Dehmer, S.E. Lewis, R.W. Parkey, C.G. Bloomquist, J.T. Willerton. Left ventricular performance in normal subjects: A comparison of responses to exercises in the supine and upright positions. *Circulation* 1980;62(3):528-534.
125. Powers, S., S. Dodd, J. Woodyard, R. Beadle, G. Church. Alterations in hemoglobin saturation during incremental arm and leg exercise. *Br. J. Sports Med.* 1984;18:212-216.
126. Powers, S.K., S. Dodd, J. Lawler, et al. Incidence of exercise induced hypoxemia in elite endurance athletes at sea level. *Eur. J. Appl. Physiol.* 1988;58:298-302.
127. Powers, S.K., J. Lawler, J.A. Dempsey, S. Dodd, G. Landry. Effects of incomplete pulmonary gas exchange on VO_2 max. *J. Appl. Physiol* 1989;66(6):2491-2495.
128. Powers, S.K., J. Lawler, D. Criswell, et al. Endurance -training-induced cellular adaptations in respiratory muscles. *J. Appl. Physiol.* 1990;69(5):2114-2118.
129. Rasmussen, B.S., B. Hanel, K. Jensen, B. Serup, N.H. Secher. Decrease in pulmonary diffusion capacity after maximal exercise. *J. Sports Sci.* 1984;4:185-188.
130. Rasmussen, B.S., P. Elkjaer, B. Juhl. Impaired pulmonary and cardiac function after maximal exercise. *J. Sports Sci.* 1988;6:219-228.
131. Rebuck, A.S., E.J.M. Campbell. A clinical method for assessing the ventilatory response to hypoxia. *Am. Rev. Resp. Dis.* 1974;109:345-350.
132. Rebuck, A.S., A.S. Slutsky. Measurement of ventilatory responses to hypercapnia and hypoxia. In: Hornbein TF, ed. Regulation of Breathing, Part II. New York: Marcel Dekker Inc., 1981: 745-773.
133. Reid, M.B., R.L. Johnson. Efficiency, maximal blood flow and aerobic work capacity of canine diaphragm. *J. Appl. Physiol.* 1983;54(3):763-772.
134. Rerych, S.K., P. M. Scholz, D. C. Sabiston and R. H. Jones. Effects of exercise training on left ventricular function in normal subjects: a longitudinal study by radionuclide angiography. *Am J. Cardiol* 1980;45:244-252.
135. Reuschlein, P.L., W.G. Reddan, J.F. Burpee, J.B.L. Gee, J. Rankin. The effect of physical on the pulmonary diffusing capacity during submaximal work. *J. Appl. Physiol.* 1968;24:152-158.
136. Robertson, C.H., G.H. Foster, R.L. Johnson. The relationship of respiratory failure to the oxygen consumption of, lactate production by, and distribution of blood flow among respiratory muscles during increased inspiratory resistance. *J. Clin. Invest.* 1977;59:31-42.

137. Robertson, C.H., M.A. Pagel, J. R. L. Johnson. The distribution of blood flow, oxygen consumption and work output among the respiratory muscles during unobstructed hyperventilation. *J. Clin. Invest.* 1977;59:43-50.
138. Robertson, H.T., R.L. Coffey, T.A. Standaert, W.E. Truog. Respiratory and inert gas exchange during high-frequency ventilation. *J. Appl. Physiol.* 1982;52:683-689.
139. Roca, J., M.C. Hogan, D. Storey, et al. Evidence for tissue diffusion limitation of $\dot{V}O_2$ max in normal humans. *J. Appl. Physiol.* 1989;67(1):291-299.
140. Rochester, D.F., G. Bettini. Diaphragmatic blood flow and energy expenditure in the dog. *J. Clin. Invest.* 1976;57:661-672.
141. Rochester, D.F., A.M. Briscoe. Metabolism of the working diaphragm. *Am. Rev. Respir. Dis.* 1979;119:101-106.
142. Rochester, D.R. Measurement of diaphragmatic blood flow and oxygen consumption in the dog by the Kety-Schmidt Technique. *J. Clin. Invest.* 1974;53:1216-1225.
143. Roncoroni, A.J., H.A. Adrogué, C.W. DeObrutski, M.L. Marchisio, M.R. Herrera. Metabolic acidosis in status asthmaticus. *Respiration* 1976;33:85-94.
144. Roughton, F.J.W. The average time spent in the pulmonary capillary and its relation to the rates of CO uptake and elimination in man. *Am. J. Physiol.* 1943;143:621-633.
145. Roughton, F.J.W., R.E. Forster. Relative importance of diffusion and chemical reaction rates in determining the rate of exchange of gases in the human lung, with special reference to true diffusing capacity of pulmonary membrane and volume of blood in the lung capillaries. *J. Appl. Physiol.* 1957;11(290-302).
146. Rowell, L.R., H.L. Taylor, Y. Wang and W. S. Carlson. Saturation of arterial blood with oxygen during maximal exercise. *J. Appl. Physiol.* 1964;19(2):284-286.
147. Schaffartzik, W., D.C. Poole, T. Derion, et al. $\dot{V}A/\dot{Q}$ distribution during heavy exercise and recovery in humans: implications for pulmonary edema. *J. Appl. Physiol.* 1992;72(5):1657-1667.
148. Schoene, R.B. Control of ventilation in climbers to extreme altitude. *J. Appl. Physiol.* 1982;53(4):886-896.
149. Shephard, R.J. The oxygen cost of breathing during vigorous breathing. *Quart. J. Exper. Physiol* 1966;51:336-360.
150. Shephard, R.J. The maximum sustained voluntary ventilation in exercise. *Clin. Sci.* 1967;32:189-197.

151. Slutsky, R., J. Karliner, D. Rocci, et al. Left ventricular volumes by gated equilibrium radionuclide angiography: a new method. *Circulation* 1979;60(3):556-564.
152. Smith, T.D., P. Richards. A simple kit for the preparation of ^{99m}Tc-labeled red blood cells. *J. Nucl. Med* 1975;17(2):126-131.
153. Starmer, C.F., D.O. Clarke. Computer computations of cardiac output using the gamma function. *J. Appl. Physiol.* 1970;28:219-220.
154. Staub, N.C., J.M. Bishop, R.E. Forster. Importance of diffusion and chemical reactions in O₂ uptake in the lung. *J. Appl. Physiol.* 1962;18:673-680.
155. Stockley, R.A. The contribution of the reflex hypoxic drive to the hyperpnoea of exercise. *Respirat. Physiol.* 1978;35:79-87.
156. Suskind, M., R.A. Bruce, M.E. McDowell, F.W. Lovejoy. Normal variations in end-tidal and arterial blood carbon dioxide and oxygen tensions during moderate exercise. *J. Appl. Physiol.* 1950;3:282-290.
157. Suzuki, S., J. Suzuki, T. Okubo. Expiratory muscle fatigue in normal subjects. *J. Appl. Physiol.* 1991;70(6):2632-2639.
158. Szal, S.A., R.B. Schoene. Ventilatory response to rowing and cycling in elite oarswomen. *J. Appl. Physiol.* 1989;64(1):264-269.
159. Thompson, J.M., J. A. Dempsey, L. W. Chosy, N. T. Shahidi and W. G. Reddan. Oxygen transport and oxyhemoglobin dissociation during prolonged muscular work. *J. Appl. Physiol.* 1974;37(5):658-664.
160. Thomsen, J.K., N.F. Anderson, K. Bulow, A. Devantier. Blood and plasma volumes determined by carbon monoxide gas, ^{99m}Tc-labelled erythrocytes, ¹²⁵I-albumin and T 1824 technique. *Scan. J. Clin. Lab. Invest.* 1991;51:185-190.
161. Torre-Bueno, J.R., P.D. Wagner, H. A. Saltzman, G. E. Gale and R. E. Moon. Diffusion limitation in normal humans during exercise at sea level and simulated altitude. *J. Appl. Physiol.* 1985;58:989-995.
162. Tsu, M.E., A.L. Babb, E.M. Sugiyama, M.P. Hlastala. Dynamics of soluble gas exchange in the airways: II. Effects of breathing conditions. *Resp. Physiol.* 1991;83:261-276.
163. Turner, P.S. The effect of furosemide on exercise induced hypoxemia in highly trained athletes. [M.P.E.]. University of British Columbia, 1992.
164. Vaughn, T.R., E.M. DeMarino, N.C. Staub. Indicator dilution lung water and capillary blood volume in prolonged heavy exercise in normal men. *Am. Rev. Respir. Dis.* 1976;133:757-162.
165. Viires, N., M. Aubier, A. Rassidakis, C. Roussos. Regional blood flow distribution in dog during induced hypotension and low cardiac output. *J. Clin. Invest.* 1983;72:935-947.

166. Wagner, P.D. Diffusion and chemical reaction in pulmonary gas exchange. *Physiol. Rev.* 1977;57:257-312.
167. Wagner, P.D., P.F. Naumann, R.B. Laravuso. Simultaneous measurement of eight foreign gases in blood by gas chromatography. *J. Appl. Physiol.* 1974;36:600-605.
168. Wagner, P.D., H.A. Saltzman, J.B. West. Measurement of continuous distributions of ventilation-perfusion ratios:theory. *J. Appl. Physiol.* 1974;36(5):588-599.
169. Wagner, P.D., C.M. Smith, N.J.H. Davies, R.D. McEvoy, G.E. Gale. Estimation of ventilation-perfusion inequality by inert gas elimination without arterial sampling. *J. Appl. Physiol.* 1985;59(2):376-383.
170. Ward, S.A., B.J. Whipp, C.S. Poon. Density dependant air flow and ventilatory control during exercise. *Resp. Physiol.* 1982;49:267-277.
171. Warren, G.L., K.J. Cureton, W.F. Middendorf, C.A. Ray, J.A. Warren. Red blood cell pulmonary capillary transit time during exercise in athletes. *Med. Sci. Sport Exerc.* 1991;23(12):1353-1361.
172. Wasserman, K., B.J. Whipp, J.A. Davis. Respiratory physiology of exercise: metabolism, gas exchange and ventilatory control. In: Widdicombe JG, ed. *International Review of Physiology, Physiology III*. Baltimore: University Park Press, 1981:
173. Weinstein, W.B., W.M. Smoak. Technical difficulties in ^{99m}Tc labeling of erythrocytes. *J. Nucl. Med.* 1970;11:41-42.
174. West, J.B. Ventilation-perfusion inequality and overall gas exchange in computer models of the lung. *Resp. Physiol.* 1969;7:88-110.
175. West, J.B. State of the art. Ventilation-perfusion relationships. *Am. Rev. Respir. Dis.* 1977;116:919-943.
176. West, J.B. *Respiratory physiology—the essentials*. (3rd ed.) Baltimore, MA: Williams & Wilkins, 1985:85-127.
177. West, J.B., S.J. Boyer, D.J. Graber, et al. Maximal exercise at extreme altitudes on the summit of Mount Everest. *J. Appl. Physiol.* 1983;55(3):688-698.
178. West, J.B., P.H. Hackett, K.H. Maret, et al. Pulmonary gas exchange on the summit of Mount Everest. *J. Appl. Physiol.* 1983;*J. Appl. Physiol.*; 55(3):678-687.
179. West, J.B., K. Tsukimoto, O. Mathieu-Costello, R. Prediletto. Stress failure in pulmonary capillaries. *J. Appl. Physiol.* 1991;70(4):1731-1742.
180. West, J.B., P.D. Wagner. Pulmonary gas exchange. In: West JB, ed. *Bioengineering Aspects of the Lung*. New York: Marcell Dekker, 1977: 361-457. *Lung Biology in Health and Disease*;
181. West, J.B., P.D. Wagner. Ventilation-perfusion relationships. In: Crystal RG, West JB, et al., ed. *The Lung: Scientific Foundations*. New York: Raven Press Ltd., 1991: 1289-1305.

182. Whipp, B.J., and K. Wasserman. Alveolar arterial gas pressure differences during exercise. *J. Appl. Physiol.* 1969;27:361-365.
183. Whipp, B.J., J.A. Davis. Peripheral chemoreceptors and exercise hyperpnoea. *Med. Sci. Sports Exerc.* 1979;11(2):204-212.
184. Williams, J., S. Powers, M. Stuart. Hemoglobin desaturation in highly trained athletes during heavy exercise. *Med. Sci. Sports Exerc.* 1986;18:168-173.
185. Young, I.H., J. Woolcock. Changes in arterial blood gas tensions during unsteady-state exercise. *J. Appl. Physiol.* 1978;44(1):93-96.

APPENDIX A

REVIEW OF LITERATURE

Introduction

A debate of the factors providing a limit to maximal oxygen consumption ($\dot{V}O_2\text{max}$) has occupied exercise physiologists for decades. An increase in $\dot{V}O_2\text{max}$ is associated with hyperoxia and infusion of red blood cells and a decline in $\dot{V}O_2\text{max}$ is observed in anemia and hypoxia. This information is generally interpreted that oxygen delivery to the working muscle provides the major limit to maximal oxygen uptake (39). In humans, increases in $\dot{V}O_2\text{max}$ have been considered to be a result of both increases in cardiac output (\dot{Q}) and oxygen extraction ($a-vO_2$).

As the first step in the supply of oxygen to the working muscle, the respiratory system has not been thought to limit maximal performance. In most individuals, arterial oxygen tension is maintained during heavy exercise (20), and maximal capacity to ventilate during non-exercising conditions greatly exceeds observed exercise ventilation at maximal exercise (67, 118). Recently, reports of arterial hypoxemia in individuals exercising at maximal levels (35, 125, 126, 146, 159) and respiratory muscle fatigue in marathon runners after prolonged exercise (93) have focused attention on the respiratory system as a possible limiting factor to performance in individuals capable of maintaining very high levels of work.

In our laboratory (72), we have documented hypoxemia with arterial PO_2 as low as 68 torr in athletes exercising for five minutes at $\dot{V}O_2\text{max}$. These subjects exhibited only partial respiratory compensation for the metabolic acidosis of exercise; despite a mean pH of 7.21, mean pCO_2 levels of 36.4 torr, indicate only partial respiratory compensation of the acidosis. This has been observed by other authors in highly trained individuals (35) with less trained subjects showing compensatory hyperventilation to a pCO_2 of approximately 30 torr (34). In resting individuals, respiratory compensation for a metabolic acidosis could result in a pCO_2 as low as 15 torr (92). In highly trained athletes who have ample

stimulation (acidosis, hypoxia) to breathe, why are such profound disturbances in homeostasis tolerated without adequate compensation?

Recently some authors (25, 34), have recognized several factors, specifically energetics, muscle fatigue, respiratory drives and gas exchange, which may limit maximal exercise performance. The following review will discuss the ways in which the respiratory system could limit aerobic performance, with particular emphasis on the respiratory system during short term, near maximal, exercise.

Respiration and the respiratory muscles:

During quiet breathing the primary muscle of inspiration is the diaphragm, which as it contracts, increases thoracic volume. Abdominal viscera are displaced, leading to protrusion of the anterior abdominal wall. The quadratus lumborum acts in synergy with the diaphragm, opposing the the tendency to elevate the 12th rib. The scalene muscles exhibit activity even during quiet inspiration, and act to fix or elevate the thoracic inlet. Expiration is passive, and mainly due to elastic recoil of the lungs.

As ventilation increases, more of the respiratory muscle mass becomes active and at maximal exercise almost all of the muscles of the chest and back may be important. In inspiration, in addition to the muscles previously described, the sternocleidomastoid, external intercostal, serratus posterior superior and possibly portions of trapezius are recruited. Expiration becomes active, with strong contractions of the oblique and transverse muscles acting to compress the abdomen, increase intra-abdominal pressure, and displace the diaphragm upwards. In addition, the internal intercostal muscles and serratus posterior inferior act to assist expiration. The muscles of the back also have a role in respiration, acting as a counterbalance to the flexion induced by the contraction of the abdominal muscles.

Energetics

Many investigators have not considered respiratory muscles to receive a substantial fraction of \dot{Q} or $\dot{V}O_2$ during exercise. At high levels of ventilation if oxygen consumption by, and blood flow to, the respiratory muscles were substantial, this could limit maximal exercise by direct competition between the working muscle and respiratory muscles.

Blood flow to the diaphragm and other respiratory muscles

Investigation into the blood flow and metabolism of the respiratory muscles has focused mainly on the diaphragm, however, as exercise intensity increases other muscles of respiration become progressively more important. Data collection in humans is hampered by methodology; most studies have relied on data obtained from dogs, ponies, sheep and rats.

Estimates of blood flow of the various respiratory muscles are summarized in Table 12 and have been made during rest, inspiratory loads and exercise (19, 50, 98-100, 137, 140, 142). At rest, dog respiratory muscle comprising about 3-4% of body weight, receives about 1.5% of cardiac output (136, 137). During inspiratory resistive work, this value rises to greater than 10% of cardiac output. Blood flow to the diaphragm increases by 275% and 500% during mild and moderate exercise, which is roughly double the increase observed in gastrocnemius muscle (50). Intercostal muscle blood flow increases two to three times, similar to values for working skeletal muscle (50, 141). Blood flow to the respiratory muscles under work stress varies with the species investigated and type of stress applied. As outlined in the table below the resting blood flow of the diaphragm is about 150 % of intercostal muscle. During maximal exercise, these values may be higher than 260 and 130 $\text{ml}\cdot\text{min}^{-1}\cdot 100\text{g}^{-1}$ for diaphragm and intercostal muscle respectively. Blood flow values for the diaphragm are similar to maximal values reported for locomotor muscles in exercising dogs ($239 \text{ ml}\cdot\text{min}^{-1}\cdot 100\text{g}^{-1}$) (116), horses ($135\text{-}237 \text{ ml}\cdot\text{min}^{-1}\cdot 100\text{g}^{-1}$) (98) and isolated working quadriceps muscle ($240 \text{ ml}\cdot\text{min}^{-1}\cdot 100\text{g}^{-1}$) in humans (2).

Table 12. Blood flow of respiratory muscles

Study	\dot{Q}_{di} (ml·min ⁻¹ ·100g ⁻¹)		\dot{Q}_i (ml·min ⁻¹ ·100g ⁻¹)		Comments
	$\bar{x} \pm SD$		$\bar{x} \pm SD$		
	Rest	Stress	Rest	Stress	
Reid and Johnson, (1983)(133)	-	20±5			inspiratory load dogs
Rochester and Bettini,(1976) (140)	18±7	52±30			inspiratory load dogs
Rochester,(1974) (142)	22±6	-			dogs
Robertson et al.,(1977a)(136)	8±2	207±41	10	59	inspiratory load dogs
Brancatisano et al., (19)			7.3±0.8§ 8.2±0.4*	9.1±1.4§ 6.2±0.4*	inspiratory load dogs
Robertson et al.,(1977b)(137)	9±1	33±2			hypercapnia dogs
Fixler et al.,(1976)(48)	16±3	96±18	15±4	43±18	moderate exercise dogs
Manohar et al.,(1988a)(99)	12-13	151-245	7±2	119±9	maximal exercise ponies
Manohar,(1986)(98)	11±3	261±23	6±1	131±10	maximal exercise ponies
Manohar, (1990) (100)	~ 30	~330	~ 18	~ 150-170	maximal exercise trained ponies
Viires,(1983)(165)	~14	~50	~8-9	~16-21	cardiac tamponade dogs

\dot{Q}_{di} = diaphragmatic blood flow, \dot{Q}_i = intercostal blood flow, * = internal intercostal muscle, § = external intercostal muscle.

Manohar et al.,(99) originally used the data obtained in their investigations in ponies to argue that the amount of cardiac output diverted to respiratory muscles during maximal exercise is relatively small, based on the measurement of diaphragm blood flow, and excluding other muscles of respiration. More recent investigations (100), in exercising ponies suggest that blood flow for the entire respiratory mass is actually much higher and may be close to 15% of the total cardiac output during maximal exercise. In humans, cardiac output has been shown to increase by 50% over resting conditions in subjects breathing through an inspiratory resistance of 50-60% of maximum inspiratory pressure (29) and by 76% in isocapnic hyperventilation at maximal sustainable ventilation $>150 \text{ l}\cdot\text{min}^{-1}$ (3). No direct measures of respiratory muscle blood flow have been made.

Oxygen consumption of respiratory muscles

In animal models, oxygen consumption of the diaphragm has been shown to be linearly related to the work of breathing (136, 137). Like skeletal muscle, demands for increased oxygen are met by both increased flow and oxygen extraction (79, 101, 136, 137). In dogs breathing through inspiratory flow resistance, oxygen extraction becomes maximal at low work rates; increasing demand for oxygen is met by increasing blood flow (136, 137, 140). In ponies exercising at heavy and maximal levels increasing O_2 demands are met by both increments in perfusion and oxygen extraction (102).

Direct measures of respiratory muscle oxygen consumption have been made in dogs in a wide variety of experimental conditions (Table 13) (133, 136, 137, 140, 142). During mechanical ventilation, $\dot{\text{V}}\text{O}_2$ of the diaphragm is less than $1 \text{ ml}\cdot\text{min}^{-1}\cdot 100 \text{ g}^{-1}$ (137, 142) and doubles during quiet breathing (136, 137, 140, 142). During hypercapnic hyperventilation, oxygen consumption triples (142), although this level of hyperventilation is less than would be expected during heavy exercise. When resistance to inspiratory flow is

used to stress the respiratory muscles, diaphragmatic $\dot{V}O_2$ increases to about 15 ml·min⁻¹·100g⁻¹ (7.1-22.6) (133, 136, 140).

Table 13. $\dot{V}O_2$ of respiratory muscles

Study	$\dot{V}O_{2di}$ (ml·min ⁻¹ ·100g ⁻¹)		$\dot{V}O_{2i}$ (ml·min ⁻¹ ·100g ⁻¹)		Comments
	$\bar{x} \pm sd$		$\bar{x} \pm sd$		
	Rest	Stress	Rest	Stress	
Manohar, (1986)(98)	1.6	58.6	0.9	29.6	horses max exercise
Manohar et al.,(1988b)(101)	0.4	45.1			horses max exercise
Reid and Johnson, (1983)(133)	-	12.0±2.8			insp. flow resistance dogs
Rochester, (1974)(142)	1.2±0.3	2.8±0.9			hypercapnia dogs
Rochester and Bettini, (1976)(140)	1.4±0.6	7.1±4.3			insp. flow resistance dogs
Robertson et al., 1977(136)	1.7	22.6			insp. flow resistance dogs

$\dot{V}O_2 di$ = oxygen consumption diaphragm; $\dot{V}O_2 i$ = oxygen consumption intercostal muscle

Data during heavy and maximal exercise have been obtained in the pony (98, 101); $\dot{V}O_2$ of the diaphragm reaches as high as 31 ml·min⁻¹·100g⁻¹ during heavy and 45-58 ml·min⁻¹·100g⁻¹ during maximal exercise. Oxygen extraction by the diaphragm increases progressively as work rate increases, but has not been shown to reach a value where it would limit O_2 consumption, although observed blood flow is close to maximal.

Direct measures of oxygen consumption of the diaphragm or other muscles of respiration have not been made in humans. Instead most investigators have measured the increase in $\dot{V}O_2$ which accompany an increase in $\dot{V}E$. The estimate in the total cost of ventilation at maximal levels of exercise varies from 3% (112) to as much as 25% (54) of

$\dot{V}O_2$ max. This variation is in part due to different means of increasing $\dot{V}E$: exercise, hyperventilation, CO_2 and inspiratory flow resistance, as well as difficulty in obtaining steady state CO_2 and accurate $\dot{V}O_2$ measures (81). The results of these investigations are summarized in Table 14. The relationship of oxygen cost to ventilation is not a linear function but rather a series of curves (11, 109, 119) with a rapidly increasing slope as the upper limit of ventilation is approached (109). The oxygen cost of a particular ventilation varies with respiratory rate (11) and most investigators agree that healthy subjects spontaneously select the tidal volume and respiratory rate that minimizes respiratory work (110, 120). At any metabolic level the $\dot{V}O_2$ of respiratory muscles is less in trained than untrained subjects, reflecting the lower level of pulmonary ventilation for any given oxygen uptake (112).

Table 14. Oxygen cost of unobstructed hyperventilation

STUDY	$\dot{V}E$ studied	O_2 cost calculation	Cost of 120 $l \cdot \text{min}^{-1} \dot{V}E$ ($\text{ml} \cdot \text{min}^{-1}$)	Cost of 170 $l \cdot \text{min}^{-1} \dot{V}E$ ($\text{ml} \cdot \text{min}^{-1}$)
Anholm et al., (1987)(3)	50-220 l	$.049[\dot{V}E^{(1.776)}]$	241	546
Bradley and Leith, (1978)(18)	103-250 l	$-682+8.31\dot{V}E$	315	813
Shephard,(1966)(149)	90-130 l	$4.3\dot{V}E$	516	-
Bartlett et al., (1958)(11)	20-200 l	estimated from curve	~ 300 $\bar{x} = 343$	~ 900 $\bar{x} = 753$

Lactate Production

No evidence of net diaphragmatic lactate production is seen in ponies during exercise at maximal levels ($\dot{V}O_2 > 120 \text{ ml} \cdot \text{kg}^{-1} \cdot \text{min}^{-1}$) (101) even when inspiratory work of breathing is increased by laryngeal hemiplegia (102). Similar findings are observed in the

dog when animals are subjected to an inspiratory flow resistance (137). In low cardiac output states, net diaphragmatic lactate production is observed only when the mixed venous PO_2 falls below 20 torr (6). Indirect evidence suggests that other respiratory muscles may contribute to net lactate production. During cardiac tamponade, spontaneously breathing dogs have been shown to have blood lactate levels roughly double that of mechanically ventilated dogs (~ 7 vs $3 \text{ mmol}\cdot\text{l}^{-1}$) (165). In humans, Roncoroni et al., (143) documented metabolic acidosis in almost 40 % of patients in status asthmaticus, which could not be attributed to poor gas exchange in these individuals leading to the conclusion that respiratory muscles in the presence of severe airway obstruction may increase blood lactate levels via anaerobic glycolysis. In healthy humans small ($\sim 1 \text{ mmol}\cdot\text{l}^{-1}$) increases in blood lactate have been recorded in isocapnic hyperventilation at approximately 70% of maximum breathing capacity (52).

Theoretical calculations of respiratory muscle $\dot{V}O_2$ and \dot{Q} in humans exercising at maximal levels

Difficulty in making direct measures of respiratory muscle metabolism in human subjects has restricted research in this area. It is also difficult to compare the work in different animal species because of different methods of inducing stress on the respiratory muscles (hypercapnia, inspiratory loading, maximal exercise, cardiac tamponade) as well as interspecies differences. Nonetheless a certain pattern arises: During resting conditions, oxygen consumption of the diaphragm is remarkably constant across species, and is generally less than $2 \text{ ml}\cdot\text{min}^{-1}\cdot 100\text{g}^{-1}$. During maximal exercise this value increases to about $45\text{-}60 \text{ ml}\cdot\text{min}^{-1}\cdot 100\text{g}^{-1}$ in horses (98, 101). Data are not available for other animal species. The values for intercostal muscle are roughly half of these values (<1 and $\sim 30 \text{ ml}\cdot\text{min}^{-1}\cdot 100\text{g}^{-1}$ (98)) both at rest and during exercise. Diaphragmatic blood flow at rest is also similar between species ($\sim 10\text{-}30 \text{ ml}\cdot\text{min}^{-1}\cdot 100\text{g}^{-1}$) and has been reported higher than $300 \text{ ml}\cdot\text{min}^{-1}\cdot 100\text{g}^{-1}$ in ponies (99). Again the values for intercostal muscle blood flow

during resting and exercising conditions are about half (~10 and as high as 130 ml·min⁻¹·100g⁻¹) of the values reported for the diaphragm.

This information can be used to calculate theoretical values of blood flow and oxygen consumption for human respiratory muscle during maximal exercise, provided the following assumptions are made:

1. The total respiratory muscle mass in humans is ~ 4 kg.
2. The diaphragm is roughly 15 % of the total respiratory muscle mass or 600g.
3. The other 3400g, which includes intercostal muscle, is relatively homogeneous, allowing calculations to be made for the entire respiratory mass.
4. Meaningful comparisons can be made between animal species and humans.

The pony is the mostly completely studied species and the only one in which systematic observations have been made at heavy and maximal exercise. Therefore data from these investigations are used in the following calculations.

$$Q_{di} = 260 \text{ ml}\cdot\text{min}^{-1}\cdot 100\text{g}^{-1} \times 600 \text{ g} = 1560 \text{ ml}\cdot\text{min}^{-1}$$

$$Q_i = 120 \text{ ml}\cdot\text{min}^{-1}\cdot 100\text{g}^{-1} \times 3400 \text{ g} = \underline{4080 \text{ ml}\cdot\text{min}^{-1}}$$

$$5640 \text{ ml}\cdot\text{min}^{-1}$$

$$\dot{V}O_2 \text{ di} = 59 \text{ ml}\cdot\text{min}^{-1}\cdot 100\text{g}^{-1} \times 600 \text{ g} = 354 \text{ ml}\cdot\text{min}^{-1}$$

$$\dot{V}O_2 \text{ i} = 30 \text{ ml}\cdot\text{min}^{-1}\cdot 100\text{g}^{-1} \times 3400 \text{ g} = \underline{1020 \text{ ml}\cdot\text{min}^{-1}}$$

$$1374 \text{ ml}\cdot\text{min}^{-1}$$

Assuming a $\dot{V}E$ of 150 l·min⁻¹, $\dot{V}O_2$ of 4.6 l·min⁻¹ (72) and \dot{Q} of 27 l·min⁻¹ (5) then these figures represent 30% of $\dot{V}O_2$ and 20% of \dot{Q} for exercising humans at maximal work loads. Clearly these numbers are substantial and support the idea that respiratory muscles may be in direct competition with skeletal muscle for oxygen and cardiac output.

The resistance of the diaphragm to lactate production has also been clearly demonstrated in a number of species and under a wide variety of experimental conditions.

However the diaphragm constitutes less than 20% of the total respiratory muscle mass and no data is available for the other muscles of respiration under exercising conditions. There is no reason to expect that intercostal, abdominal and other muscles of respiration should behave differently than other exercising skeletal muscle. Any increase in ventilation, rather than increasing pH and lessening the impact of metabolic acidosis, may actually worsen it through increasing respiratory work. This line of thought, while highly speculative, is not new. Otis (119) argued that a critical ventilation could be reached above which any increase in $\dot{V}O_2$ would go entirely to respiratory muscles and estimated this ventilation at 140 l·min⁻¹. It is logical to consider that exercise ventilation represents an optimum level of ventilation balancing respiratory muscle oxygen consumption and blood flow against the demands of skeletal muscle and pH homeostasis. The level of ventilation achieved is a compromise between supply and the cost of supplying ventilation.

Respiratory muscle fatigue

Respiratory muscle fatigue is commonly seen in chronic obstructive lung disease, or in acute medical situations such as adult respiratory distress syndrome, where pulmonary edema increases respiratory work. In the normal exercising human, respiratory muscles have been considered to be fatigue resistant under most conditions, however reports of decrements in respiratory muscle strength after prolonged exercise (93) and decrease in performance following respiratory work (97, 105), indicate that this is not the case.

Histochemical properties of mammalian respiratory muscles

The histochemical and biochemical characteristics of respiratory muscles have been investigated in both animals and humans. The diaphragm of most mammals are composed of varying percentages of the three skeletal muscle fiber types. Biopsy specimens taken during thoracotomy in humans show the composition of the diaphragm to be 55% SG, 21% FOG and 24%FG fibers (90). The oxidative capacity of diaphragm is greater than other mixed skeletal muscle, and closely resembles an intermediate between skeletal and cardiac

muscle (62, 114). The oxidative capacity can be trained by imposing inspiratory resistive loads (1, 82) and in induced emphysema (48). The effect of endurance exercise on the respiratory muscles is controversial, with some authors documenting an increase in the respiratory capacity of the rat diaphragm and intercostal muscles with endurance training (114, 128) and no change reported by others (53) using an almost identical protocol.

After endurance exercise, depletion of muscle glycogen stores has been found in both diaphragm and intercostal muscle (62, 75, 114) as well as triglyceride depletion in the diaphragm (62). This evidence points to the diaphragm as a muscle with high aerobic capacity, relying on aerobic glycolysis and fatty acid oxidation to offset the metabolic cost of work. Other muscles of respiration have not been as extensively evaluated, but would appear to have characteristics in common with other skeletal muscle.

Evidence for fatigue

Muscular fatigue has been defined as a reversible reduction in force generating capacity which is relieved by rest (117). Task failure is defined as the inability to maintain or continue the force required to perform a particular task. For the respiratory system this can be defined as the failure of the respiratory muscles to generate a given pleural pressure. The unique characteristics of diaphragm muscle with ability to maintain very high oxidative capacity, renders this muscle relatively resistant to fatigue compared with skeletal muscle (172) however, as a correlate to the histochemical data, several studies have shown that high levels of ventilation cannot be maintained indefinitely (14, 24, 107). A decline in the strength of the ventilatory muscles at the end of a marathon race, with a fall in maximum inspiratory and expiratory mouth pressures and transdiaphragmatic pressures suggests that these considerations may be of practical concern (93). Reduced time to exhaustion has been observed during short-term maximal exercise after 150 minutes of maximal ventilation (105) and after inspiratory threshold loading (97). Expiratory muscle fatigue has also been reported as a result of increased expiratory work in normal subjects, persisting for up to an

hour after cessation of expiratory muscle loading (157). Expiratory loading also induces inspiratory muscle fatigue and these findings may have important implications for the athlete with exercise induced asthma.

Taken together the histochemical and whole body information point to the respiratory system as a system that is fatigue resistant under healthy, non-exercising conditions but that will demonstrate substrate depletion and a decline in performance with levels of exercise that are not uncommon in today's active society.

Respiratory drives

After the preceding discussion, the advantages of a blunted ventilatory response to exercise to an athlete appear obvious. If at any given level of exercise the ventilation is reduced, the individual will be less likely to develop respiratory muscle fatigue, will require a smaller fraction of total cardiac output and $\dot{V}O_2$ diverted to respiratory muscles and will experience less dyspnoea.

Although controversial, most authors would agree that the peripheral chemoreceptors contribute to exercise ventilation to a substantial degree. The estimated contribution of the hypoxic ventilatory response to exercise ventilation ranges from 16 to 30% of the total $\dot{V}E$ (106, 155, 183). Resting hypoxic and hypercapnic drives are positively related (131) and also correlate with drives measured during moderate exercise (106) and with exercise ventilation (106, 132). During maximal levels of exercise the relationship between respiratory drives and exercise ventilation is less clear and it is likely that, during exercise near maximal levels, other stimuli to ventilate over-ride any contribution by hypoxic drives (35, 72). The relationship between hypercapnic drives and ventilation during maximal or very heavy exercise has not been determined.

A link has been postulated between outstanding endurance performance and chemoreception (106) as some studies have shown endurance athletes to have blunted responses to hypoxia and hypercapnia, compared to other athletes and sedentary controls

(26, 106, 148) . It is tempting to speculate that these blunted respiratory drives may be related to exercise induced hypoxemia. Dempsey et al., (35) felt that hypoventilation was a major contributing factor to the hypoxemia seen in the athletes studied. The athlete with a blunted respiratory response to hypoxia, would ventilate less in response to the hypoxic stimulus with substantial savings in the cost of maintaining a high level of ventilation at the expense of less than optimal arterial oxygenation and presumably O₂ delivery. A more recent study (72), failed to demonstrate a relationship between hypoxemia in maximal exercise and resting hypoxic drives and implicated widening alveolar-arterial differences as being the most important contributor to the hypoxemia seen in their subject population. Further investigation is needed to determine the relationship between exercising hypoxic and hypercapnic responses and hypoxemia in exercise, however it would appear that the role of respiratory drives in determining exercise ventilation is a minor one during maximal exercise, although at less intense levels of exertion, respiratory drives modify the respiratory response to submaximal exercise.

Pulmonary mechanics and expiratory flow limitation

Pressure-volume relationships

In order for air to flow through a tube a difference in pressure must exist between the two ends. In the lung, this pressure difference is generated at rest by the contraction of the diaphragm in inspiration, and by passive elastic recoil during expiration. During quiet breathing, intra-alveolar pressure becomes slightly negative with respect to atmospheric pressure during inspiration and slightly positive during expiration (± 1 torr). During exercise inspiration is aided by the external intercostal muscles and other accessory muscles of inspiration. Expiration becomes active, with contraction of the muscles of the abdominal wall and internal intercostal muscles contributing to driving pressure.

Characteristics of flow inside tubes

At low flow rates air flow in a tube is in smooth streams parallel to the walls of the tube. This phenomenon is termed laminar flow and the flow rate is related to the length and diameter of the tube, the driving pressure and the viscosity of the flowing material. As flow rates increase, turbulent flow becomes more likely. The viscosity of the material becomes relatively unimportant, however driving pressure must increase to maintain flow as gas density increases. The complexity of the branching system, and irregularity of the surface in the lung makes laminar flow unlikely in much of the bronchial tree. In most parts of the lung, transitional flow predominates with eddy formation at the branch points of the bronchial tree.

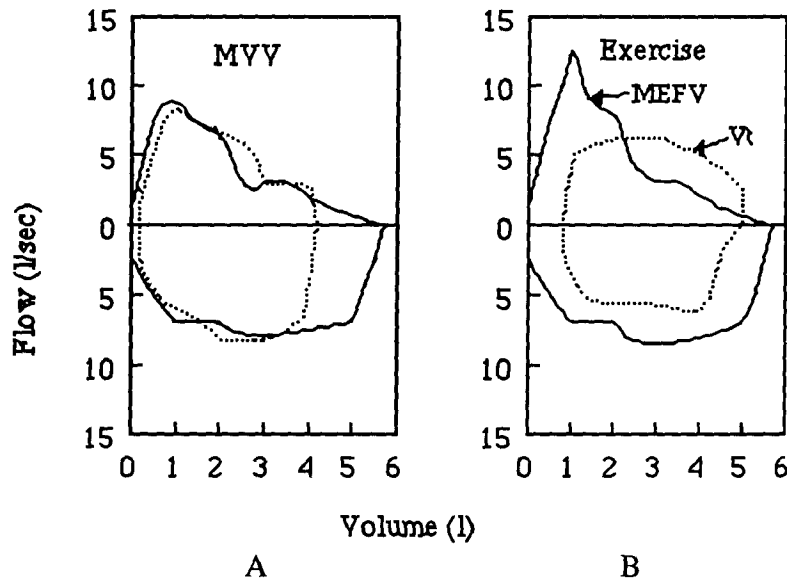
Airways resistance to flow can be modified by disease states and chemical agents. The effect of exercise is modest bronchodilation secondary to sympathetic nervous system stimulation. Intuitively, it seems logical that much of the resistance to flow should be located in the very small airways, however direct measures have shown that the majority of the drop

in pressure takes place over the first 10 generations of bronchial branching (176). The explanation for this is likely the large number of small airways relative to larger airways.

Flow-volume relationships

Maximal expiratory flow-volume (MEFV) curves have been used for many years as a clinical assessment of pulmonary function. At rest normal tidal breathing falls well within the limits defined by the MEFV curve, however in certain circumstances these limits may be approached or even exceeded (Figure 9). During progressive exercise the demands for increased ventilation are met by an increase in tidal volume, to about 50% of forced vital capacity (30, 51) and breathing frequency.

Figure 9. Maximal expiratory flow volume loop with exercise and maximum voluntary ventilation manoeuvre



(adapted from Jensen et al., 1980 (78))

Solid line = maximal expiratory flow volume loop. Dotted line = tidal volume during maximal voluntary ventilation (A) and exercise (B)

The ventilation at maximal exercise is approximately 75% of that during maximal voluntary ventilation manoeuvres (MVV) (67) and this information has been interpreted as indicating that mechanical factors do not limit ventilation during exercise. During very heavy exercise, there is some evidence to suggest that this may be inaccurate. Peak expiratory

flows have been measured, that approach or even exceed maximal expiratory flow measured during MEFV loops (67, 78, 118). Several explanations are possible: Firstly, during MVV measurements subjects breathe at higher lung volumes and therefore have higher expiratory flow (118); Secondly, during exercise, maximum flow may be increased by increased elastic recoil pressure; Thirdly, during exercise there may be decreased resistance to flow as a result of bronchodilation secondary to increased sympathetic or decreased parasympathetic tone (78). Finally, an increase in ventilation, alveolar PO_2 and arterial oxygenation is seen with the administration of He: O_2 mixtures during heavy exercise, and is associated with a decrease in $PaCO_2$ (35, 36, 170). In interpreting the information gained from administration of low density gases caution must be exercised to avoid attributing all of the improvement to the effects on the MEFV curve as there will also be a reduction in the work of breathing for any given level of ventilation, with attendant interaction with respiratory muscle blood flow and metabolism.

A final factor which should be considered is entrainment, the alteration of breathing frequency to be in step with exercise rhythm. One to one entrainment in galloping horses is well known (34, 121), and has been proposed as a factor causing hypoxemia in these animals (34). During exercise in humans, entrainment is much less complete and depends on the form of exercise. During walking about half of normal subjects are partially or completely entrained, increasing to about 80% during running. Entrainment during cycling is found in about 30% of subjects (13) and is apparent in oarswomen, at low work intensities (158). From the preceding arguments it is clear the respiratory mechanics have the potential to limit exercise ventilation, and by inference maximal exercise through entrainment, expiratory flow limitation or by interaction with the work of breathing.

Pulmonary diffusion and gas exchange

In the preceding pages some of the factors that may contribute to a respiratory constraint to exercise have been discussed. Diffusion and gas exchange may interact with these factors on several levels as well as directly contributing to limitation of performance. For example, if through hypo-ventilation or mechanical limitation of flow, alveolar PO_2 is reduced, then the driving pressure for diffusion is also reduced and may lead to a decline in arterial oxygen content and subsequent decrease in oxygen delivery. It is not the purpose of this review to completely discuss the physics of respiratory gas exchange as it has been the subject of several excellent reviews. The reader is referred to the work of Peter Wagner (166) for a more in-depth discussion of the points discussed below.

As air travels from the atmosphere to the alveolus it becomes fully saturated with water vapor and in the alveolus becomes mixed with alveolar air containing lower concentration of oxygen and a higher concentration of carbon dioxide. It is usually assumed that alveolar gas is fully saturated with water which gives a partial pressure of 47 torr at a barometric pressure of 760 torr and $37^\circ C$. Under resting conditions the gas tensions of alveolar air are approximately $PO_2 = 105$ torr, $PCO_2 = 40$ torr, $PH_2O = 47$ torr and $PN_2 = 568$ torr.

Once a gas has arrived at the alveolus it must pass through alveolar fluid, alveolar epithelium, epithelial basement membrane, interstitial space, capillary basement membrane and through capillary endothelium into the blood.

Factors related to diffusion of oxygen

The rate of combination of oxygen with hemoglobin is not instantaneous but rather occurs as a finite rate. The uptake of oxygen can be considered in two steps (145): 1. Diffusion across the alveolar membrane and plasma to the red blood cell and 2. Combination with hemoglobin. The rate of combination of hemoglobin with oxygen (given by θ) is a

function of hemoglobin saturation, being greatest at low saturation and approaching zero at saturations above 80% (154). The overall transfer from the alveolus to the red cell and diffusing capacity of the lung (D_L) can be related by:

$$\frac{1}{D_L} = \frac{1}{D_M} + \frac{1}{\theta V_c}$$

Where V_c is capillary blood volume, and D_M is the diffusing capacity of the alveolar membrane. D_M is close in value to V_c , therefore for θ greater than 1, the major resistance to uptake would be that determined by combination of hemoglobin with oxygen. Most of the changes in PO_2 and O_2 content take place in the first 0.2 second of the red blood cell transit in the pulmonary capillary when saturation is low and θ is high, and rate is predominantly determined by D_M . Later as saturation rises, θ decreases and the chemical reaction resistance predominates. The amount of oxygen dissolved in plasma is linearly related to partial pressure and is about $0.3 \text{ ml} \cdot 100 \text{ ml}^{-1}$, less than 2% of that bound to hemoglobin and it is generally neglected in order to simplify calculations. The rate of rise in PO_2 is affected by simultaneous CO_2 exchange: as capillary PCO_2 falls the oxygen hemoglobin equilibrium curve is shifted towards the left and more oxygen is taken up by hemoglobin, delaying the rise in PO_2 .

Factors related to diffusion of carbon dioxide

Although the diffusion across alveolar membrane is approximately 20 times greater for carbon dioxide than for oxygen, the diffusion rate for CO_2 may be similar, or even slower, than for O_2 . The reason for this becomes apparent when the chemical reactions within the blood necessary for CO_2 exchange are examined. Transfer of CO_2 in the blood is in three forms: dissolved CO_2 , HCO_3^- , and bound to protein (carbamino compounds), primarily hemoglobin. In arterial blood, HCO_3^- is the predominant form of CO_2 transport

(90%), with 5% bound to proteins and 5% as dissolved CO₂. Plasma CO₂ accounts for about 2/3 of the total CO₂, with the remainder present intracellularly, bound to hemoglobin. As CO₂ diffuses into the alveolar gas, it is replaced by plasma carbamino-CO₂ and by the conversion of HCO₃⁻ and H⁺ to CO₂ and water. In the plasma, this reaction is not catalyzed by carbonic anhydrase, as it is within the red blood cell and therefore proceeds much (~10⁴) more slowly. As HCO₃⁻ from the plasma is consumed, it is replaced by red cell HCO₃⁻ which is exchanged with chloride ion (chloride shift). CO₂ also diffuses out of the red blood cell where it has been produced by the much more rapid carbonic anhydrase catalyzed conversion of HCO₃⁻. Deoxy-hemoglobin acts as a buffer for H⁺, as oxygen combines with hemoglobin H⁺ is released, which facilitates the conversion of bicarbonate to carbon dioxide and water (the Haldane effect). Although for CO₂ D_M is 20 times that for O₂, the slowness of chemical reactions, particularly the chloride shift, with a t^{1/2} of 0.15 seconds renders the time for CO₂ diffusion equilibrium, if anything, slower than that for O₂. Due to the absence of carbonic anhydrase in the plasma, the plasma concentrations of CO₂, H⁺, and HCO₃⁻ are not in equilibrium at the end of the pulmonary transit. This leads to a post-capillary increase in pH and CO₂ and a fall in HCO₃⁻.

Factors affecting pulmonary gas exchange

In the intact organism gas exchange can be modified by a number of factors.

1. **Shunt:** In the normal human, small amounts of blood by-pass the pulmonary capillaries and therefore do not participate in gas exchange. This includes blood from the bronchial arteries and coronary veins that drains directly into the left ventricle via the thesbian veins. Normally shunt accounts for less than 2% of cardiac output.
2. **Hypoventilation:** The level of alveolar O₂ and CO₂ is determined by a balance between supply and removal. Hypoventilation from any cause will impair pulmonary gas exchange

by decreasing the driving pressure across the alveolar membrane for both carbon dioxide (decreased removal) and oxygen (decreased supply).

3. Ventilation-perfusion (\dot{V}_A/\dot{Q}) mis-match: If ventilation is abolished in a particular area of the lung then the blood passing through this portion of the lung is essentially shunted through the lung; no gas exchange takes place, and no change in gas content is observed. If on the other hand perfusion tends towards zero, the gas content of that blood will resemble that of alveolar gas. Ventilation and perfusion are not uniform throughout the lung, the effects of gravity render the bases better perfused than the apices of the lungs and the apices relatively better ventilated than the bases. (\dot{V}_A/\dot{Q}) mis-match will tend to depress P_{aO_2} as more blood will be poorly oxygenated.

4. Reduction of alveolar surface area: Through disease states, such as chronic obstructive pulmonary disease, alveolar surface area can be reduced thus reducing the available surface area for gas exchange. When advanced, this will be manifest in decreased diffusing capacity for CO and impaired gas exchange during exercise.

5. Diffusing capacity: The diffusing capacity of the lung can be diminished by pulmonary disease. In order to produce abnormalities of gas exchange it must be reduced to 20-25% of normal.

6. Altitude: The effect of altitude is to decrease total barometric pressure and therefore the partial pressure of inspired oxygen. Some compensation is made by increasing alveolar ventilation (and decreasing alveolar CO_2) however the overall effect is to decrease PAO_2 , and the driving pressure for oxygen across the alveolar membrane.

7. Transit time: Under normal conditions, partial pressure equilibrium is reached after about 0.25 seconds of gas exchange. The average transit time of red cells in the pulmonary capillaries is obtained by the ratio of capillary blood volume to cardiac output (V_c/\dot{Q}) or about 0.75 seconds for a person at rest with a V_c of 75 ml and \dot{Q} of $6000 \text{ ml}\cdot\text{min}^{-1}$ (80). During exercise, V_c may increase by a factor of 2 while cardiac output may increase to $30 \text{ l}\cdot\text{min}^{-1}$ giving an average transit time of 0.30 seconds. Cardiac output in excess of 40

$l \cdot \text{min}^{-1}$ has been reported in some elite athletes (43) which would reduce average transit time to 0.23 seconds using these calculations. It should be pointed out that these numbers represent average transit times, and some red cells will travel faster than these values.

Capillary flow is not uniform but rather is pulsatile, which may reduce transit time further.

8. Exercise: The effects of exercise on diffusion of oxygen across the alveolar membrane can be seen in Table 15 . At rest, the normal alveolar-arterial difference is about 7 to 10 torr (60, 161, 182). During light exercise, gas exchange may improve (182), as a result of improved ventilation-perfusion relationships. As exercise intensity increases, gas exchange deteriorates and reported mean $[A-a]DO_2$ ranges from 11 to 41 torr at $\dot{V}O_2$ of $2.7 l \cdot \text{min}^{-1}$ and above.

Table 15. Alveolar-arterial differences at rest and during exercise

Study	$\dot{V}O_2$ l·min ⁻¹	\dot{Q} l·min ⁻¹	PAO ₂ torr	PaO ₂ torr	[A-a]DO ₂ torr
Gledhill et al., 1978 (60)	0.29±0.03	5.9±1.6	97.8±2.2	86.9±1.6	10.1±2.5
Whipp and Wasserman, 1969 (182)	0.32±0.07	-	105.0±1.2	97.0±1.9	7.4±1.9
Torre-Bueno et al., 1985 (161)	0.35±0.04	6.6±1.3	111*	102.7±10.8	8.6±5.4
Whipp and Wasserman, 1969 (182)	1.65±.45	-	102.0±4.6	98.0±5.5	3.8±2.9
Gledhill et al., 1978 (60)	1.84±.07	15.5±3.1	102.9±2.2	87.5±2.7	15.5±1.6
Torre-Bueno et al., 1985 (161)	2.71±.53	21.7±3.4	113.0*	89.9±3.8	23.1±7.5
Whipp and Wasserman, 1969 (182)	3.31±.58	-	108.0±6.4	97.0±3.73	10.8±3.6
Hammond et al., 1986 (63)	3.97±.29	24.9±3.2	113.7*	90.7±8.2	23.0±8.0
Hopkins and McKenzie, 1989 (72)	4.54±.45	-	119.0±1.5	78.0±8.6	41.0±7.7

*= Standard deviation not reported

Pulmonary gas exchange has been studied using multiple inert gas techniques, at rest and during exercise at sea level and simulated altitude to 15,000 feet, allowing the contributing factors to [A-a]DO₂ to be dissected. At sea level, ventilation-perfusion relationships worsen with exercise, with the major factor contributing to [A-a]DO₂ being

\dot{V}_A/\dot{Q} mis-match at $\dot{V}O_2$ up to $3.0 \text{ l}\cdot\text{min}^{-1}$. At rest, the contribution of post-pulmonary shunt to $[A-a]DO_2$ is undetectably small and does not increase with exercise, simulated altitude or exercise at simulated altitude (161). Of particular interest is the effect of exercise on the diffusion component of $[A-a]DO_2$. Gale et al. (55), at exercise corresponding to a $\dot{V}O_2$ greater than $3.0 \text{ l}\cdot\text{min}^{-1}$, found a trend toward greater $[A-a]DO_2$ than could be predicted from inert gas data, and suggested diffusion limitation was the likely cause. Similar results were obtained at $\dot{V}O_2 = 2\text{-}3 \text{ l}\cdot\text{min}^{-1}$ at simulated altitude of 5000 ft. Statistical conclusions were hampered by the small "n" of the study.

In an attempt to clarify this issue, Hammond et al., (63) studied gas exchange in men at various exercise intensities up to $\dot{V}O_2 \sim 4.0 \text{ l}\cdot\text{min}^{-1}$ (essentially maximum). During the very heavy exercise levels, $[A-a]DO_2$ was measured at 23.0 ± 8.0 torr of which 10.7 ± 7.8 torr could be predicted by inert gas data. Administration of 100% O_2 did not alter the \dot{V}_A/\dot{Q} relationships. They observed that $[A-a]DO_2$ increased linearly with $\dot{V}O_2$. Analysis of data provided by Torre-Bueno et al., (161) yields a correlation between cardiac output and $[A-a]DO_2$ of $r = 0.68$. As cardiac output increases pulmonary transit time will decrease from resting levels, therefore at the higher levels of exercise it is possible that some individuals will exhibit increased $[A-a]DO_2$ because of shortened pulmonary transit time and diffusion dis-equilibrium. No inert gas studies have been made on highly trained athletes capable of high cardiac output, and the possibility for shortened pulmonary transit and significant arterial hypoxemia.

Does the pulmonary system constrain exercise?

In the preceding pages, the evidence that the pulmonary system may constrain maximal exercise performance has been explored in five areas: energetics, fatigue, respiratory drives, mechanics and diffusion. These arguments will now be applied to data obtained from several studies (Table 16) in an attempt to integrate this information.

Group one subjects are sedentary individuals who are unlikely to have a respiratory limitation to performance. This is borne out by the blood gas data indicating that the arterial PO_2 and saturation are maintained and the metabolic acidosis of exercise is relatively well compensated ($pH = 7.31$). At a ventilation of $80 \text{ l}\cdot\text{min}^{-1}$ the oxygen cost of breathing is about 12% of the total $\dot{V}O_2$ (from mean of Table 14) and flow volume loops are unlikely to be mechanically constraining, confirmed by maintenance of alveolar PO_2 . Blunted respiratory drives are unlikely in sedentary subjects such as these and have not contributed to significant hypoventilation as indicated by pH and alveolar PO_2 and CO_2 status. The observed alveolar-arterial difference is only slightly greater than that predicted from multiple inert gases therefore they are not likely to be diffusion limited (161). The predicted mean pulmonary transit time based on a capillary blood volume of 150 ml (80) is 0.41 seconds, well within that which will allow full O_2 equilibration.

Group Two subjects, again show minimal evidence for pulmonary constraint; Alveolar PO_2 is maintained as is arterial PO_2 (91 torr) and SaO_2 (94.5 %). Hypoventilation secondary to fatigue, blunted drives or mechanics are unlikely to be a factor as evidenced by maintenance of alveolar PO_2 , although the pH values indicate less compensation for the metabolic acidosis of exercise. In these subjects measured alveolar-arterial differences are approximately 12 torr greater than predicted for inert gas data (63) suggesting some diffusion limitation. Calculated mean pulmonary transit time is 0.36 seconds, closer to the 0.25 seconds required for full equilibration.

Some interesting comparisons can be made between groups three, four and five who are all highly trained individuals exercising at a $\dot{V}O_2$ greater than $4 \text{ l}\cdot\text{min}^{-1}$, with similar levels of ventilation and predicted cardiac output, but quite different alveolar and blood gas data. Group three is able to maintain arterial saturation above 92 % and PO_2 above 80 by maintaining a very high alveolar PO_2 in the face of widening alveolar-arterial differences to about 37 torr. $\dot{V}CO_2$ is very high in these subjects as evidenced by R values greater than 1.15 and hypocapnia to 37 torr despite this level of ventilation. Dempsey et al., (35) have

suggested that to maintain a PaCO_2 of 30 torr in subjects with a $\dot{V}\text{CO}_2$ of 5 - 6 $\text{l}\cdot\text{min}^{-1}$ the required ventilation is $\sim 240 \text{ l}\cdot\text{min}^{-1}$, a level unlikely to be sustained even by highly trained individuals. Group four subjects, despite very similar ventilatory data, are unable to maintain arterial PO_2 and SaO_2 and have extremely high alveolar-arterial differences. Inert gas data has not been obtained in these individuals but it is tempting to speculate that the trend in $[\text{A-a}]\text{DO}_2$ due to diffusion observed at $\dot{V}\text{O}_2 = 3.0 \text{ l}\cdot\text{min}^{-1}$ and statistically significant difference at $4.0 \text{ l}\cdot\text{min}^{-1}$, may continue to increase at higher intensity exercise. If a cardiac output of $31 \text{ l}\cdot\text{min}^{-1}$ (43) can be assumed for these subjects, predicted mean pulmonary transit time would be less than 0.30 seconds and almost half of the RBC transit times would be less than that required for full oxygen equilibration.

Why group three and four subjects, who are identical in so many respects, should behave so differently with respect to PaO_2 and $[\text{A-a}]\text{DO}_2$ is unclear but perhaps some answers can be found in inspection of the Fick equation. Whole body $\dot{V}\text{O}_2$ is the product of blood flow (in this case cardiac output) and the arterio-venous difference, therefore two strategies are available to increase $\dot{V}\text{O}_2$: oxygen delivery can be increased, (increase in \dot{Q}) or a-v difference can be increased (increased peripheral extraction). It is possible that group three subjects despite similar $\dot{V}\text{O}_2$, may have a lower cardiac output and maintain $\dot{V}\text{O}_2$ by superior peripheral extraction. The net result would be a longer pulmonary transit time and lower $[\text{A-a}]\text{DO}_2$ due to diffusion.

Group five subjects are different again, and clearly have evidence of hypoventilation as evidenced by the inability to maintain alveolar PO_2 greater than 108 torr, as well as a widened alveolar-arterial difference indicative of possible diffusion limitation. pH is higher and PaCO_2 lower, most likely due to lower intensity exercise - 90% vs 100% of $\dot{V}\text{O}_2$ max. It is likely that in these subjects, mechanical factors may also play a role in the genesis of hypoxemia. It is also possible that at this submaximal exercise level that there may be a role for respiratory drives, which is not evident during exercise at 100% of $\dot{V}\text{O}_2$ max.

Table 16. Blood gas and cardio-respiratory data obtained at 70-100% of $\dot{V}O_2$ max

Group	1	2	3	4	5
Training status	Untrained	Moderately Trained	Highly Trained	Highly Trained	Highly Trained
$\dot{V}O_2$ (l·min ⁻¹)	2.71	3.97	4.45	4.65	4.81
$\dot{V}CO_2$ (l·min ⁻¹)	2.75	4.19	5.27	5.42	4.62
R	1.05	1.04	1.18	1.17	0.96
\dot{Q} (l·min ⁻¹)	27.1	24.9	?	?	?
PAO ₂ (torr)	113	114	119	119	108
PaO ₂ (torr)	90	91	82	71	75
[A-a]DO _{2(o)} (torr)	23	23	37	48	33
[A-a]DO _{2(p)} (torr)	22	11	?	?	?
SaO ₂ (%)	95.6§	94.5§	93.0	89.9	91.9
PaCO ₂ (torr)	37	35	37	37	33
pH	7.31	7.24	7.21	7.20	7.29
n	9	8	7	5	16

§ = SaO₂ calculated from normogram; 1 = data from Gale et al., 1985 (55) and Torre-Bueno et al., 1985 (161); 2 = Hammond et al., 1986 (63); 3,4 = Hopkins and McKenzie, 1989 (72) and unpublished data, 5 = Dempsey et al., 1984 (35), respiratory exchange ratio; \dot{Q} = cardiac output (l·min⁻¹); $\dot{V}E$ = minute ventilation (l·min⁻¹); PAO₂ = alveolar O₂ (torr); PaO₂ = arterial O₂ (torr); [A-a]DO_{2(o)} = observed alveolar-arterial difference (torr); [A-a]DO_{2(p)} = predicted alveolar-arterial difference (torr); SaO₂ = arterial hemoglobin saturation (%); PaCO₂ = arterial CO₂ (torr).

Summary

This review has identified several factors by which the respiratory system may constrain exercise performance. In sedentary or moderately trained individuals, the data does not favor evidence of pulmonary limitation and it seem likely that these individuals are constrained by other factors, such as O₂ delivery and extraction. In highly trained individuals exercising at high intensity, the picture is different, with falling PaO₂, widening [A-a]DO₂ and inability to maintain acid-base homeostasis suggesting a pulmonary constraint. The relative contribution of various factors is unclear, but the balance of the evidence favours mechanical limitation of ventilation and diffusion limitation at the lung as the most attractive possibilities.

APPENDIX B:

METHODOLOGICAL BACKGROUND

Quantitative radiocardiography

Red blood cell labeling

Labeling red blood cells with ^{99m}Tc provides a stable intravascular marker that has wide spread clinical applications, particularly in blood flow measurements. Simple incubation of the erythrocytes with ^{99m}Tc does not provide a satisfactory result because of loss of radioactivity with washing of the cells (173). The addition of stannous citrate acting as a reducing agent, allows the ^{99m}Tc -pertechnetate to cross the red cell membrane, improving the stability of the label, while still providing labeling efficiency of over 90% (152). Commercial kit preparations (152) have the advantage of allowing the preparation of small quantities of labelled cells with high yields with a minimal amount of handling thus reducing the risk of contamination. The kit consists of a sterile reagent tube containing 100 units of sodium heparin, 2.6 μg stannous citrate (1.0 μg stannous ion), sodium citrate and anhydrous dextrose. About 6 ml of whole blood is added to the vial followed, after mixing with 4 ml of sterile saline. After centrifuging, 2 ml of erythrocytes are withdrawn and added to a sterile vial containing ^{99m}Tc -pertechnetate and incubated for five minutes. The resulting mixture is assayed for radioactivity prior to injection for RBC label studies.

First pass determination of cardiac output

After injection into a flowing stream eventually all of a tracer, although diluted, will eventually pass by an observational point down-stream and the amount of indicator (given by I) can be calculated by

$$I = F \int_0^{\infty} C_1(t) dt$$

where F is flow and $C_i(t)$ is the observed concentration at time t . In tracers confined to the vascular space the equilibrium concentration (C_{eq}) times volume of distribution (Vd) will equal the total amount of tracer injected and

$$C_{eq} \cdot Vd = F \int_0^{\infty} C_i(t) dt.$$

This method can be applied to all tracers, but for radioisotopes where concentrations cannot be measured directly by an external counter it is necessary to relate concentration to count-rate by allowing for the counting efficiency of the detector for the tracer material in the volume of interest. After summation the following equation can be derived:

$$F = \frac{E \cdot Vd}{A}$$

where E is the observed equilibrium count rate, Vd is the volume of distribution and A is the area under the first pass time activity curve after correction for re-circulation.

To determine cardiac output this analysis is applied to a first pass time activity curve derived from gamma camera imaging of a region of interest in the left ventricle, following a bolus injection of ^{99m}Tc -pertechnetate label red cells. The equilibrium count rate is measured in the same region of interest after complete mixing of the tracer has occurred. Sources of error with this method arise from poor bolus technique at the time of injection, difficulties in extrapolation of the down slope of the first pass curve, dead time count losses by the detector system, and incomplete mixing of the tracer. Volume of dilution of the tracer must also be determined and can also be measured using radioisotopes (76). Determination of cardiac output by first pass radiocardiography has shown excellent correlation with other methods (83, 84) and has the advantages of being non-invasive, able to evaluate separately the right and left ventricle and provide information about pulmonary transit times.

Gated radionuclide angiography:

Gated radionuclide angiography is based on the principle that if cardiac volumes can be determined in end-systole and end-diastole, and if heart rate is known, cardiac output can be determined from the product of stroke volume and heart rate. After injection and equilibration of labeled erythrocytes, data acquisition is performed by dividing the R-R interval into a discrete number of frames (usually 16), and using the QRS complex as a gate. A series of images are acquired that provides a dynamic picture of cardiac function. By measuring the number of counts in the left ventricle over the sixteen frames end-systolic and end-diastolic counts can be determined and left ventricular ejection fraction can then be calculated from the difference between background subtracted end-diastolic and end-systolic counts and expressed as a percentage of end-diastolic counts.

Samples of blood are drawn at the end of each data acquisition and imaged in petri dishes for five minutes. The average background subtracted count rate for 5 ml of blood is obtained, and the left ventricular count rate is corrected for loss by decay of ^{99m}Tc using standard tables. Left ventricular end-diastolic volume is obtained by dividing the left ventricular count rate by the 5 ml count rate; cardiac output is obtained by multiplying the stroke volume by the average heart rate during data acquisition, usually 2 to 3 minutes. The advantage of gated studies are that sequential evaluations are possible and that dynamic information about cardiac wall motion can be obtained. The major disadvantage is that movement artifact becomes more likely as exercise intensity is increased and a correction factor must be applied to correct the ventricular counts for attenuation by the structures of the chest. This last problem can be overcome for sequential studies if a first pass determination of cardiac output is performed prior to the acquisition of gated information. The ventricle depth for the gated studies is set with the first pass information obtained at the identical workload so that the two studies agree and the result is applied to subsequent determinations of cardiac output. Gated equilibrium ventriculography has been shown to be a reliable and valid means of measuring cardiac output and ventricular volumes (111, 122,

123). Data obtained by this method correlates well with that obtained by contrast and first-pass ventriculography (122).

Measurement of blood volume:

Plasma volume can be measured relatively simply and accurately by the use of radioisotopes. Currently, the use of radioiodine (^{131}I) labelled serum albumin (RISA) is the method recommended by The International Committee for Standardization in Haematology (76). Briefly, 5ml of radioiodine labelled human serum albumin is injected intravenously and the time of injection recorded. At 10, 20 and 30 minutes from the time of the original injection 5ml of blood is withdrawn and plasma volume is calculated as:

$$P_v = \frac{S \cdot D \cdot V}{P_0}$$

where S is the concentration of radioactivity in a prepared standard solution, D is the dilution of the standard, V is the volume of RISA injected, and P_0 is the concentration of radioactivity in the sample extrapolated back to time zero, based on the radioactivity counts in the three measured samples. This method can also be used with only a single sample taken at 10 minutes. Total blood volume can then be calculated from the hematocrit (H_v) and the plasma volume:

$$BV = \frac{P_v}{1 - 0.9H_v}$$

where 0.9 is a correction factor for relating whole body hematocrit to venous hematocrit.

Pulmonary transit time:

Theory: The mean transit time for a well mixed indicator to flow through a specific volume at a given flow rate is described by the relationship: $\text{transit time} = \text{volume}/\text{flow}$. The time required for an indicator to flow past an observation point down stream from an entry point is related not only to the time it take the bolus to flow past the point but also how quickly it arrived there. Transit time is the time that it takes a bolus to remain in a compartment if it is injected directly and instantaneously into the compartment. The first moment describes not only the time that the indicator is in the compartment but also how quickly or slowly it arrived there. The first moment therefore represents the summation of all transit times up to that point. If it were possible to deliver indicator material instantaneously into the compartment of interest the first moment would be the same as the transit time. Transit time of a compartment can be determined by subtracting the first moment of the bolus from that of the compartment.

To measure pulmonary transit times, the bolus or input curve is derived from a labeled RBC time activity curve of the right ventricle, the output curve is derived from the left ventricle and transit time is determined by subtracting the first moment of the right ventricular curve from the first moment of the left ventricular curve. This method is referred to as the centroid method. Deconvolution is a mathematical process by which a frequency distribution of transit times (a transfer function, $h(t)$) can be derived from the input (right ventricular) and output (left ventricular) time activity curves. It is important to note that the transit time obtained from either method represents the the delay of the bolus through pulmonary arteries, arterioles, capillaries, venules, veins, left atrium and left ventricle and does not just represent pulmonary transit time.

Frequency distribution of pulmonary transit times:

A frequency distribution ($h(t)$), such that the transformation of the input curve by the transfer function produces the output curve can be written as:

$$i(t)*h(t) = o(t)$$

where $i(t)$ is the input curve, $o(t)$ is the output curve and $*$ represents convolution or a complex transformation. The process of determining the shape of $h(t)$ is termed deconvolution.

Several methods have been used to determine the shape of $h(t)$. For example,

$$o(t) = \int_0^t i(\tau)h(t-\tau)d\tau$$

where τ is a variable used only for integration. If this is the case then a numerical solution can be sought by assuming that the integral can be approximated by a sum. Then the approximation of the output curve is given by:

$$o(n\Delta t) = \sum i(s\Delta t)h(n-s+1)\Delta t$$

where n is an integer which varies between 1 and m (m is the number of data points in the input and output functions) Δt is the time interval between the two data points and s is the integer variable for the summation. Knowing $o(n\Delta t)$ and $i(n\Delta t)$ it is possible to solve for the frequency distribution of transit times. Unfortunately this method is extremely unstable in the initial part of the input curve where it is required to extrapolate towards zero. This uncertainty is then propagated throughout the solution.

Fourier analysis which describes $h(t)$ in terms of a Fourier transform (\mathfrak{F}) has also been used for calculation of transit times.

$$\begin{aligned}\mathfrak{F}[o(t)] &= \mathfrak{F}[i(t)*h(t)] \\ &= \mathfrak{F}[i(t)] \cdot \mathfrak{F}[h(t)]\end{aligned}$$

and solving for $h(t)$:

$$h(t) = \mathfrak{Z} \left[\frac{\mathfrak{Z}[o(t)]}{\mathfrak{Z}[i(t)]} \right]$$

this analysis, however also suffers from the same problem as solution one, namely propagation of error.

More recently, deconvolution analysis using multiple fitting functions has been used to determine $h(t)$. This has the advantage that knowledge of $h(t_0)$ is not crucial and therefore eliminates the problem of propagation of error. The first step in this process is to fit a smooth function to $i(t)$ and $o(t)$. This involves elimination of noise from movement artifact during data collection, re-circulation of tracer and background radiation. Application of a gamma function to indicator dilution curves gives an excellent fit (153). The family of curves given by this model are described by

$$C(t_n) = k(t_n - t_a)^\alpha e^{-(t_n - t_a)/\beta},$$

where k , α and β are arbitrary, t_a and t_n are times of appearance and n th time respectively and $C(t_n)$ is the indicator concentration at t_n . This function can be linearized (see (153) for details) and then weighted least squares procedure can be used to fit the preceding equation to the input and output curves.

The area under the curve can then be determined using

$$\int_0^{\infty} C(t) dt = t_a + \beta^2(\alpha + 1).$$

Since for the determination of transit times the absolute area under the curve is not important, the area under both the input curve and the output curve can be set equal to 1 (all indicator that appears in the right ventricle must at some time appear in the left ventricle). The next step is to determine many $h(t)$ s, each with an area under the curve equal to 1, making the assumption that since both the input curve and output curve are described by a γ function that $h(t)$ is also γ distributed. A family of twenty to fifty curves (ie $h_1(t)$, $h_2(t)$... $h_{50}(t)$) is then generated with a mean transit time for these curves that is equal to the

difference between the first moments of the input and output curves and variances that range from the variance of the input curve to the variance of the output curve. Each of these curves is then convoluted with the input curve to produce a unique output curve each of which contributes to the final output curve:

$$o(t) = i(t)*h(t)$$

$$=i(t)*[h_1(t) + h_2(t) + \dots h_{50}(t)]$$

Given many $h_n(t)$ it should be possible to be able to approximate $h(t)$. If the area under $h(t)$ is set equal to 1 then:

$$o(t) = i(t)*[ah_1(t) + bh_2(t) + ch_3(t)\dots]$$

$$\text{where } a + b + c \dots = 1$$

and

$$o(t) = ai(t)*h_1(t) + bi(t)*h_2(t) + ci(t)*h_3(t)\dots$$

Multiple regression analysis is then applied to determine the contribution of each of these curves to $h(t)$. Unfortunately, each of the generated curves are highly correlated with one another (a situation termed multicollinearity) resulting in either a highly unstable result, such as negative numbers for a, b, c, \dots (since $i(t) = 1$ and $o(t) = 1$ the area under each $h_n(t)$ must also equal one and a, b, c, \dots must add up to 1 and vary between 0 and 1). Another problem is the refusal of least squares regression software packages to complete the regression since every curve is very similar. In order to overcome these difficulties, constrained ridge regression is used to determine the relative contribution of a, b, c, \dots to the final solution. Ridge regression acts on the assumption that the least squares estimation of the regression coefficients tends to be too large and therefore applies a shrinkage factor to the least squares estimator biasing it towards zero. The amount of shrinkage that ridge regression applies to each regression coefficient is proportional to the coefficient's

variance; it is assumed that the greater the variance the less the certainty that the estimated coefficient reflects the true value.

The final step in this process involves convoluting the input curve with the derived transfer function. If the resulting $o(t)$ is the same as the measured $o(t)$ then the transfer function must be correct and the analysis is complete. If the result is unacceptable then the entire process is repeated until a good fit is obtained.

A further problem associated with deconvolution analysis revolves around the definition and quantification of a "good fit" of the derived $o(t)$ with the actual $o(t)$. The curves under discussion represent complex mathematical functions which are difficult to assign numerical values to determine goodness of fit. If a numerical scale is assigned, a further problem arises with quantification. For example a numerical score of 7 may fit better than 10, but how much better? The usual method relies on manual observation to determine goodness of fit. While not entirely satisfactory it should be noted that small changes in fit are associated with minimal, if any, changes in transit time.

Incomplete mixing of the bolus can lead in either over or underestimation of times, therefore it is preferable to measure transit time downstream from the site of injection. Other sources of error include poor bolus technique and cross contamination of time activity curves from overlying structures in the chest.

Multiple inert gas elimination

Ventilation and perfusion relationships

The partial pressure of O_2 , CO_2 and N_2 in any gas exchanging unit is determined by three major factors: the ventilation perfusion ratio, the composition of the inspired gases and the composition of mixed venous blood. If CO_2 is the gas of interest the following equation can be derived:

$$\dot{V}CO_2 = \dot{V}_A \cdot P_A CO_2 \cdot K$$

where \dot{V}_{CO_2} is CO₂ output, \dot{V}_A is alveolar ventilation, $P_A CO_2$ is alveolar PCO₂ and K is a constant. Similarly the loss of CO₂ from the capillary blood can be described by :

$$\dot{V}_{CO_2} = \dot{Q}(C\bar{v}_{CO_2} - C_c'CO_2)$$

Where \dot{Q} is blood flow, $C\bar{v}_{CO_2}$ is mixed venous CO₂, and $C_c'CO_2$ is end capillary CO₂.

Under steady state conditions these equations must be the same and

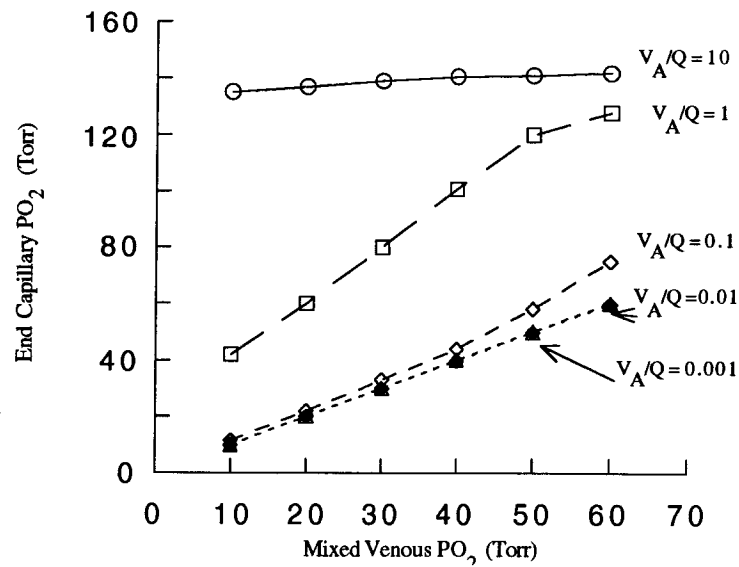
$$\dot{V}_A \cdot P_A CO_2 \cdot K = \dot{Q}(C\bar{v}_{CO_2} - C_c'CO_2)$$

rearranging:

$$\frac{\dot{V}_A}{\dot{Q}} = \frac{C\bar{v}_{CO_2} - C_c'CO_2}{P_A CO_2 \cdot K}$$

The effect of changing inspired oxygen concentration on arterial blood gases is determined by the ventilation perfusion ratio. For lung units with $\dot{V}_A/\dot{Q} > 1$ end capillary O₂ is high regardless of F_IO₂, whereas lung units with $\dot{V}_A/\dot{Q} \sim 0.1$ end capillary O₂ will increase rapidly as the F_IO₂ is increased. Those with $\dot{V}_A/\dot{Q} < .01$ show little response to increasing O₂ unless the inspired O₂ is greater than 50%. The effect of changing the mixed venous PO₂ is the most marked in lung units with \dot{V}_A/\dot{Q} between 0.1 and 1, and end capillary O₂ will decrease rapidly when the mixed venous PO₂ falls (Figure 10). This is especially important when one considers the effect of exercise on mixed venous PO₂ as values of about 25 torr are not uncommon (27) in normal subjects and in athletes exercising near max ($\dot{V}O_2 \sim 5.0 \text{ l}\cdot\text{min}^{-1}$, $\dot{Q} \sim 33 \text{ l}\cdot\text{min}^{-1}$) this can be calculated to be less than 20 torr by the Fick equation. Alterations in the inspired PO₂ can also alter the \dot{V}_A/\dot{Q} relationship by causing hypoxic vasoconstriction with low F_IO₂, or collapse of low \dot{V}_A/\dot{Q} units as O₂ is absorbed with high F_IO₂.

Figure 10. The relationship between end capillary PO_2 and mixed venous PO_2 for lung units of differing \dot{V}_A/\dot{Q}



From West, 1977 (175)

Multiple inert gas elimination theory:

An inert gas can be defined as one that obeys Henry's law, that is, that at constant temperature the solubility of the gas in a liquid is directly proportional to the pressure the gas exerts on the liquid. The diffusion of gas through tissues is described by Fick's law of diffusion. This states that the rate of transfer of a gas through a tissue or membrane is proportional to the difference in partial pressure of the gas on either side of the tissue. This can be written as :

$$F = K(P_1 - P_2) \tag{1}$$

Where F is flow of the gas across the membrane, K is a constant and P₁ and P₂ are partial pressures of the gases on either side of the membrane. The constant K is related to the surface area that is in contact with the gas, the solubility of the gas in the tissue, and is inversely proportional to the thickness of the membrane and the square root of the molecular weight of the gas of interest (166). Fick's law when applied to a finite volume of blood (a "slug") makes several assumptions: the blood is perfectly mixed, with a homogeneous capacity for the gas, there is no axial diffusion and the slug of blood is flowing at a uniform rate. The preceding equation can be expressed in terms of diffusing capacity:

$$V_{\chi}(t) = -D_{\chi}[P_{A\chi} - P_{\chi}(t)] \quad (2)$$

Where V_χ is the flow rate and D_χ is the diffusing capacity for gas χ, P_{Aχ} is the alveolar pressure and P_χ(t) is the instantaneous capillary pressure of gas χ. This equation can also be expressed as a rate in change in partial pressure in pulmonary capillary blood:

$$V_{\chi}(t) = \beta_{\chi} \cdot P_{\chi}(t) \frac{V_c}{100} \quad (3)$$

where P_χ(t) is the rate of change of capillary partial pressure, V_c is the capillary blood volume and β is the solubility of the gas in blood.

Diffusing capacity can also be expressed in terms of its component parts:

$$D_{\chi} = k \frac{A}{d} \cdot \frac{\alpha_{\chi}}{\sqrt{M W_{\chi}}} \quad (4)$$

where k is the diffusion coefficient of gas χ in the blood-gas barrier, A is the cross-sectional area over which diffusion is occurring, d is the thickness of the blood-gas barrier, α_χ is the solubility of the gas χ in the blood-gas barrier and MW is the molecular weight of the gas.

Equation 3 and 4 can be combined with equation 2 and integrated with respect to time, giving the following:

$$P_\chi(t) = P_{A\chi} + (P_{\bar{v}\chi} - P_{A\chi}) \cdot e^{-\left[\frac{100}{60} \cdot \frac{kA}{dV_c} \cdot \frac{\alpha_\chi}{\beta_\chi \sqrt{MW_\chi}} \right] t} \quad (5)$$

Where t = time and $P_{\bar{v}}$ is mixed venous P_χ . Although complicated, equation 5 can be used to make the following points: Absolute solubility of a gas is less important than the ratio of solubilities in blood and alveolar wall tissue, making the ratio of α_χ to β_χ an important regulator of equilibrium rate. In the same fashion, if two gases are equal in other factors they will differ in their equilibration rates on the basis of molecular weight.

The Fick principle can also be applied to an inert gas (χ):

$$\dot{V}_I \cdot P_{I\chi} - \dot{V}_A \cdot P_{A\chi} = \lambda_\chi \dot{Q} (P_{c'\chi} - P_{\bar{v}\chi})$$

where \dot{V}_I is the inspired ventilation in the lung unit, \dot{V}_A is expired ventilation in the lung unit of interest, $P_{I\chi}$, $P_{c'\chi}$ and $P_{\bar{v}\chi}$ are inspired, end capillary and mixed venous concentrations of gas χ , and λ_χ is the blood gas partition coefficient:

$$\lambda_\chi = \beta_\chi (P_{\text{bar}} - P_{H_2O} \text{ body temp}) / 100$$

For most inert gases $P_{I\chi}$ can be considered to be zero and in steady state the equation simplifies to :

$$\frac{P_{A\chi}}{P_{\bar{v}\chi}} = \frac{P_{c'\chi}}{P_{\bar{v}\chi}} = \frac{\lambda_\chi}{\lambda_\chi + \dot{V}_A / \dot{Q}}$$

This analysis has considered \dot{V}_A/\dot{Q} relationships in one lung unit or a perfectly homogeneous lung, but it can be applied to gas exchange in a heterogeneous lung divided into N compartments each representing a given \dot{V}_A/\dot{Q} ratio by summation (69, 168):

$$\mathbf{R} = \frac{\overline{P^{\text{exp}} \chi}}{P \dot{V}_\chi} = \sum_{j=1}^{j=N} \dot{V}_{Aj} \cdot \left(\frac{\lambda_\chi}{\lambda_\chi + \dot{V}_A/\dot{Q}} \right)$$

$$\mathbf{E} = \frac{\overline{P^{\text{art}} \chi}}{P \dot{V}_\chi} = \sum_{j=1}^{j=N} \dot{Q}_j \cdot \left(\frac{\lambda_\chi}{\lambda_\chi + \dot{V}_A/\dot{Q}} \right)$$

where $\overline{P^{\text{exp}} \chi}$ is the mixed expired partial pressure of the gas and $\overline{P^{\text{art}} \chi}$ is the mixed arterial partial pressure. $\frac{\overline{P^{\text{exp}} \chi}}{P \dot{V}_\chi}$ has been termed the excretion (E) of gas χ and $\frac{\overline{P^{\text{art}} \chi}}{P \dot{V}_\chi}$ is referred to as the retention (R) of gas χ .

Practical aspects

Although theoretically it would be possible to apply this model to a single gas of known λ , it is preferable to use six to eight gases of varying λ . A gas mixture of 20% SF₆ ($\lambda \sim 0.005$), 20% cyclopropane ($\lambda \sim 0.5$) and 60% ethane ($\lambda \sim 0.1$) is bubbled under sterile conditions into a bag of 5% dextrose followed by injections of 2 ml·l⁻¹ enflurane ($\lambda \sim 2$), 0.5 ml·l⁻¹ diethyl ether ($\lambda \sim 12$) and 6 ml·l⁻¹ acetone ($\lambda \sim 300$). This mixture is infused into a vein and after a period of equilibration arterial blood and mixed expired gas samples are simultaneously obtained in ungreased gas tight syringes (167). The gases in the blood are extracted into the gaseous phase by the addition of helium and then analyzed using electron capture (in the case of SF₆) and flame ionization (in the case of the other

five gases) gas chromatography. The results (P_{eqm} - equilibrium pressure) are corrected back to the original concentrations in blood (P_0) using the following equation:

$$P_0 = P_{eqm} \cdot \left[1.0 + \frac{V_g}{k \cdot S} \right]$$

where k is the barometric pressure-saturated water vapour pressure/100, S is the solubility of the gas in blood (measured directly by a second equilibration) and V_l and V_g are the volume of liquid and gas in the sample respectively. Mixed venous concentrations of the gas are then calculated using the Fick equation for inert gases.

$$P_{\bar{v}} = P_a + \frac{P_{\bar{e}} \dot{V}_E}{\lambda \dot{Q}_T}$$

\dot{V}_E is measured in the usual fashion, \dot{Q}_T is total cardiac output and λ is obtained from the measured solubility:

$$\lambda_x = S_x \cdot \frac{(P_{bar} - P_{H_2O})}{100}$$

Dead space

Retentions (R) and Excretions (E) are calculated as described previously. An enormous amount of information can be obtained from this analysis (69, 181). The inert gas dead space (V_{DIG}) represents ventilation that does not come into contact with perfusion and results in a decreased excretion ratio of the gas.

$$V_{DIG} = \frac{R_{homo} - E_{homo}}{R_{homo}}$$

Where R_{homo} and E_{homo} are retentions and excretions of the homogeneous lung respectively. Physiological dead space represents both inert gas dead space and that resulting from excess ventilation to a lung unit. Physiological dead space ratio can be calculated as:

$$\frac{V_D}{V_T} = \frac{P_a - P_E}{P_a} = \frac{\frac{P_a - P_E}{P_a}}{\frac{P_a - P_a}{P_a}} = \frac{R - E}{R}$$

Where R and E are retention and excretion in the heterogeneous lung. The alveolar dead space which is physiological dead space minus inert gas dead space can also be determined directly from retention and excretion data:

$$\frac{V_{D_{alv}}}{V_T} = \frac{(P_a - P_{a_{homo}}) \frac{P_{E_{homo}}}{P_{a_{homo}}} + (P_{E_{homo}} - P_E)}{P_a}$$

The effect of \dot{V}_A/\dot{Q} heterogeneity is to increase the retention and decrease the excretion of a gas.

Shunt

Shunt refers to that portion of blood flow that bypasses gas exchanging areas and can be divided into intra-pulmonary and extra-pulmonary shunt. The effect of either is to increase the retention of any gas without an effect on the excretion of a gas. Note that the inert gas analysis does not consider extra-pulmonary shunt. Venous admixture (\dot{Q}_{va}) includes both pure intra pulmonary shunt and that from over perfusion of lung units and can be calculated by:

$$\frac{\dot{Q}_{va}}{\dot{Q}_T} = \frac{P_A - P_a}{P_A - P_{\bar{v}}} = \frac{P_a - P_A}{P_{\bar{v}} - P_A}$$

Alveolar partial pressure can be calculated using mixed expired partial pressure from:

$$\frac{P_E}{P_A} = 1 - \frac{V_{DIG}}{V_T}$$

and the preceding equation becomes:

$$\frac{\dot{Q}_{va}}{\dot{Q}_T} = \frac{R - E'}{1 - E'} \text{ where } E' = \frac{E}{1 - \frac{V_{DIG}}{V_T}}$$

\dot{V}_A/\dot{Q} distributions

The \dot{V}_A/\dot{Q} distribution can be estimated from the inert gas data using a linear least squares regression with enforced smoothing (69, 168) and from this model, predicted PaO_2 and PaCO_2 can be calculated. Diffusion limitation for inert gases and O_2 can be determined from this model. Diffusion limitation for inert gases would manifest as retention of gases with high molecular weight (SF_6 and enflurane), while that of O_2 would be evident as a much lower PaO_2 than predicted from the model.

The degree of \dot{V}_A/\dot{Q} mismatch is generally evaluated from two types of indices of dispersion (55) one derived from the model described above and the other derived directly from the retention and excretion data. The log standard deviations of blood flow ($\log \text{SD}\dot{Q}$) and ventilation ($\log \text{SD}\dot{V}$) are calculated as the square root of the second moment about the mean for both blood flow and ventilation (174). Normally this value is about 0.3-0.4 with 0.6 being at the upper limit of normal in young healthy subjects (181), and representing an alveolar-arterial difference of about 5 torr. In addition the curves resulting from the graph of ventilation of blood flow versus ventilation/perfusion ratio are centered on \dot{V}_A/\dot{Q} of 1 and do not have very high or low \dot{V}_A/\dot{Q} , or areas of shunt.

More recently Gale et al., (55) derived three indices of dispersion: DISP_{R^*} analogous to $\log \text{SD}\dot{Q}$, DISP_E analogous to $\log \text{SD}\dot{V}$ and DISP_{R^*-E} an overall index of dispersion.

$$\text{DISP}_{R^*-E} = 100 \times \sqrt{\frac{\sum_{i=1}^n (\text{Ri} - \text{Ei}^*)^2}{n}}$$

$$\text{DISP}_{R^*} = 100 \times \sqrt{\frac{\sum_{i=1}^n (\text{Ri} - \text{R}_{\text{homoi}}^*)^2}{n}}$$

$$DISP_E = 100 \times \sqrt{\frac{\sum_{i=1}^n (E_{homoi} - E_i^*)^2}{n}}$$

where

$$E_{homoi} = R_{homoi} = \frac{\lambda_i}{\lambda_i + \frac{\dot{V}_A}{\dot{Q}_T}}$$

and E_i and R_i represent excretions and retentions of the gas of interest and E_i^* is excretion corrected for dead space:

$$E_i^* = \frac{E_i}{1 - \frac{V_D}{V_T}}$$

These have been shown to correlate well with $\log SD\dot{Q}$ and $\log SD\dot{V}$ (55), although it should be noted that $DISP_R$ unlike $\log SD\dot{Q}$ includes shunt ($\dot{V}_A/\dot{Q} = 0$) and $DISP_E$ includes areas of dead space ($\dot{V}_A/\dot{Q} = \infty$) which is not true of $\log SD\dot{V}$.

Alveolar arterial difference

For a distribution of ventilation and perfusion ratios the partial pressure of mixed expired gas is given by:

$$P_{\bar{A}} = \frac{\sum_{j=1}^{j=N} P_{Aj} \cdot \dot{V}_{Aj}}{\sum_{j=1}^{j=N} P_{Aj}}$$

and the mixed mixed arterial partial pressure is given by :

$$P_{\bar{a}} = \frac{\sum_{j=1}^{j=N} P_{aj} \cdot \dot{Q}_j}{\sum_{j=1}^{j=N} \dot{Q}_j}$$

As the distribution of ventilation and perfusion broadens the PAO_2 and PaO_2 move further away from each other; in the perfectly homogeneous lung without shunt, or \dot{V}_A/\dot{Q} mismatch they would be equal. The alveolar-arterial difference tends to zero as λ tends to zero or infinity, and $[A-a]DO_2$ is the greatest for gases of intermediate solubility. Reducing the \dot{V}_A/\dot{Q} has the most effect on gases of low solubility, while raising the \dot{V}_A/\dot{Q} has the most pronounced effect on gases of high solubility (180).

APPENDIX C STATISTICAL ANALYSES AND RAW DATA

* = significant at $p \leq 0.05$

Anova tables

Metabolic data

Temperature

Source	Degrees of freedom	F- test	P value	Comparison	Scheffe F-test
Between subjects	9	2.367	0.0371	Rest vs Light exercise	4.167*
Within subjects	30			Rest vs Heavy exercise	4.167*
treatment	3	24.33	0.0001	Rest vs Maximal exercise	24.000*
residual	27			Light vs Heavy	0
total	39			Light vs Maximal	8.167*
				Heavy vs Maximal	8.167*

Ventilation

Source	Degrees of freedom	F- test	P value	Comparison	Scheffe F-test
Between subjects	9	0.085	0.9997	Rest vs Light exercise	9.280*
Within subjects	30			Rest vs Heavy exercise	101.007*
treatment	3	296.57	0.0001	Rest vs Maximal exercise	244.312*
residual	27			Light vs Heavy	49.054*
total	39			Light vs Maximal	158.360
				Heavy vs Maximal	31.140*

$\dot{V}O_2$

Source	Degrees of freedom	F- test	P value	Comparison	Scheffe F-test
Between subjects	9	0.032	1	Rest vs Light exercise	58.312*
Within subjects	30			Rest vs Heavy exercise	293.176*
treatment	3	524.67	0.001	Rest vs Maximal exercise	426.225*
residual	27			Light vs Heavy	89.988*
total	39			Light vs Maximal	169.234*
				Heavy vs Maximal	12.410*

$\dot{V}CO_2$

Source	Degrees of freedom	F- test	P value	Comparison	Scheffe F-test
Between subjects	9	0.028	1	Rest vs Light exercise	25.803*
Within subjects	30			Rest vs Heavy exercise	188.121*
treatment	3	439.65	0.0001	Rest vs Maximal exercise	364.961*
residual	27			Light vs Heavy	74.638*
total	39			Light vs Maximal	196.680*
				Heavy vs Maximal	28.997*

 $\dot{V}E/\dot{V}O_2$

Source	Degrees of freedom	F- test	P value	Comparison	Scheffe F-test
Between subjects	9	1.064	0.42	Rest vs Light exercise	18.191*
Within subjects	30			Rest vs Heavy exercise	4.043*
treatment	3	28.248	0.0001	Rest vs Maximal exercise	0.245
residual	27			Light vs Heavy	5.082*
total	39			Light vs Maximal	22.657*
				Heavy vs Maximal	6.279*

 $\dot{V}E/\dot{V}CO_2$

Source	Degrees of freedom	F- test	P value	Comparison	Scheffe F-test
Between subjects	9	0.746	0.66	Rest vs Light exercise	20.476*
Within subjects	30			Rest vs Heavy exercise	13.818*
treatment	3	23.298	0.0001	Rest vs Maximal exercise	7.616*
residual	27			Light vs Heavy	0.653
total	39			Light vs Maximal	3.117*
				Heavy vs Maximal	0.917

Respiratory exchange ratio

Source	Degrees of freedom	F- test	P value	Comparison	Scheffe F-test
Between subjects	9	0.633	0.76	Rest vs Light exercise	0.580
Within subjects	30			Rest vs Heavy exercise	6.460*
treatment	3	37.573	0.0001	Rest vs Maximal exercise	25.928*
residual	27			Light vs Heavy	7.740*
total	39			Light vs Maximal	28.435*
				Heavy vs Maximal	6.504*

Blood gas data

pH

Source	Degrees of freedom	F- test	P value	Comparison	Scheffe F-test
Between subjects	9	0.481	0.88	Rest vs Light exercise	1.288
Within subjects	30			Rest vs Heavy exercise	15.624*
treatment	3	72.959	0.0001	Rest vs Maximal exercise	61.266*
residual	27			Light vs Heavy	7.940*
total	39			Light vs Maximal	44.787*
				Heavy vs Maximal	15.012*

PaCO₂

Source	Degrees of freedom	F- test	P value	Comparison	Scheffe F-test
Between subjects	9	0.941	0.51	Rest vs Light exercise	2.908
Within subjects	30			Rest vs Heavy exercise	1.425
treatment	3	31.565	0.0001	Rest vs Maximal exercise	14.074*
residual	27			Light vs Heavy	8.404*
total	39			Light vs Maximal	29.777*
				Heavy vs Maximal	6.543*

PAO₂

Source	Degrees of freedom	F- test	P value	Comparison	Scheffe F-test
Between subjects	9	0.577	0.83	Rest vs Light exercise	1.435
Within subjects	30			Rest vs Heavy exercise	6.551*
treatment	3	48.435	0.0001	Rest vs Maximal exercise	27.046*
residual	27			Light vs Heavy	14.119*
total	39			Light vs Maximal	40.093*
				Heavy vs Maximal	6.976*

PaO₂

Source	Degrees of freedom	F- test	P value	Comparison	Scheffe F-test
Between subjects	9	4.319	0.0011	Rest vs Light exercise	3.634*
Within subjects	30			Rest vs Heavy exercise	12.774*
treatment	3	13.581	0.0001	Rest vs Maximal exercise	1.214
residual	27			Light vs Heavy	2.782
total	39			Light vs Maximal	0.647
				Heavy vs Maximal	6.111*

[A-a]DO₂(o)

Source	Degrees of freedom	F- test	P value	Comparison	Scheffe F-test
Between subjects	9	1.41	0.22	Rest vs Light exercise	0.292
Within subjects	30			Rest vs Heavy exercise	33.422*
treatment	3	65.419	0.0001	Rest vs Maximal exercise	37.938*
residual	27			Light vs Heavy	27.647*
total	39			Light vs Maximal	31.574*
				Heavy vs Maximal	0.143

SaO₂

Source	Degrees of freedom	F- test	P value	Comparison	Scheffe F-test
Between subjects	9	1.173	0.12	Rest vs Light exercise	1.228
Within subjects	30			Rest vs Heavy exercise	7.45*
treatment	3	18.555	0.0001	Rest vs Maximal exercise	15.915*
residual	27			Light vs Heavy	2.629
total	39			Light vs Maximal	8.301*
				Heavy vs Maximal	1.587

P \bar{v} O₂

Source	Degrees of freedom	F- test	P value	Comparison	Scheffe F-test
Between subjects	9	0.34	0.95	Rest vs Light exercise	17.943*
Within subjects	30			Rest vs Heavy exercise	33.802*
treatment	3	41.473	0.0001	Rest vs Maximal exercise	27.379*
residual	27			Light vs Heavy	2.490
total	39			Light vs Maximal	0.993
				Heavy vs Maximal	0.338

(a- \bar{v})O₂

Source	Degrees of freedom	F- test	P value	Comparison	Scheffe F-test
Between subjects	9	2.983	0.01	Rest vs Light exercise	3.985*
Within subjects	30			Rest vs Heavy exercise	4.075*
treatment	3	11.262	0.0001	Rest vs Maximal exercise	11.02*
residual	27			Light vs Heavy	0.001
total	39			Light vs Maximal	1.751
				Heavy vs Maximal	1.692

MIGET data for all six gases

Residual sum of squares

Source	Degrees of freedom	F- test	P value	Comparison	Scheffe F-test
Between subjects	9	2.821	0.02	Rest vs Light exercise	1.054
Within subjects	30			Rest vs Heavy exercise	3.357*
treatment	3	4.612	0.01	Rest vs Maximal exercise	3.466*
residual	27			Light vs Heavy	0.649
total	39			Light vs Maximal	0.698
				Heavy vs Maximal	0.001

Mean of Q distribution

Source	Degrees of freedom	F- test	P value	Comparison	Scheffe F-test
Between subjects	9	0.133	0.98	Rest vs Light exercise	8.065*
Within subjects	30			Rest vs Heavy exercise	14.191*
treatment	3	45.611	0.0001	Rest vs Maximal exercise	44.748*
residual	27			Light vs Heavy	0.860
total	39			Light vs Maximal	14.818*
				Heavy vs Maximal	8.540*

Mean of V distribution

Source	Degrees of freedom	F- test	P value	Comparison	Scheffe F-test
Between subjects	9	0.81	0.60	Rest vs Light exercise	2.917
Within subjects	30			Rest vs Heavy exercise	15.917*
treatment	3	61.187	0.0001	Rest vs Maximal exercise	54.555*
residual	27			Light vs Heavy	5.206*
total	39			Light vs Maximal	32.243*
				Heavy vs Maximal	11.537*

Log SD \dot{O}

Source	Degrees of freedom	F- test	P value	Comparison	Scheffe F-test
Between subjects	9	1.536	0.91	Rest vs Light exercise	0.551
Within subjects	30	31.046	0.0001	Rest vs Heavy exercise	10.258*
				Rest vs Maximal exercise	24.488*
treatment	3			Light vs Heavy	6.054*
residual	27			Light vs Maximal	17.963*
total	39			Heavy vs Maximal	3.048*

Log SD \dot{V}

Source	Degrees of freedom	F- test	P value	Comparison	Scheffe F-test
Between subjects	9	3.61	0.005	Rest vs Light exercise	0.579
Within subjects	30	1.347	0.28	Rest vs Heavy exercise	0.002
				Rest vs Maximal exercise	0.131
treatment	3			Light vs Heavy	0.600
residual	27			Light vs Maximal	1.262
total	39			Heavy vs Maximal	0.122

DISP_R*

Source	Degrees of freedom	F- test	P value	Comparison	Scheffe F-test
Between subjects	9	4.428	0.0013	Rest vs Light exercise	0.168
Within subjects	30	25.757	0.001	Rest vs Heavy exercise	8.232*
				Rest vs Maximal exercise	19.110*
treatment	3			Light vs Heavy	6.048*
residual	27			Light vs Maximal	15.696*
total	39			Heavy vs Maximal	2.257

DISP_E

Source	Degrees of freedom	F- test	P value	Comparison	Scheffe F-test
Between subjects	9	4.094	0.001	Rest vs Light exercise	0.001
Within subjects	30			Rest vs Heavy exercise	1.992
treatment	3	2.453	0.089	Rest vs Maximal exercise	1.884
residual	27			Light vs Heavy	1.949
total	39			Light vs Maximal	1.841
				Heavy vs Maximal	0.108

DISP_{R*-E}

Source	Degrees of freedom	F- test	P value	Comparison	Scheffe F-test
Between subjects	9	3.773	0.003	Rest vs Light exercise	0.111
Within subjects	30			Rest vs Heavy exercise	3.694*
treatment	3	8.449	0.0004	Rest vs Maximal exercise	5.909*
residual	27			Light vs Heavy	2.524
total	39			Light vs Maximal	4.400*
				Heavy vs Maximal	0.259

R(A-a)D

Source	Degrees of freedom	F- test	P value	Comparison	Scheffe F-test
Between subjects	9	2.899	0.0136	Rest vs Light exercise	0.631
Within subjects	30			Rest vs Heavy exercise	8.095*
treatment	3	20.998	0.001	Rest vs Maximal exercise	16.684*
residual	27			Light vs Heavy	4.205*
total	39			Light vs Maximal	10.825*
				Heavy vs Maximal	1.536

E(A-a)D

Source	Degrees of freedom	F- test	P value	Comparison	Scheffe F-test
Between subjects	9	1.709	0.1304	Rest vs Light exercise	0.517
				Rest vs Heavy exercise	0.176
				Rest vs Maximal exercise	0.043
Within subjects treatment	30	0.567	0.6418	Light vs Heavy	0.090
				Light vs Maximal	0.262
				Heavy vs Maximal	0.045
residual	27				
total	39				

(A-a)D

Source	Degrees of freedom	F- test	P value	Comparison	Scheffe F-test
Between subjects	9	3.809	0.0027	Rest vs Light exercise	0.0780
				Rest vs Heavy exercise	3.555*
				Rest vs Maximal exercise	6.443*
Within subjects treatment	30	9.094	0.0003	Light vs Heavy	2.581
				Light vs Maximal	5.106*
				Heavy vs Maximal	0.426
residual	27				
total	39				

[A-a]DO₂ (p)

Source	Degrees of freedom	F- test	P value	Comparison	Scheffe F-test
Between subjects	9	1.326	0.2652	Rest vs Light exercise	0.745
				Rest vs Heavy exercise	7.900*
				Rest vs Maximal exercise	7.969*
Within subjects treatment	30	12.124	0.0001	Light vs Heavy	3.793*
				Light vs Maximal	3.840*
				Heavy vs Maximal	0.0001
residual	27				
total	39				

[A-a]DO₂ (o-p)

Source	Degrees of freedom	F- test	P value	Comparison	Scheffe F-test
Between subjects	9	4.593	0.0013	Rest vs Light exercise	0.0530
Within subjects	30			Rest vs Heavy exercise	4.029*
				Rest vs Maximal exercise	4.609*
treatment	3	9.679	0.0002	Light vs Heavy	5.001*
residual	27			Light vs Maximal	5.646*
total	39			Heavy vs Maximal	0.0200

Cardiac data

Stroke volume

Source	Degrees of freedom	F- test	P value	Comparison	Scheffe F-test
Between subjects	9	0.488	0.87	Rest vs Light exercise	8.813*
Within subjects	30			Rest vs Heavy exercise	22.487*
				Rest vs Maximal exercise	59.456*
treatment	3	62.601	0.001	Light vs Heavy	3.245*
residual	27			Light vs Maximal	22.487*
total	39			Heavy vs Maximal	8.813*

End diastolic volume

Source	Degrees of freedom	F- test	P value	Comparison	Scheffe F-test
Between subjects	6	1.11	0.40	Rest vs Light exercise	10.429*
Within subjects	14			Rest vs Heavy exercise	20.124*
treatment	2	21.421	0.0001	Light vs Heavy	1.777
residual	12				
total	20				

End systolic volume

Source	Degrees of freedom	F- test	P value	Comparison	Scheffe F-test
Between subjects	6	2.02	0.13	Rest vs Light exercise	2.272
Within subjects	14			Rest vs Heavy exercise	4.069*
treatment	2	4.40	0.37	Light vs Heavy	0.26
residual	12				
total	20				

Ejection fraction

Source	Degrees of freedom	F- test	P value	Comparison	Scheffe F-test
Between subjects	6	0.621	0.71	Rest vs Light exercise	35.118*
Within subjects	14			Rest vs Heavy exercise	59.657*
treatment	2	65.338	0.0001	Light vs Heavy	3.232
residual	12				
total	20				

Regression

$\dot{V}E/\dot{V}CO_2$ vs PaO_2 during heavy exercise

Degrees of Freedom	R	R ²	Slope	Intercept
9	0.43	0.19	0.266	4.233
Source	Degrees of freedom	F test	P (one tailed)	
Regression	1	1.85	0.11	
Residual	8			
Total	9			

$\dot{V}E/\dot{V}CO_2$ vs PaO_2 during maximal exercise

Degrees of Freedom	R	R ²	Slope	Intercept
9	0.53	0.28	0.184	12.657
Source	Degrees of freedom	F test	P (one tailed)	
Regression	1	3.18	0.06	
Residual	8			
Total	9			

$\dot{V}E/\dot{V}O_2$ vs PaO_2 during heavy exercise

Degrees of Freedom	R	R ²	Slope	Intercept
9	0.402	0.161	0.3	1.895
Source	Degrees of freedom	F test	P (one tailed)	
Regression	1	1.539	0.12	
Residual	8			
Total	9			

$\dot{V}E/\dot{V}CO_2$ vs PaO_2 during maximal exercise

Degrees of Freedom	R	R ²	Slope	Intercept
9	0.11	0.13	0.055	29.721
Source	Degrees of freedom	F test	P (one tailed)	
Regression	1	0.109	0.37	
Residual	8			
Total	9			

Transit time at rest centroid method vs deconvolution

Degrees of Freedom	R	R ²	Slope	Intercept
9	0.993	0.987	0.963	0.339
Source	Degrees of freedom	F test	P (one tailed)	
Regression	1	605.419	0.0001	
Residual	8			
Total	9			

Transit time during exercise centroid method vs deconvolution

Degrees of Freedom	R	R ²	Slope	Intercept
9	0.955	0.899	1.152	-0.432
Source	Degrees of freedom	F test	P (one tailed)	
Regression	1	72.437	0.0001	
Residual	8			
Total	9			

Pulmonary transit time vs PaO₂ at maximal exercise

Degrees of Freedom	R	R ²	Slope	Intercept
9	0.648	0.420	17.9	42.243
Source	Degrees of freedom	F test	P (one tailed)	
Regression	1	5.795	0.02	
Residual	8			
Total	9			

Pulmonary transit time vs [A-a]DO₂(o) at maximal exercise

Degrees of Freedom	R	R ²	Slope	Intercept
9	0.591	0.35	-17.861	78.643
Source	Degrees of freedom	F test	P (one tailed)	
Regression	1	4.301	0.04	
Residual	8			
Total	9			

Pulmonary transit time vs [A-a]DO₂ (o-p)

Degrees of Freedom	R	R ²	Slope	Intercept
9	0.63	0.39	-23.814	78.304
Source	Degrees of freedom	F test	P (one tailed)	
Regression	1	5.283	0.025	
Residual	8			
Total	9			

Exercising pulmonary blood index vs whole blood volume (ml·kg⁻¹)

Degrees of Freedom	R	R ²	Slope	Intercept
9	0.656	0.43	14.379	-458.816
Source	Degrees of freedom	F test	P (one tailed)	
Regression	1	6.040	0.020	
Residual	8			
Total	9			

Pulmonary blood volume index vs [A-a]DO₂(o) at rest

Degrees of Freedom	R	R ²	Slope	Intercept
9	0.651	0.423	-0.088	51.175
Source	Degrees of freedom	F test	P (one tailed)	
Regression	1	5.871	0.02	
Residual	8			
Total	9			

Pulmonary blood volume index vs [A-a]DO₂(o) at maximal exercise

Degrees of Freedom	R	R ²	Slope	Intercept
9	0.569	0.34	-8.367	1024.178
Source	Degrees of freedom	F test	P (one tailed)	
Regression	1	3.84	0.04	
Residual	8			
Total	9			

Pulmonary blood volume index vs PaO₂ at maximal exercise

Degrees of Freedom	R	R ²	Slope	Intercept
9	0.689	0.475	11.073	-242.825
Source	Degrees of freedom	F test	P (one tailed)	
Regression	1	7.23	0.01	
Residual	8			
Total	9			

Pulmonary blood volume index vs [A-a]DO₂ (o-p) at maximal exercise

Degrees of Freedom	R	R ²	Slope	Intercept
9	0.679	0.46	-0.058	56.446
Source	Degrees of freedom	F test	P (one tailed)	
Regression	1	6.836	0.015	
Residual	8			
Total	9			

Multiple regression to predict PaO₂ at maximal exercise

Degrees of Freedom	R	R ²	
9	0.94	0.844	
Parameter	Value	Partial F	P value
Intercept	-25.224		
inert gas (A-a)D	28.356	5.064	0.0327
transit time	19.141	26.926	0.0012
$\dot{V}E/\dot{V}CO_2$	1.714	2.503	0.0028

APPENDIX D: INDIVIDUAL SUBJECT DATA.

*=missing data or not collected at this exercise level

Subject 1.				
Workload (watts)	R	150	300	420
Temp. (°C)	36.9	37.0	37.0	37.8
HCT	40			45
PaCO ₂ (torr)	36	36	36	31
PAO ₂ (torr)	89	102	112	120
PaO ₂ (torr)	89	96	82	85
[A-a]DO ₂ (o) (torr)	0	6	30	35
[A-a]DO ₂ (p) (torr)	5	8	10	15
[A-a]DO ₂ (o-p) (torr)	-4	-2	19	20
pH	7.45	7.46	7.41	7.24
SaO ₂ %	97.2	97.6	96.5	93.8
Pv̄O ₂ (torr)	30	19	14	11
$\dot{V}E$ (l·min ⁻¹)	15.7	43.4	105.4	195.4
$\dot{V}O_2$ (l·min ⁻¹)	638	2001	4191	6192
$\dot{V}CO_2$ (l·min ⁻¹)	430	1683	4316	7112
$\dot{V}E/\dot{V}O_2$	24.6	21.7	25.1	31.6
$\dot{V}E/\dot{V}CO_2$	36.5	25.8	24.4	27.5
\dot{Q} (l·min ⁻¹)	7.3	15.2#	26.6#	34.4
End diastolic volume (ml)	*	*	*	*
End systolic volume (ml)	*	*	*	*
Stroke volume (ml)	126	143	186	206
Ejection fraction	*	*	*	*
Transit time deconvolution (s)	10.19			2.92
Transit time centroid (s)	10.09			2.99
Pulmonary blood volume (l)	1.234			1.694
Mean residual sum of squares	99.6	69.05	94.65	33.3
Mean of \dot{Q}	0.955	2.145	2.82	4.31
Mean of \dot{V}	1.045	2.79	3.46	7.575
LogSD \dot{Q}	0.24	0.37	0.44	0.63
LogSD \dot{V}	0.42	0.80	0.47	0.91
DISP R*-E	1.052	3.292	2.657	6.439
DISP R*	0.476	1.447	1.400	3.422
DISP E*	0.559	2.151	1.478	3.522
Inert Gas A-a area	0.039	0.122	0.087	0.237

Subject 2				
Workload (watts)	R	150	300	350
Temp. (°C)	35.5	36.7	36.7	36.9
HCT	45			48
PaCO ₂ (torr)	33	43	30	29
PAO ₂ (torr)	108	102	124	123
PaO ₂ (torr)	88	88	87	91
[A-a]DO ₂ (o) (torr)	20	14	37	32
[A-a]DO ₂ (p) (torr)	12	9	22	16
[A-a]DO ₂ (o-p) (torr)	8	5	15	16
pH	7.48	7.40	7.32	7.29
SaO ₂ %	98.3	97.0	96.4	96.4
PvO ₂ (torr)	40	21	24	19
$\dot{V}E$ (l·min ⁻¹)	11.9	44.8	133.1	175.4
$\dot{V}O_2$ (l·min ⁻¹)	273	1867	3668	4494
$\dot{V}CO_2$ (l·min ⁻¹)	240	1834	4720	5431
$\dot{V}E/\dot{V}O_2$	43.59	24.00	36.29	39.03
$\dot{V}E/\dot{V}CO_2$	49.58	24.43	28.20	32.30
\dot{Q} (l·min ⁻¹)	6.1	13.9	24.7	27.6
End diastolic volume (ml)	132	159	190	*
End systolic volume (ml)	45	43	31	*
Stroke volume (ml)	87	116	158	161
Ejection fraction	0.67	0.74	0.83	*
Transit time deconvolution (s)	7.37			2.78
Transit time centroid (s)	7.24			2.77
Pulmonary blood volume (l)	0.743			1.277
Mean residual sum of squares	9	37	19	22
Mean of \dot{Q}	0.89	4.53	2.26	3.98
Mean of \dot{V}	1.61	5.50	5.30	8.66
LogSD \dot{Q}	0.64	0.47	0.77	0.67
LogSD \dot{V}	1.33	0.44	1.26	1.13
DISP R*-E	5.211	1.750	6.273	8.547
DISP R*	1.809	0.969	3.098	4.371
DISP E*	3.997	0.926	3.764	4.847
Inert Gas A-a area	0.215	0.059	0.241	0.327

Subject 3				
Workload (watts)	R	150	300	390
Temp. (°C)	36.5	36.7	37.0	37.6
HCT	48			48
PaCO ₂ (torr)	38	41	35	31
PAO ₂ (torr)	103	92	113	124
PaO ₂ (torr)	98	95	91	96
[A-a]DO ₂ (o) (torr)	5	-3	22	28
[A-a]DO ₂ (p) (torr)	4	7	16	16
[A-a]DO ₂ (o-p) (torr)	2	-10	6	12
pH	7.47	7.42	7.37	7.27
SaO ₂ %	97.9	97.4	96.7	95.8
Pv̄O ₂ (torr)	31	17	20	29
$\dot{V}E$ (l·min ⁻¹)	17.1	45.0	177.7	195.8
$\dot{V}O_2$ (l·min ⁻¹)	520	2393	4367	5176
$\dot{V}CO_2$ (l·min ⁻¹)	468	1889	4499	6657
$\dot{V}E/\dot{V}O_2$	32.9	18.8	40.7	37.8
$\dot{V}E/\dot{V}CO_2$	36.5	23.8	39.5	29.4
\dot{Q} (l·min ⁻¹)	6.5	14.4	21.9	34.6
End diastolic volume (ml)	121	158	178	*
End systolic volume (ml)	42	36	37	*
Stroke volume (ml)	79	122	140	197
Ejection fraction	0.66	0.77	0.80	*
Transit time deconvolution (s)	8.75			3.16
Transit time centroid (s)	8.60			3.18
Pulmonary blood volume (l)	0.94			1.83
Mean residual sum of squares	66	67	35	72
Mean of \dot{Q}	0.92	2.16	2.62	4.73
Mean of \dot{V}	1.25	2.68	5.61	10.31
LogSD \dot{Q}	0.24	0.29	0.51	0.69
LogSD \dot{V}	0.82	0.65	1.29	1.16
DISP R*-E	3.213	2.283	8.303	8.071
DISP R*	1.054	0.989	3.718	4.214
DISP E*	2.469	2.511	5.283	4.381
Inert Gas A-a area	0.126	0.086	0.321	0.328

Subject 4				
Workload (watts)	R	150	300	360
Temp. (°C)	37.3	37.5	38.1	38.8
HCT	40			46
PaCO ₂ (torr)	36	39	35	30
PAO ₂ (torr)	115	101	113	124
PaO ₂ (torr)	94	83	74	81
[A-a]DO ₂ (o) (torr)	21	18	39	43
[A-a]DO ₂ (p) (torr)	1	4	6	13
[A-a]DO ₂ (o-p) (torr)	19	14	33	30
pH	7.44	7.41	7.29	7.18
SaO ₂ %	97.1	95.5	90.7	88.1
P \bar{v} O ₂ (torr)	36	19	13	19
$\dot{V}E$ (l·min ⁻¹)	18.5	43.4	114.3	183.7
$\dot{V}O_2$ (l·min ⁻¹)	548	2086	4654	5178
$\dot{V}CO_2$ (l·min ⁻¹)	611	1835	4895	6586
$\dot{V}E/\dot{V}O_2$	33.76	20.81	24.56	35.48
$\dot{V}E/\dot{V}CO_2$	30.28	23.65	23.35	27.89
\dot{Q} (l·min ⁻¹)	8.5	15.7#	29.0#	31.9#
End diastolic volume (ml)	*	*	*	*
End systolic volume (ml)	*	*	*	*
Stroke volume (ml)	147	141	187	197
Ejection fraction	*	*	*	*
Transit time deconvolution (s)	7.45			2.67
Transit time centroid (s)	7.72			2.68
Pulmonary blood volume (l)	1.075			1.422
Mean residual sum of squares	198	125	86	86
Mean of \dot{Q}	1.19	3.15	2.91	4.56
Mean of \dot{V}	1.23	3.55	4.83	11.95
LogSD \dot{Q}	0.18	0.28	0.40	0.73
LogSD \dot{V}	0.18	0.39	0.97	1.18
DISP R*-E	0.430	1.261	5.597	10.124
DISP R*	0.230	0.668	2.480	5.525
DISP E*	0.237	0.706	3.653	5.419
Inert Gas A-a area	0.014	0.045	0.221	0.405

Subject 5				
Workload (watts)	R	150	300	400
Temp. (°C)	36.7	37.0	36.8	38.3
HCT	43.0			44.0
PaCO ₂ (torr)	41	46	44	33
PAO ₂ (torr)	103	94	103	122
PaO ₂ (torr)	99	86	74	93
[A-a]DO ₂ (o) (torr)	4	8	29	29
[A-a]DO ₂ (p) (torr)	11	12	23	15
[A-a]DO ₂ (o-p) (torr)	-7	-4	6	14
pH	7.48	7.45	7.38	7.20
SaO ₂ %	97.9	96.8	94.8	93.5
P \bar{v} O ₂ (torr)	34	24	13	25
$\dot{V}E$ (l·min ⁻¹)	9.9	36.4	75.8	147.6
$\dot{V}O_2$ (l·min ⁻¹)	414	1913	3974	5291
$\dot{V}CO_2$ (l·min ⁻¹)	372	1621	3752	6072
$\dot{V}E/\dot{V}O_2$	23.91	19.03	19.07	27.9
$\dot{V}E/\dot{V}CO_2$	26.61	22.46	20.2	24.31
\dot{Q} (l·min ⁻¹)	7.6	17.8	24.4	36.0
End diastolic volume (ml)	154	185	185	*
End systolic volume (ml)	45	33	31	*
Stroke volume (ml)	108	152	154	227
Ejection fraction	0.71	0.84	0.84	*
Transit time deconvolution (s)	9.23			2.99
Transit time centroid (s)	9.12			2.74
Pulmonary blood volume (l)	1.162			1.719
Mean residual sum of squares	27.1	19.7	17.2	61.9
Mean of \dot{Q}	0.91	2.38	1.99	3.38
Mean of \dot{V}	1.67	3.40	4.16	11.30
LogSD \dot{Q}	0.42	0.51	0.61	0.79
LogSD \dot{V}	1.32	0.66	0.86	1.35
DISP _{R*-E}	6.791	3.634	7.120	12.974
DISP _{R*}	2.366	1.843	3.495	6.760
DISP _{E*}	5.017	2.128	4.307	7.292
Inert Gas A-a area	0.261	0.132	0.264	0.508

Subject 6				
Workload (watts)	R	150	300	370
Temp. (°C)	37.1	37.5	37.8	39.0
HCT	43.0			42.0
PaCO ₂ (torr)	40	40	38	33
PAO ₂ (torr)	109	105	109	119
PaO ₂ (torr)	107	104	100	110
[A-a]DO ₂ (o) (torr)	2	1	9	9
[A-a]DO ₂ (p) (torr)	3	13	22	21
[A-a]DO ₂ (o-p) (torr)	-1	-13	-12	-12
pH	7.41	7.39	7.30	7.20
SaO ₂ %	97.8	97.3	95.5	94.7
PvO ₂ (torr)	43	24	18	12
$\dot{V}E$ (l·min ⁻¹)	12.4	44.1	105.4	159.2
$\dot{V}O_2$ (l·min ⁻¹)	371	1938	4350	4911
$\dot{V}CO_2$ (l·min ⁻¹)	363	1753	4135	5171
$\dot{V}E/\dot{V}O_2$	33.42	22.76	24.23	32.42
$\dot{V}E/\dot{V}CO_2$	34.16	25.16	25.49	30.79
\dot{Q} (l·min ⁻¹)	8.2	16.3	21.9	34.5
End diastolic volume (ml)	165	167	186	*
End systolic volume (ml)	66	39	56	*
Stroke volume (ml)	99	128	130	197
Ejection fraction	0.60	0.77	0.77	*
Transit time deconvolution (s)	8.85			3.56
Transit time centroid (s)	8.96			3.76
Pulmonary blood volume (l)	1.217			2.105
Mean residual sum of squares	79.3	16.7	16.8	2.2
Mean of \dot{Q}	0.66	1.86	3.36	4.58
Mean of \dot{V}	1.43	5.03	10.11	14.19
LogSD \dot{Q}	0.30	0.63	0.83	0.90
LogSD \dot{V}	1.65	1.39	1.22	1.16
DISP _{R*-E}	5.216	11.457	11.900	11.974
DISP _{R*}	1.588	5.062	6.421	6.847
DISP _{E*}	4.155	7.509	6.522	6.051
Inert Gas A-a area	20.9	0.214	0.442	0.462

Subject 7				
Workload (watts)	R	150	300	370
Temp. (°C)	36.9	36.9	36.9	38.1
HCT	41.0			43.0
PaCO ₂ (torr)	41	44	37	32
PAO ₂ (torr)	107	99	114	123
PaO ₂ (torr)	105	98	94	106
[A-a]DO ₂ (o) (torr)	2	1	20	17
[A-a]DO ₂ (p) (torr)	5	10	16	19
[A-a]DO ₂ (o-p) (torr)	-3	-9	3	-2
pH	7.40	7.38	7.31	7.16
SaO ₂ %	97.8	97.2	96.6	95.1
P \bar{v} O ₂ (torr)	32	22	17	19
$\dot{V}E$ (l·min ⁻¹)	15.3	49.3	105.8	184.0
$\dot{V}O_2$ (l·min ⁻¹)	454	2424	4108	4912
$\dot{V}CO_2$ (l·min ⁻¹)	436	2165	4218	5713
$\dot{V}E/\dot{V}O_2$	33.7	20.34	25.75	37.46
$\dot{V}E/\dot{V}CO_2$	35.09	22.77	25.08	32.21
\dot{Q} (l·min ⁻¹)	6.2	18.2	26.8#	37.6
End diastolic volume (ml)	146	233	223	*
End systolic volume (ml)	57	67	39	*
Stroke volume (ml)	89	166	184	229
Ejection fraction	0.62	0.72	0.83	*
Transit time deconvolution (s)	8.73			2.91
Transit time centroid (s)	8.63			2.95
Pulmonary blood volume (l)	0.897			1.836
Mean residual sum of squares	190.2	88.5	18.8	15.4
Mean of \dot{Q}	1.20	1.72	3.04	4.72
Mean of \dot{V}	4.15	6.34	11.84	13.39
LogSD \dot{Q}	0.40	0.53	0.77	0.85
LogSD \dot{V}	1.82	1.70	1.42	1.10
DISP R*-E	12.570	13.778	14.567	11.072
DISP R*	4.484	5.630	7.338	6.316
DISP E*	9.327	9.482	8.529	5.663
Inert Gas A-a area	0.513	0.550	0.574	0.437

Subject 8				
Workload (watts)	R	150	300	340
Temp. (°C)	37.2	37.3	37.5	38.3
HCT	43.0			41.0
PaCO ₂ (torr)	42	43	36	30
PAO ₂ (torr)	97	95	110	122
PaO ₂ (torr)	99	78	83	93
[A-a]DO ₂ (o) (torr)	-2	17	27	29
[A-a]DO ₂ (p) (torr)	1	20	25	20
[A-a]DO ₂ (o-p) (torr)	-3	-3	2	9
pH	7.40	7.38	7.33	7.25
SaO ₂ %	97.2	94.6	95.0	94.3
P \bar{v} O ₂ (torr)	40	18	14	15
$\dot{V}E$ (l·min ⁻¹)	12.0	43.4	107.6	169.6
$\dot{V}O_2$ (l·min ⁻¹)	350	2163	4337	4673
$\dot{V}CO_2$ (l·min ⁻¹)	299	1813	4218	5324
$\dot{V}E/\dot{V}O_2$	34.29	20.06	24.81	36.29
$\dot{V}E/\dot{V}CO_2$	40.13	23.94	25.51	31.86
\dot{Q} (l·min ⁻¹)	6.6	15.5	22.8	35.7
End diastolic volume (ml)	145	185	188	*
End systolic volume (ml)	63	59	48	*
Stroke volume (ml)	81	126	139	209
Ejection fraction	0.56	0.68	0.74	*
Transit time deconvolution (s)	9.82			2.58
Transit time centroid (s)	9.80			2.60
Pulmonary blood volume (l)	1.079			1.541
Mean residual sum of squares	*	4.4	8.6	5.0
Mean of \dot{Q}	*	4.72	1.96	4.77
Mean of \dot{V}	*	11.43	7.23	14.63
LogSD \dot{Q}	*	0.82	0.75	0.88
LogSD \dot{V}	*	1.00	1.58	1.15
DISP R*-E	1.898	9.993	16.805	11.999
DISP R*	5.684	5.688	7.632	6.916
DISP E*	1.393	5.015	10.811	5.999
Inert Gas A-a area	0.076	0.373	0.640	0.472

Subject 9				
Workload (watts)	R	150	300	320
Temp. (°C)	37.1	37.5	37.5	38.2
HCT	43.0			45.0
PaCO ₂ (torr)	36	40	33	31
PAO ₂ (torr)	93	94	114	120
PaO ₂ (torr)	103	94	93	101
[A-a]DO ₂ (o) (torr)	-10	0	21	19
[A-a]DO ₂ (p) (torr)	26	9	24	13
[A-a]DO ₂ (o-p) (torr)	-36	-8	-3	6
pH	7.41	7.38	7.27	7.23
SaO ₂ %	97.6	96.5	95.6	95.30
Pv̄O ₂ (torr)	35	22	5	11
$\dot{V}E$ (l·min ⁻¹)	10.2	49.3	139.1	158.1
$\dot{V}O_2$ (l·min ⁻¹)	439	2476	5006	4749
$\dot{V}CO_2$ (l·min ⁻¹)	307	1947	4915	5213
$\dot{V}E/\dot{V}O_2$	23.23	19.91	27.79	33.29
$\dot{V}E/\dot{V}CO_2$	33.22	25.32	28.3	30.33
\dot{Q} (l·min ⁻¹)	5.9	18.4	26.4#	26.4#
End diastolic volume (ml)	164	191	*	*
End systolic volume (ml)	59	43	*	*
Stroke volume (ml)	105	148	165	165
Ejection fraction	0.64	0.80	*	*
Transit time deconvolution (s)	11.35			2.69
Transit time centroid (s)	11.36			2.68
Pulmonary blood volume (l)	1.117			1.181
Mean residual sum of squares	2.1	50.1	11.1	6.6
Mean of \dot{Q}	0.89	2.32	4.04	5.28
Mean of \dot{V}	2.76	5.97	13.56	17.20
LogSD \dot{Q}	0.76	0.53	0.86	0.92
LogSD \dot{V}	1.34	1.38	1.22	1.41
DISP R*-E	13.412	9.924	13.115	12.362
DISP R*	6.105	4.387	7.246	7.277
DISP E*	8.445	6.469	6.939	6.001
Inert Gas A-a area	0.480	0.391	0.513	0.497

Subject 10				
Workload (watts)	R	150	300	390
Temp. (°C)	36.9#	37.1#	37.3#	38.2#
HCT	40.0			40.0
PaCO ₂ (torr)	39	41	39	38
PAO ₂ (torr)	95	92	101	113
PaO ₂ (torr)	96	92	80	90
[A-a]DO ₂ (o) (torr)	-1	0	21	23
[A-a]DO ₂ (p) (torr)	3	11	9	18
[A-a]DO ₂ (o-p) (torr)	-3	-10	12	5
pH	7.44	7.42	7.39	7.36
SaO ₂ %	97.5	96.9	95.2	95.10
Pv̄O ₂ (torr)	35	17	8	7
$\dot{V}E$ (l·min ⁻¹)	12.4	48.9	106.2	182.7
$\dot{V}O_2$ (l·min ⁻¹)	354	2264	4562	5569
$\dot{V}CO_2$ (l·min ⁻¹)	283	1791	4026	6261
$\dot{V}E/\dot{V}O_2$	35.03	21.6	23.28	32.81
$\dot{V}E/\dot{V}CO_2$	43.82	27.3	26.38	29.18
\dot{Q} (l·min ⁻¹)	7.0	16.4	28.5	33.8
End diastolic volume (ml)	165	198	235	*
End systolic volume (ml)	63	36	48	*
Stroke volume (ml)	102	161	187	222
Ejection fraction	0.62	0.81	0.79	*
Transit time deconvolution (s)	11.43			
Transit time centroid (s)	11.75			2.15
Pulmonary blood volume (l)	1.352			1.211
Mean residual sum of squares	113	49.3	20.6	12.6
Mean of \dot{Q}	1.42	1.88	3.39	4.38
Mean of \dot{V}	2.08	2.59	6.53	11.83
LogSD \dot{Q}	0.26	0.37	0.58	0.86
LogSD \dot{V}	0.91	0.68	1.11	1.20
DISP R*-E	4.290	3.532	7.090	10.284
DISP R*	1.469	1.587	3.483	5.683
DISP E*	3.217	2.279	4.205	5.412
Inert Gas A-a area	0.171	0.130	0.275	0.418